ANL-5822
Reactors-General

ARGONNE NATIONAL LABORATORY
P. O. Box 299
Lemont, Illinois

HEAT TRANSFER FROM RODS NORMAL TO SUBCOOLED WATER FLOW FOR NON-BOILING AND SURFACE-BOILING CONDITIONS UP TO AND INCLUDING BURNOUT

by

S. P. Kezios and R. K. Lo
Illinois Institute of Technology

January 1958

Reproduced from Final Report on IIT Project No. 6074
sponsored by ANL Subcontract No. 31-109-38-453

Operated by The University of Chicago
under
Contract W-31-109-eng-38

DISCLAIMER

FOREWORD

This investigation was carried out in the Heat Transfer Laboratory of Illinois Institute of Technology under the sponsorship of the Argonne National Laboratory (Subcontract ANL No. 31-109-38-453).

The work was initiated under the direction of the late Max Jakob and was completed under the direction of the undersigned, who, prior to Dr. Jakob's death in 1955, acted in a supervisory capacity in connection with the work. Robert K. Lo, Assistant Research Engineer, was the main participant in this experimental study; student assistants were employed from time to time as the need arose. Mr. Frederick Salzberg, also a laboratory staff member at the time, set up and carried out the auxiliary tests dealing with the resistivity measurements of Chromax wire. Mr. Serge Vinogradov of IIT's Chemistry Department determined the specific resistance and pH value of the test water.

The support of Argonne National Laboratory is gratefully acknowledged.

Respectfully submitted,

S. P. Kezios

S. P. Kezios
Associate Professor of Mechanical Engineering
Director, Heat Transfer Laboratory

September 15, 1957

TABLE OF CONTENTS

TABLE OF CONTENTS (Cont'd)

LIST OF TABLES

LIST OF ILLUSTRATIONS

LIST OF ILLUSTRATIONS (Cont'd)

NOMENCLATURE

Symbol	Description	Unit
A_c	cross-sectional area	ft^2
A_s	surface area	ft^2
C	constants	
b	thickness of plate	ft
D	diameter	ft
E	electrical potential	volts
E	thermal emf	millivolts
g	acceleration of gravity	ft/hr
G	mass flow rate	$lb_m/hr\ ft^2$
h	heat transfer coefficient	$B/hr\ ft^2\ F$
h^*	heat transfer coefficient based on indicated surface temperature	$B/hr\ ft^2\ F$
h_p	heat transfer coefficient between fluid and a plate	$B/hr\ ft^2\ F$
h_{tc}	heat transfer coefficient between fluid and thermocouple wires	$B/hr\ ft^2\ F$
I	electric current	amperes
$J_o(x)$	Bessel function of the first kind, zero order	
$J_1(x)$	Bessel function of the first kind, first order	
k	thermal conductivity	$B/hr\ ft^2\ F$
$K_o(x)$	modified Bessel function of the second kind, zero order	
$K_1(x)$	modified Bessel function of the second kind, first order	
L	length	ft
N_{Nu}	Nusselt number, hD/k	

NOMENCLATURE (Cont'd)

Symbol	Description	Unit
N_{Pr}	Prandtl number, $\mu c_p/k$	
N_{Re}	Reynolds number, $\rho vD/\mu$	
p	pressure	in. Hg or psia
q	rate of heat flow	B/hr
q"	rate of heat flow per unit area	B/hr ft^2
q'''	rate of heat flow per unit volume	B/hr ft^3
q''_{BO}	rate of heat flow per unit area at burnout condition	B/hr ft^2
r	radius	ft
r_s	radius of source, $\sqrt{2}\ r_{tc}$	ft
R'	electrical resistance	ohm/ft
R	specific electrical resistance	ohm/cm^3
t_f	film temperature, $(t_s + t_w)/2$	°F
t_{ind}	indicated temperature	°F
t_s	surface temperature	°F
t_{sat}	saturation temperature	°F
t_w	water temperature	°F
V	velocity	ft/hr or ft/sec
v	volume	ft^3
Δt_{sub}	degree of subcooling, $(t_{sat} - t_w)$	F
Δt_{sat}	temperature excess, $(t_s - t_{sat})$	F
α	ratio between orifice diameter to inside pipe diameter	
β	coefficient of thermal expansion	F^{-1}

NOMENCLATURE (Cont'd)

Symbol	Description	Unit
β	defined as $(h_{p1} + h_{p2})/bk$	ft^{-2}
γ	defined as $2\pi r_{tc} \sqrt{2h_{tc} k_{tc} r_{tc}}$	$B/hr\ ft^2$
ϵ	temperature coefficient	F^{-1}
ρ	density	lb_m/ft^3
ρ	electrical resistivity	ohm ft or ohm(cir mil)/ft
σ	defined as $r \sqrt{\epsilon q'''_m / k}$	
μ	dynamic viscosity	$lb_m/hr\ ft$
θ	temperature difference	F

Subscripts

i	denoting condition inside a tube
m	mean
o	denoting condition outside a tube

CHAPTER I

INTRODUCTION

Purpose of the Investigation

Scientific investigators have, over a period of many years, contributed substantial theoretical and experimental information concerning the heat transfer, temperature distribution, boundary layer and eddy formation for flow of fluids normal to cylinders. However, for the most part, experimental studies dealing with the heat transfer between cylinders and liquids have been made for the case of heat transfer without change in phase of the liquid, that is, without boiling.

In recent years the boiling phenomenon itself has received considerable attention. Results of heat transfer from wires with free-convection surface boiling have been reported, and a number of investigations dealing with heat transfer for subcooled liquids passing through inside of cylinders or annuli of concentric cylinders have also been carried out, to mention only a few types of boiling studies. Research in this area continues.

Nevertheless, the information regarding forced-convection surface-boiling heat transfer for flow normal to wires is still extremely meager. This lack of detailed information constitutes a major handicap to engineers designing apparatus of limited size for heat transfer at very high rates of flux; such information is especially needed, for example, in the design of certain types of "boiling-water" reactors, in which rod-type arrays suggest themselves as possible fuel-element configurations.

It is the purpose of this investigation to obtain experimental data for heat transfer from heated wires or rods normal to water flow, with and without change of phase and up to the limit of burnout. A heated wire may,

in certain designs, simulate the solid fuel elements in a nuclear reactor; moreover, information obtained with a single rod is of fundamental importance, and it provides a point of departure for experiments and analyses dealing with wire assemblies of various sorts. As such, the research reported herein may be considered as an initial step toward the understanding of the complex problem of heat transfer with change of phase in an assembly of wires (or fuel rods).

Scope of the Work

This research, experimental in nature, deals with forced-convection non-boiling and surface-boiling heat transfer from an electrically heated 1/8-in. OD by 10-in. long Chromax wire to subcooled water flowing normal to it with emphasis on the following items:

1) correlation of the convective heat-transfer coefficient, velocity, and fluid properties (temperature influence) for the case of heat transfer without change in phase and the given normal flow geometry,
2) influence of the degree of subcooling and velocity on the rate of heat transfer with change of phase,*
3) correlation of heat flux density, velocity and degree of subcooling at burnout with zero quality,* and
4) photographic study of the boiling phenomenon.

The variables employed in this study range as follows:

1) mean velocity: 1 to 6.8 ft/sec,
2) system pressure: 15 to 30 psia,

*These items involve only so-called "local" or "partial" boiling.

3) degree of subcooling: 40 to 160 F (this smallest value corresponds to a bulk water temperature of 180°F),* and

4) heat flux: up to 3,750,000 B/hr ft^2, corresponding to a power input of 30 kva at a heated wire.

The test wires were centrally located in a 6-5/8-in. by 10-in. test channel with their long dimension oriented across the 10-in. channel width.

In addition to the experiments falling under the scope outlined above, some preliminary experiments dealing with the heat transfer and burnout characteristics of extremely simple matrix arrays were carried out. They are reported in Appendix B.

Some auxiliary experiments, performed with 1/8-in. OD Type 304 stainless steel tubes, were also carried out in order to provide data on boiling heat transfer using a different metal and, mainly, using different technique to measure the surface temperature. These experiments are reported in Appendix C.

Brief Review of Related Studies**

Only literature more or less directly related to this study are introduced here, and no attempt is made to cover in a comprehensive manner the rather large literature dealing with the general problem of heat transfer in surface boiling. Although this study involves heat transfer by forced-convection surface boiling, a few papers on free-convection surface-boiling heat transfer are also cited; these cover the main historical developments and the techniques for measuring surface temperatures of the heating elements.

---

*These items involve only so-called "local" or "partial" boiling.

**The reader already acquainted with the main literature on the subject of boiling can proceed at once to Chapter II, page 15.

Jakob and Fritz (1)[1] investigated boiling heat transfer by employing a horizontal copper heating element of 10-cm diameter, heated electrically, and housed in a double-walled boiler. Windows were provided for visual observation and photography. With this experimental arrangement they studied the influence of the roughness of, and the gas absorbed at, the heater surface, and also the effect of the length of immersion time. They presented their results by plotting flux density q'' and heat transfer coefficient h versus temperature excess Δt_{sat}. Employing the theory of capillarity, they also observed that there are three fundamental types of bubbles, classified according to whether they form on an unwetted surface, on a partially wetted surface, or on a totally wetted surface. The temperature variation of bulk water was carefully measured by a movable thermocouple in order to investigate the heat transfer from the bulk water to the rising bubbles. Because of the limit of heat input to the electric heater, they could only obtain heat flux up to 14,720 B/hr ft^2.

Jakob and Linke (2,3) performed experiments with a vertical heating surface. They improved their original apparatus and increased its maximum heat flux to 73,600 B/hr ft^2. As a result of their work, they proposed a correlation of the form:

$$N_{Nu} = C(N_{Gr} \cdot N_{Pr})^n \qquad (1)$$

where C represents a constant depending on the conditions of the heater surface. They found that $n = 1/4$ for vertical surfaces and $n = 3/4$ for horizontal surfaces. These values were substantiated through the use of Schlieren photography, through which it was observed that the convection

---

[1] Numbers in parentheses refer to Bibliography at the end of this report.

flow near a vertical heating surface was always laminar whereas it was invariably turbulent on a horizontal heated surface. Still photographs and motion pictures were used to determine the rate of growth of bubbles, bubble rise velocity and other characteristics. Frequency of bubble generation was also measured stroboscopically using a rotating disk and lamp.

Cryder and Gilliland (4) studied free-convection surface-boiling heat transfer from an electrically heated 1.04-in. OD brass tube to saturated water and seven other organic liquids. Brass disks were silver-soldered to the ends of the tube inside of which the heating element, made of AWG No. 22 Nichrome wire, was housed. The surface temperature was measured by means of five Chromel-copper thermocouples silver-soldered on the test surface and at the ends of the units. They reported that a maximum heat flux density of 24,000 B/hr ft^2 was attained. Heat transfer coefficients in the nucleate boiling region were expressed as varying with temperature excess Δt_{sat} to the 2.4^{th} power.

Nukiyama (5), in a classic study, was probably the first to obtain the complete heat flux q'' versus temperature excess Δt_{sat} curve showing the four distinct regions of heat transfer, that is, that by free convection, that by nucleate boiling, that by partial film boiling and that by radiation through the vapor film blanketing the heating surface. He submerged platinum wires 20-cm long and 0.14- to 0.4-mm in diameter in a pool of saturated water at atmospheric pressure. The test wire was introduced in a branch of a Wheatstone electric bridge, and the relation of its temperature to the reading of the bridge was calibrated beforehand with a small current from a battery. The wire was heated with direct current. First he observed that when heat flux reached a maximum at a temperature

excess equal to 40°C, the wire melted. Then, through the manipulation of the external resistance of the circuit, he succeeded in obtaining, beyond the heat flux of burnout, a minimum heat flux at a higher temperature difference between the wire surface and the water. Beyond this point, further increase in heat input resulted in rapid increase of wire temperature; at this state the wire was seen glowing brightly in the water. He also performed experiments with an electrically heated copper disk of 10-mm diameter. The results obtained are similar to those from platinum wires.

Drew and Mueller (6) experimentally obtained a complete boiling curve similar to that of Nukiyama. Their heating element, made of a 1/4-in. ID by 1/2-in. OD looped pipe, was placed in a fluid held in a sealed flask. Steam passing and condensing inside the pipe served as a heating medium. The use of condensing steam in conjunction with hydrocarbon fluids permitted the experiments to be carried out beyond the point of burnout for the usual electric heater and allowed for the operation in the region of film boiling. From the results of their experiments with various organic substances they plotted the curves of heat flux q'' versus temperature excess Δt_{sat} and their correlation.

Cryder and Finalborgo (7) investigated free-convection heat transfer from an electrically heated 1-1/2-in. OD by 1-in. ID brass tube to saturated water and seven other liquids at pressures below atmospheric. A resistance wire, comprising the heater, was inserted in the inside of the tube which, in turn, was mounted by fitting it to a 6-in. OD by 16-in. high brass boiler. The boiler was closed at both ends with brass plates and it was lagged with 2-1/2-in. magnesia-asbestos. The outer surface temperature of the heater was obtained by several AWG No. 28 copper-Copel thermocouple wires spot-welded to the surface. They reported that from their preliminary

measurements various methods for attaching the thermocouple wires to the surface indicated negligible differences in results. They found that in the nucleate boiling region the heat transfer coefficient varied with temperature excess Δt_{sat} to the one-fourth power which confirmed the findings of Jakob (2).

Akin and McAdams (8) determined free-convection heat transfer coefficients from a single horizontal steam-heated 3/4-in. nickel-plated copper tube to water and three alcohols boiling at atmospheric pressure and under vacuum. They also verified experimentally that the heat flux went through a maximum value as the temperature difference was increased. Film boiling occurred at the large temperature differences beyond the hump in the curve. At atmospheric pressure a maximum heat flux 360,000 B/hr ft^2 for distilled water was obtained. Approximately the same maximum heat flux was also found with tap water boiling on a scaled tube, except at a higher temperature difference.

Akin and McAdams developed a special thermocouple technique to measure the surface temperature. Their construction was as follows: a 0.026-in. hole was drilled in the tube wall, with the closed end almost at the outer surface of the tube. A single AWG 30 constantan wire, sealed in a Pyrex tube except for the tip of the wire, was then inserted and tin-soldered so that the hot junction was almost at the surface.

Farber and Scorah (9) studied heat transfer to water boiling in a pool at different pressures from four different wires, namely, nickel, tungsten, Chromel A and Chromel C. All of their wires were 6 in. long and 0.04 in. in diameter, heated electrically. To measure the surface temperature of the wire they welded an AWG 28 Chromel-Alumel thermocouple on the surface, and they also employed a pyrometer for this purpose. Both

a-c and d-c power were used to heat the wires and they reported that no difference was detected in results obtained. The shape of the boiling curves they obtained was similar to that by Nukiyama. They found that at the same pressure, different metals gave different numerical values for the boiling curve; at different pressures, the same metal gave different numerical values for the boiling curve. However, the shape of the boiling curve remained the same.

Knowles (10) employed downflow of subcooled tap water in an annulus containing centrally located stainless steel tubes, 1/8 in. and 1/4 in. in diameter, with length hydraulic-diameter ratio varying from 7.6 to 64.3. Alternating current was used to heat the tubes. The outside surface temperature of the heated tube was calculated from the electrical energy dissipated in the tube and the temperature registered by a movable copper-constantan thermocouple. Knowles obtained maximum heat flux density 2,300,000 B/hr ft^2 at a velocity of 10 ft/sec. He also found surface-boiling to increase the heat-transfer coefficient to over four times the value predicted for non-boiling conditions.

McAdams and co-workers (11) obtained data for water boiling in a pool at atmospheric pressure on horizontal platinum wires ranging in diameters from 0.004 to 0.024 in. heated with direct current from a 4 to 40-volt storage battery. The platinum wire served both as the heat-transfer surface and as a resistance thermometer. Corrections for radial temperature gradient were also made in this study, in a manner similar to that of Knowles (10).

They reported that at a given temperature Δt_{sat} wire size has a substantial effect on the heat flux in the region of free convection (Δt_{sat} from 4 to 15°F). In the region of film boiling (Δt_{sat} from

1350°F to 2350°F) the heat flux was found to be inversely proportional to the square root of the diameter of the wire. In the region of nucleate boiling (Δt_{sat} from 17 to 42°F), diameter has little effect. They also reported that in the range of nucleate boiling, experiments made with a dirty 0.0117-in. platinum wire showed the maximum heat flux density to increase from 400,000 B/hr ft^2 at 1 atmosphere to 2,000,000 B/hr ft^2 at 83 atmospheres.

No complete boiling curve, such as that found by Nukiyama, was reported by McAdams' group.

McAdams and co-workers (12) in a subsequent study investigated heat transfer at high heat flux density from a heated surface to degassed distilled water flowing upward through an annulus of a vertical glass tube containing a centrally located heater of 1/4-in. OD Type 304 stainless steel tube, which was heated with direct current. The outer wall temperature was calculated from uniform heat generation with constant thermal conductivity and constant electrical resistivity and inner wall temperature which were recorded by several iron-constantan thermocouples placed inside the heated tube at an equal spacing. The length of the heater employed was 3.75 and 11.5 in. with equivalent hydraulic diameters 0.17, 0.48 and 0.54 in.

They reported excellent results on surface boiling with quantitative relations among heat flux density, temperature difference, pressure, degree of subcooling, water velocity and geometry of the flow path; pressures ranged from 30 to 90 psia and the degree of subcooling from 20 to 150°F, while the velocity was varied from 1 to 12 ft/sec. They correlated their data for boiling and wire burnouts by the dimensional equations:

$$q'' = C(\Delta t_{sat})^{3.86} \tag{2}$$

$$q''_{BO} = (400{,}000 + 4800 \cdot \Delta t_{sub})\, V^{1/3} \tag{3}$$

where V is velocity in ft/sec.

Kreith and Summerfield (13) investigated heat transfer to subcooled distilled water from both horizontal and vertical, Type 304 stainless steel tubes, 1/2 in. in diameter, and 17 and 38 in. in length, heated with alternating current. The inner tube wall temperature was calculated from heat flux density and the outer wall temperature recorded using 0.005-in. OD iron-constantan thermocouples spot-welded on the surface.

They plotted their results for the vertical tube in the usual manner, with heat flux density q'' versus temperature excess Δt_{sat} and with curves for several pressures ranging from 16 to 200 psia. Each curve for a given pressure showed a gradual transition. This shifting was attributed to the effect of total pressure because a constant degree of subcooling was not maintained.

Comparison of forced-convection heat transfer with and without surface boiling was also made for velocities in the range of 6 to 12 ft/sec and pressures of 30, 100, and 200 psia. Under non-boiling conditions the data were closely correlated by the equation of Dittus and Boelter (14). Under surface-boiling conditions, a large increase in heat flux only resulted in a minor increase in wall temperature. At the same pressure the curve of high velocity shifted toward that of low velocity.

The velocity employed in this study ranged from 6 to 13 ft/sec and maximum heat flux obtained was 1,450,000 B/hr ft^2. Burnout data were reported only for one run.

Gunther (15) studied surface-boiling with high-speed photography (up to 20,000 frames per second) by circulating degassed, distilled water through a transparent channel of rectangular cross-section, 3/16-in. by 1/2-in. by 6 in. A 1/8-in. wide by 0.004-in. thick metal strip was suspended lengthwise to divide the channel into two passages; it was heated with direct current. The pictures showed that with low degrees of liquid subcooling the bubbles detached from the surface and condensed in the stream but at high degrees of liquid subcooling, they remained attached to the surface growing and collapsing.

He also showed that the essential feature of bubble formation in nucleate boiling was the intense oscillation in the laminar sublayer immediately next to the heater surface induced by the growth and collapse. The bubble growth and collapse caused an agitation which effectively destroyed the laminar sublayer with a resulting increase in heat transfer.

He also correlated, within a maximum deviation of 27 per cent, the results of thirty-eight experiments on burnout, with pressures ranging from 14.7 to 164 psia, velocities from 5 to 40 ft/sec, degree of subcooling from 22 to 282 F and heat flux densities from 420,000 to 11,400,000 B/hr ft^2. The correlating equation was as follows:

$$q''_{BO} = 7000\ V^{1/2}\ \Delta t_{sub} \qquad (4)$$

Buchberg and co-workers (16) employed upward vertical flow of subcooled de-aerated and degassed, distilled water through the inside of a 1/4-in. OD by 25-in. long Type 347 stainless steel tube heated with direct current. The inner wall temperature was calculated from heat energy dissipated, thermal conductivity of the tube, and temperature recorded by Chromel-Alumel thermocouples spot-welded on the outer surface. The

variables ranged with pressure up to 2500 psia, mass velocity up to 770,000 lb/hr ft^2, water temperature up to 650°F and heat flux density up to 3,800,000 B/hr ft^2.

Their results for non-boiling heat transfer could be correlated within 12 per cent using the equation of Colburn (17).

They found that the inner wall temperature was independent of mass velocity and heat flux for pressures above approximately 1000 psia, but a trend indicating a small increase in surface temperature with increasing heat flux was observed for pressures below 1000 psia. The presence of nitrogen in the water (up to 900 cc/liter at 2000 psia and 110 cc/liter at 500 psia) was found to have no significant effect on tube wall temperature during fully established surface boiling.

A correlation for burnout was also reported,

$$q''_{BO} = 520\ G^{0.5}\ (\Delta t_{sub})^{0.2} \qquad (5)$$

Similar to the work reported by Buchberg, et al (16), Rohsenow and Clark (18) also employed upward flow of de-aerated, distilled water through a 0.1805-in. ID by 9.4-in. long nickel tube heated with direct current. Variables in their study covered heat flux up to 3,500,000 B/hr ft^2, inlet velocities up to 30 ft/sec, pressures up to 2000 psia and liquid subcooling between 50°F and 250°F. The temperature of the inner tube wall was calculated from measurements of the outer wall temperature, the electric current and the geometrical and physical properties of the nickel tube. The outer wall temperature of the tube was measured by Chromel-constanten thermocouples wrapped around and electrically insulated from the tube wall by a small sheet of 0.0015-in. thick mica. Guard heaters

were also provided to ascertain the true tube wall temperature recorded by the thermocouples.

The correlation of their results of non-boiling heat transfer was below Colburn's equation (17) by about 17 per cent. In boiling region they reported that at higher pressures less wall superheat existed at a given rate of heat transfer, and at higher heat transfer rates decreased the effect of velocity which were reported by previous investigators (10,12,13).

Jens and Lottes (19) summarized the work reported by Buchberg, et al (16) and Rohsenow and Clark (18) on surface boiling of water flowing upward in a vertical electrically heated tube of stainless steel and nickel. The data were correlated by the dimensional equation:

$$t_{sat} = \frac{1.9(q'')^{1/4}}{e^{p/900}} \qquad (6)$$

where p is the absolute pressure in psia. The burnout heat flux was correlated within $\pm$ 25 per cent by the dimensional equation:

$$q''_{BO} \times 10^{-6} = C \left[\frac{G}{10^{-6}}\right]^{m} (\Delta t_{sub})^{0.22} \qquad (7)$$

As pressure increased from 1000 to 2000 psia the average value of C decreased from 0.76 to 0.50 and m increased from 0.27 to 0.50.

Lowdermilk and co-workers (20) studied burnout heat transfer by employing upward flow of distilled water through 0.12, 0.067, and 0.040-in. ID stainless steel tubes heated with alternating current. Measurements were made for ranges of velocities from 0.1 to 19 ft/sec, pressures from atmospheric to 2000 psia, length diameter ratio of 25, 37.5, and 50, inlet subcooling from zero to 400°F and maximum heat fluxes from 28,000 B/hr ft^2 to 6,110,000 B/hr ft^2, but no correlation was reported.

Dingee and co-workers (21) performed experimental study of burnout heat transfer to distilled water flowing in a rectangular Zircaloy channel, 0.087-in. by 1-in. in cross section and 12-1/16 in. long, heated with alternating current. The tests were performed at an ambient pressure of 2000 psia and at flow rates from about 200,000 lb/hr ft^2 to 500,000 lb/hr ft^2. Qualitative burnout data were obtained for two inlet subcoolings, 10 and 60°F. Maximum heat flux obtained was 643,000 B/hr ft^2. No correlation was reported.

CHAPTER II

SUMMARY OF RESULTS

The experimental work reported herein covers the results of forced-convection non-boiling and surface-boiling heat transfer, heat flux at burnout, and qualitative results of some photographic studies. The principal results are summarized below according to the above classifications.

It may be only mentioned here that surface temperatures of the heated wire were measured with thermocouples carefully silver-soldered to the wire surface, and the observed temperatures were corrected for the error due to conduction. Details of the technique as well as other discussion relating to temperature measurement of the wire are presented later.

Forced-convection Non-boiling Heat Transfer Results

The results of non-boiling heat transfer from heated wires under normal flow obtained at different heat flux densities, namely, 0.0860 x 10^6, 0.1383 x 10^6, and 0.1786 x 10^6 B/hr ft^2, each for velocities of 1, 2, 3, 4, 5, and 6.8 ft/sec and at constant water temperature of 85°F, are listed in Test No. 1, Appendix E. They are plotted in Fig. 1 with heat flux q'' as a function of the difference between the surface temperature and the bulk water temperature $(t_s - t_w)$.

Figure 1 shows clearly the proportionality between log q'' and log $(t_s - t_w)$ for any given fluid velocity under non-boiling conditions. The slopes of the representative lines, drawn through the data for each velocity, range from just about unity at a flow velocity of 6.8 ft/sec to approximately 1.25 for a flow velocity of 1 ft/sec, increasing

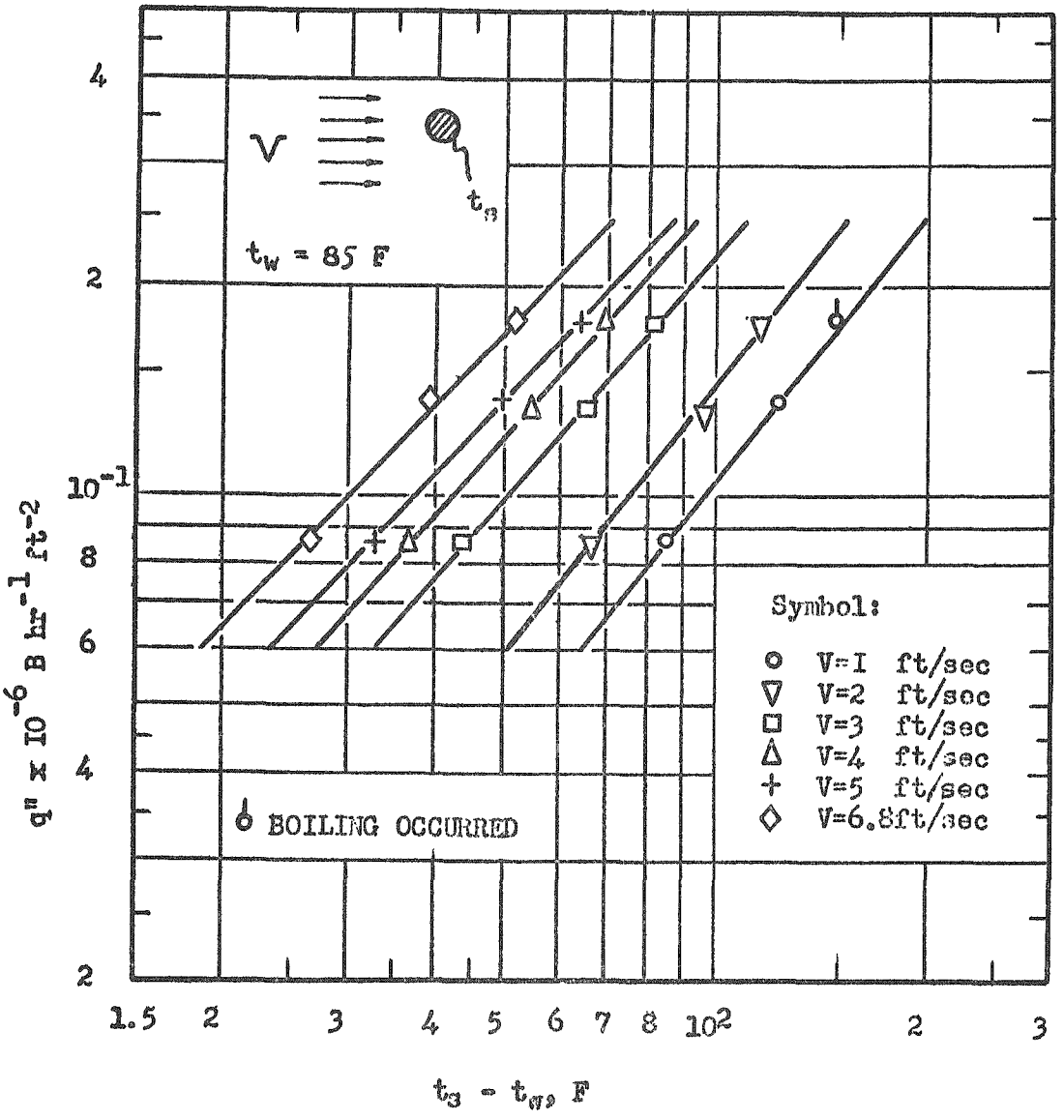

Fig. 1 Heat Flux versus Temperature Difference of Non-Boiling Heat Transfer

progressively with decreasing flow speed. At the lowest speeds, and particularly at 1 ft/sec, the dependence of the heat flux rate q' on about the 1.25 power of the temperature difference between the surface and the bulk water suggests some influence of free convection effects considering that the coefficient of convective heat transfer is seen to depend on about the one fourth power of the temperature difference (see Discussion, Chapter IV).

The results correlated employing the method of averages (22), are shown in Table 1 and they are plotted in Fig. 7. Table 1 shows maximum deviation of 7.5 per cent and an average deviation of 1.9 per cent from the correlating line. The correlation in non dimensional form and valid for Reynolds numbers between 1500 and 11,000, is given by the following equations:

$$N_{Nu} = f\left(N_{Pr}^{0.6}\right) \quad \text{or} \quad N_{Nu} = \Phi\left(N_{Re}\right) \cdot N_{Pr}^{0.6} \qquad (8.$$

where Φ stands for "function of".

Results obtained on heat transfer characteristics of the boiling heat transfer from single cylinders using water and liquid nitrogen cold in cross flow are summarized by McAdams (23) in the form of empirical correlation for Reynolds numbers between 150 and 2500:

$$N_{Nu} = f\left(N_{Pr,f}^{1/3}\right) = 0.683\, N_{Re}^{0.466} \cdot N_{Pr}^{1/3} \qquad (9.$$

Both Equations (8) and (9) along with an extrapolation (dotted line), are plotted in Fig. 7 for comparison. In addition to the known correlation for liquids introduced above the well-established correlation for air in normal flow over cylinders representing results of many investigators and presented by McAdams (23), has been modified by the introduction of $N_{Pr,f}^{0.6}$

Table 1 Results of Forced-Convection Non-Boiling Heat Transfer

p_{atm} = 29.48 in. Hg, t_w = 85°F, t_{rm} = 76°F

Run No.	p_{abs}	q'' ($\times 10^{-6}$)	t_s	V	$\frac{\rho_f VD}{\mu_f}$	$\left(\frac{N_{Nu,f}}{N_{Pr,f}^{0.3}}\right)_{exp}$	$\left(\frac{N_{Nu,f}}{N_{Pr,f}^{0.3}}\right)^{*}_{corr}$	Deviation**
	in.Hg	$\frac{B}{hr\ ft^2}$	°F	ft/sec	—	—	—	%
1	37.72	0.0860	169.6	1	1655	19.3	19.3	0
2	40.07	"	151.1	2	3310	30.0	30.5	+ 0.6
3	44.67	"	128.5	3	4550	37.1	37.6	+ 1.0
4	47.97	"	121.4	4	59.10	44.0	44.7	+ 1.5
5	53.97	"	117.9	5	7480	48.5	52.2	+ 7.6
6	61.97	"	111.4	6.8	9300	59.6	60.3	+ 1.1
7	37.72	0.1364	207.2	1	2085	22.7	22.5	- 0.9
8	40.07	0.1348	179.3	2	37.20	32.2	33.2	+ 0
9	44.67	"	150.8	3	4970	39.6	39.8	+ 0.5
10	47.97	"	139.2	4	6310	45.8	46.7	+ 1.9
11	53.97	0.1383	134.5	5	7740	53.2	53.4	+ 0.4
12	61.97	"	123.9	6.8	11120	64.8	67.8	+ 4.6
13	37.72	0.1786	231.9	1	←—Boiling occurred—→			-
14	40.07	"	198.1	2	4100	35.6	35.1	- 1.4
15	44.67	"	165.6	3	5350	39.5	41.9	+ 6.1
16	47.97	"	153.7	4	6880	49.7	49.5	- 0.4
17	53.97	"	149.0	5	8300	53.6	55.9	+ 4.3
18	61.97	"	136.5	6.8	10750	66.0	66.4	- 0.6
							Average	1.9

$N_{Nu,f} = hD/k_f$; $N_{Pr,f} = \mu_f C_p/k_f$; $N_{Re,f} = \rho_f VD/\mu_f$.

*Calculated from Equation (8).

**Based on experiment.

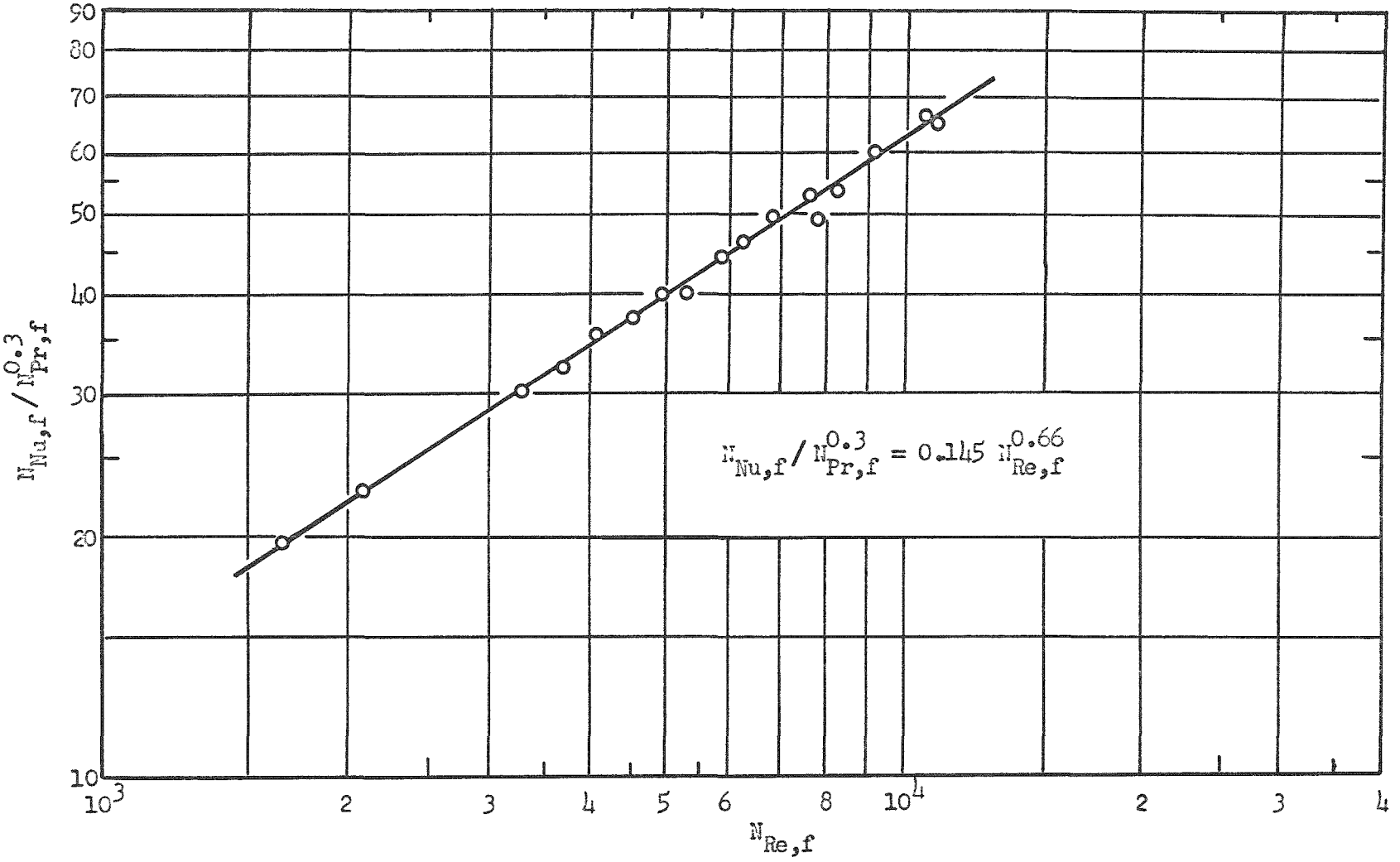

Fig. 2 Correlation of Non-Boiling Heat Transfer Data

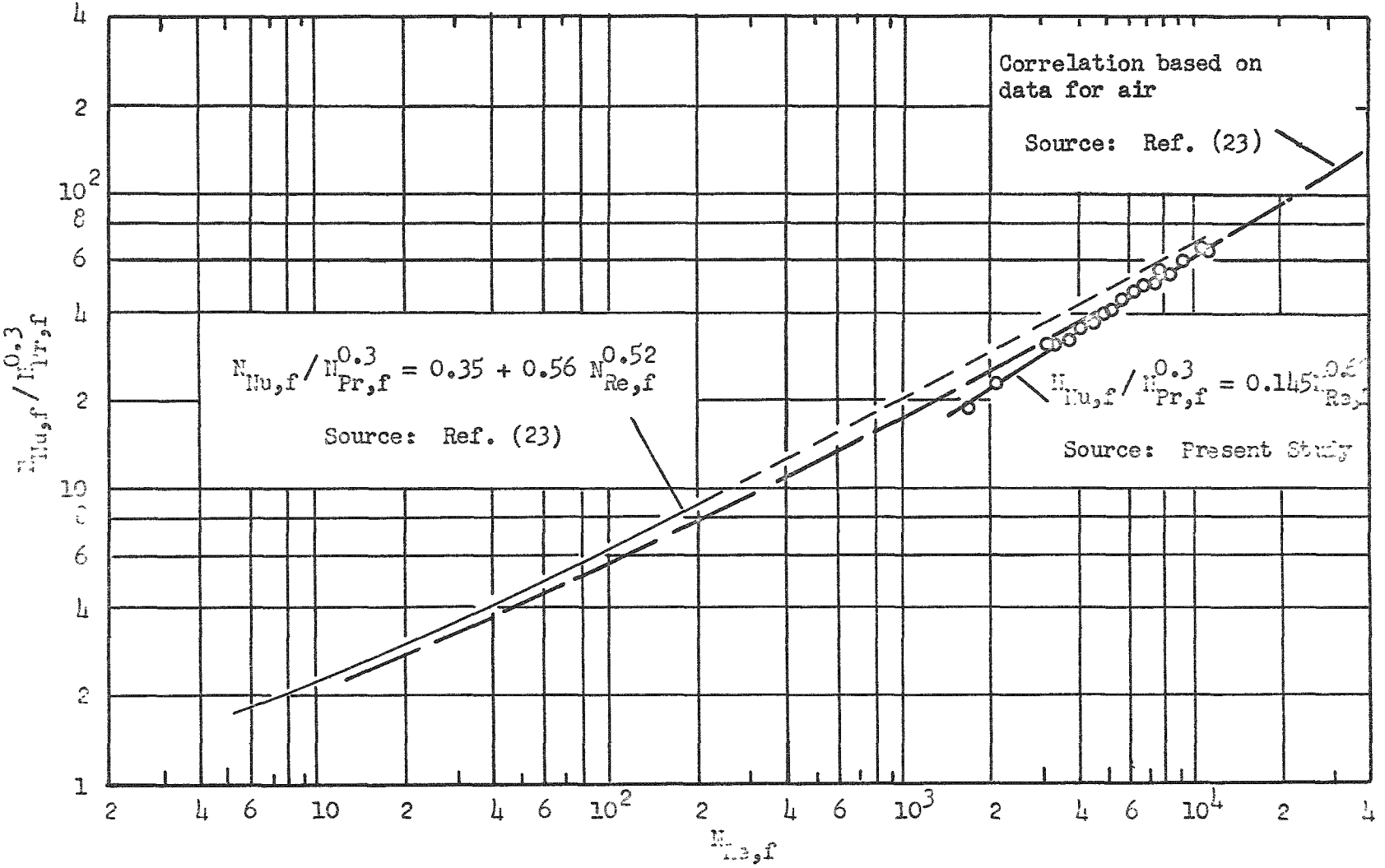

Fig. 3 Comparison of Non-Boiling Heat Transfer Correlations

to represent fluids in general, and its more general form is plotted in Fig. 3 to provide additional basis for comparison. It also provides a rather good check on the extrapolation of the correlation for liquids into a flow regime in which apparently no data have heretofore been available for liquids.

Forced-Convection Surface-Boiling Heat Transfer

In order to isolate any possibilities of error in temperature measurement it is usual and, in fact, good practice to plot heat flux density q'' versus temperature difference $(t_s - t_w)$ rather than heat transfer coefficient versus temperature difference. All of the boiling data have been plotted in this way.

Figures 4 through 9 show the effect of subcooling on boiling at velocities ranging from 1 to 6.8 ft/sec. Boiling curves for a given velocity and for 80 F and 140 F subcooling are plotted in each figure. It may be observed at this point that the boiling curve at 80 F subcooling tends to merge with that at 140 F subcooling, as heat flux increases.

Theoretically speaking, boiling would commence when the temperature of the heater surface reaches the saturation temperature corresponding to the prevailing static pressure p_o in the test section.[1] It can be seen in Fig. 4 through 9 that all the boiling curves inflect upward at, or in the vicinity of, the degree of subcooling. It seems in agreement with the

---

[1] Neglecting, in first approximation, the variation of total pressure p over the cylinder which, expressed in terms of pressure excess above the prevailing static pressure p_o, starts with a value of $(p - p_o)/(\rho V^2/2) = 1$ at the forward stagnation, decreases to zero at approximately 40° from the leading edge, takes on negative values (approximately -1) between about 60° and 300°, and then increases again to $+1$ at 360°. Local saturation temperature around the cylindrical profile of the test rods is not considered quantitatively.

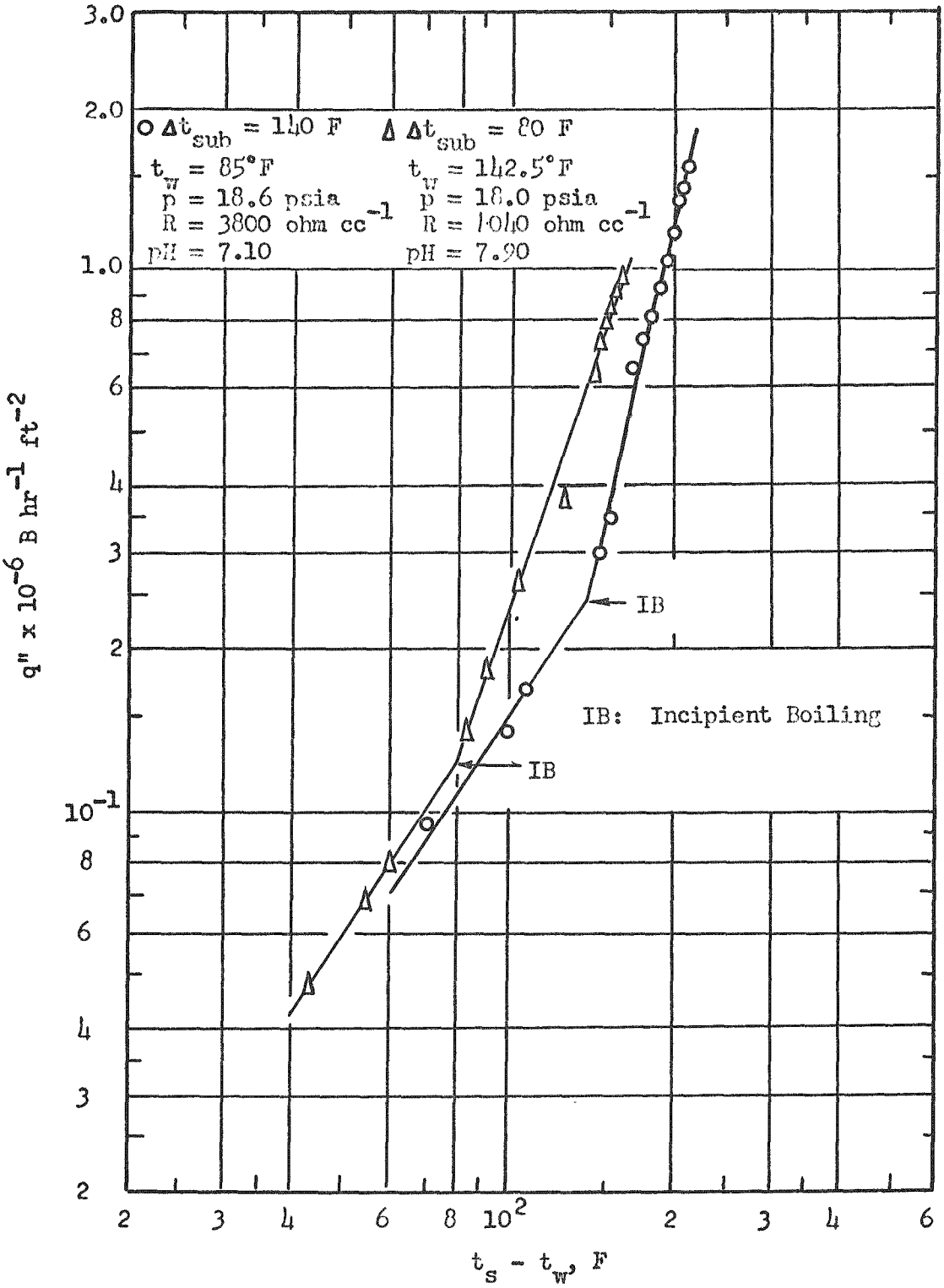

Fig. 4 Effect of Subcooling on Boiling at Velocity 1 ft/sec

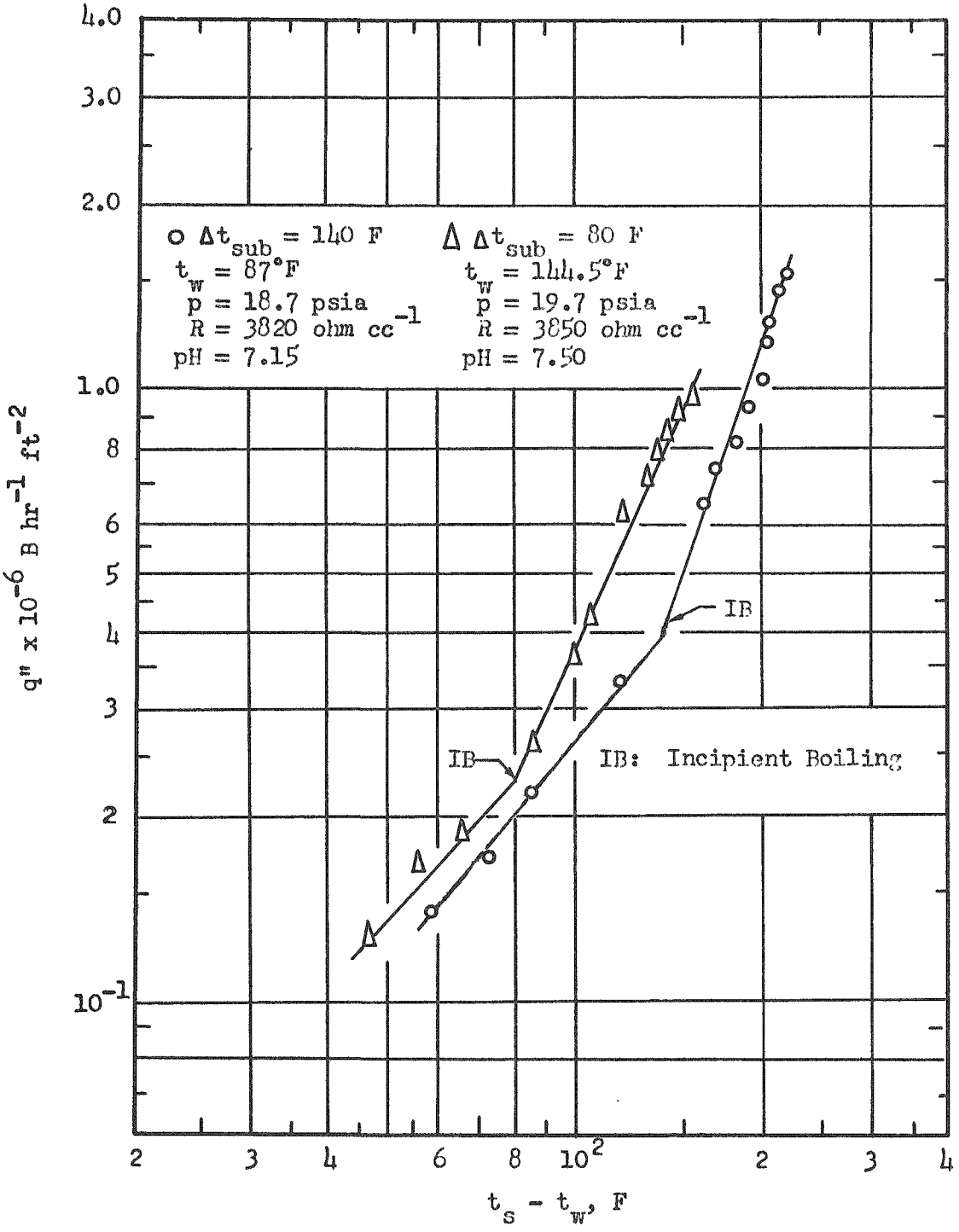

Fig. 5 Effect of Subcooling on Boiling at Velocity 2 ft/sec

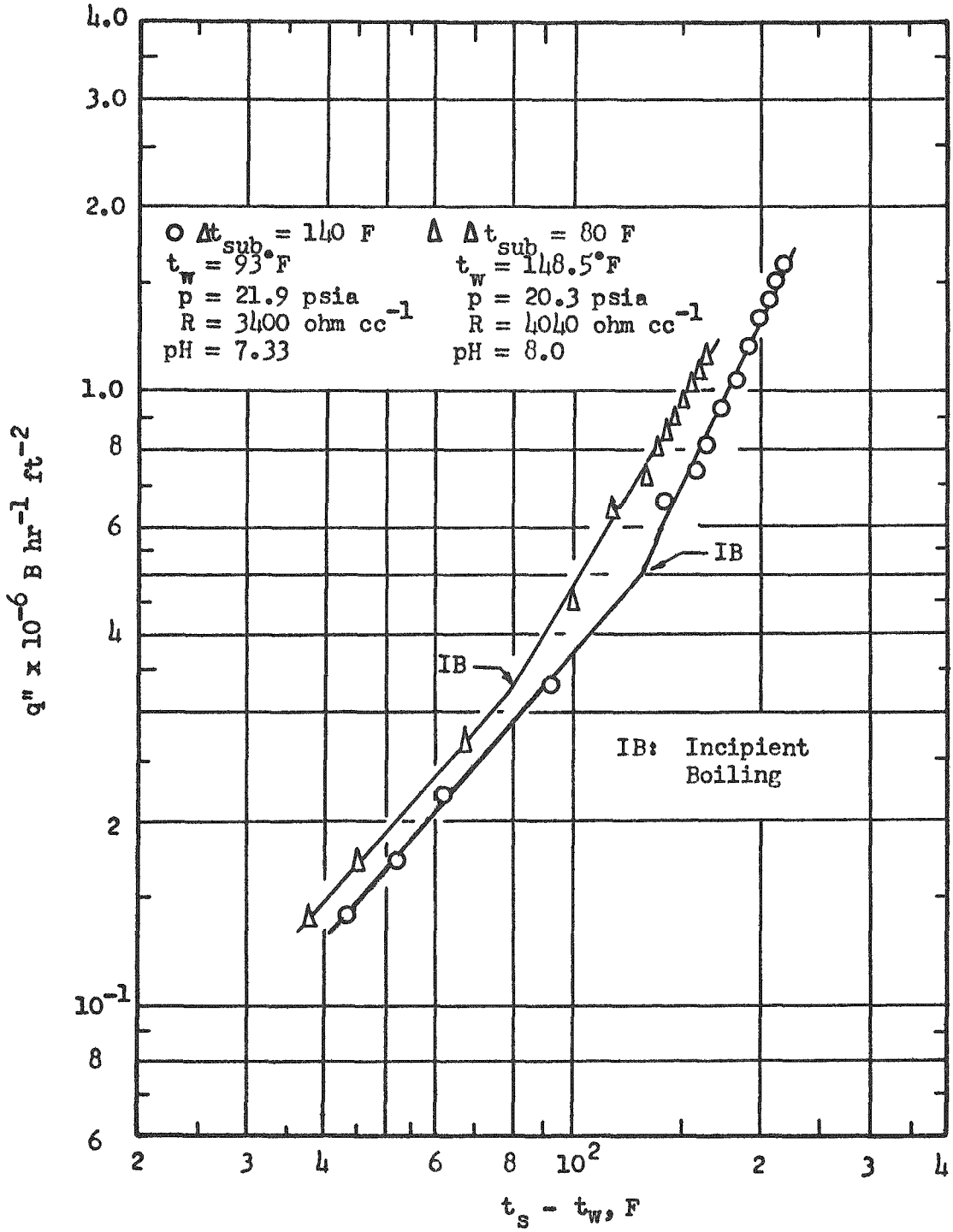

Fig. 6 Effect of Subcooling on Boiling at Velocity 3 ft/sec

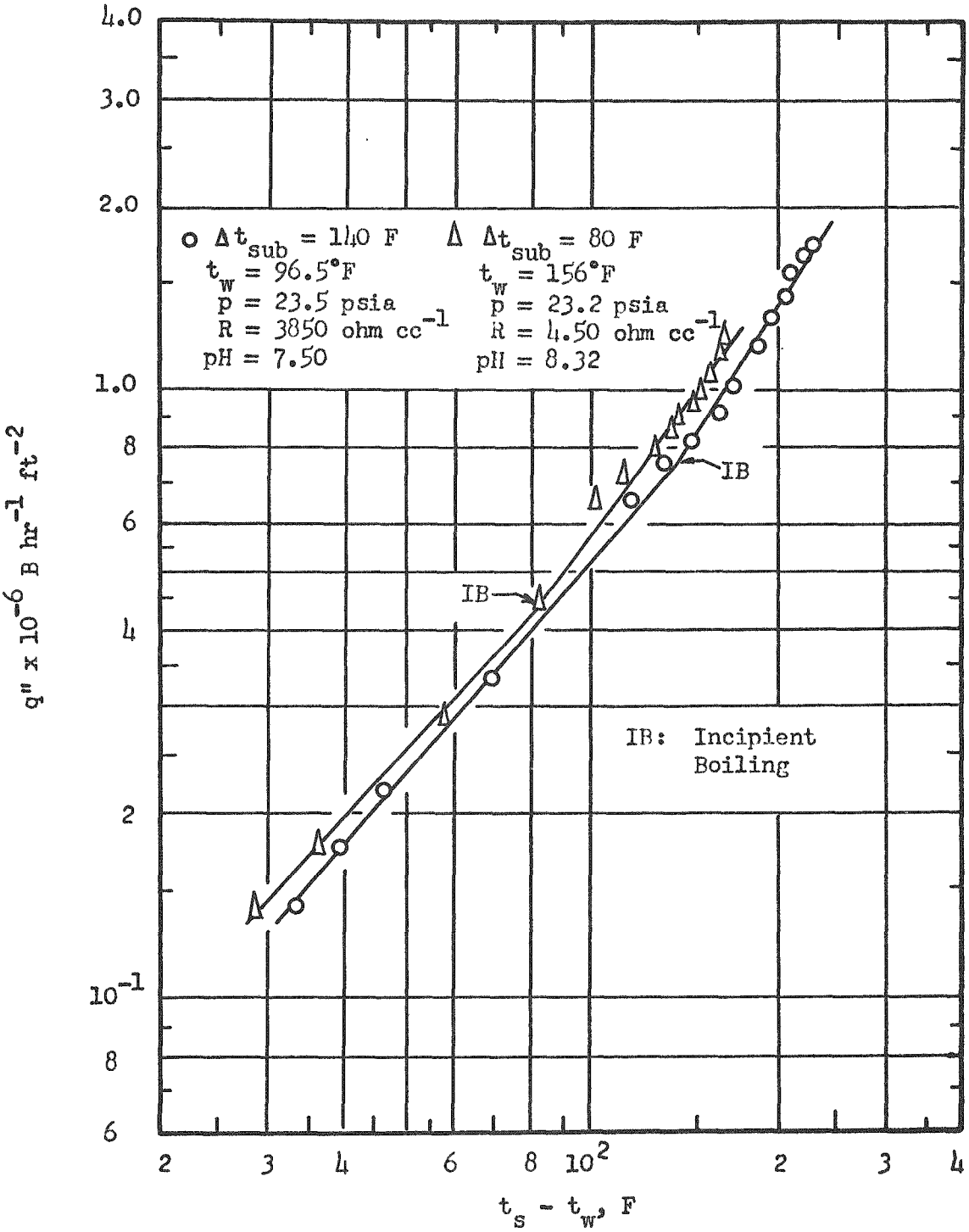

Fig. 7 Effect of Subcooling on Boiling at Velocity 4 ft/sec

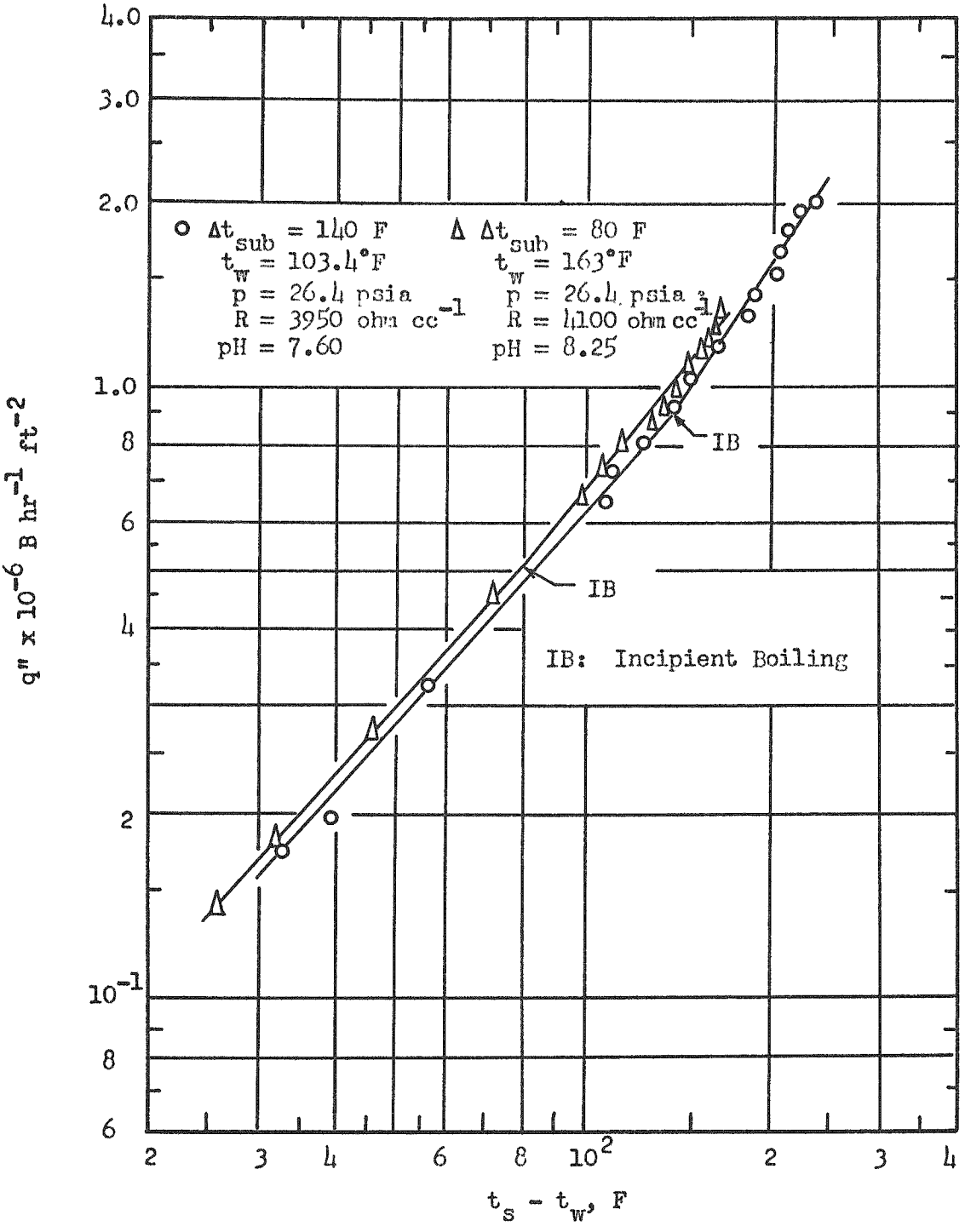

Fig. 8 Effect of Subcooling on Boiling at Velocity 5 ft/sec

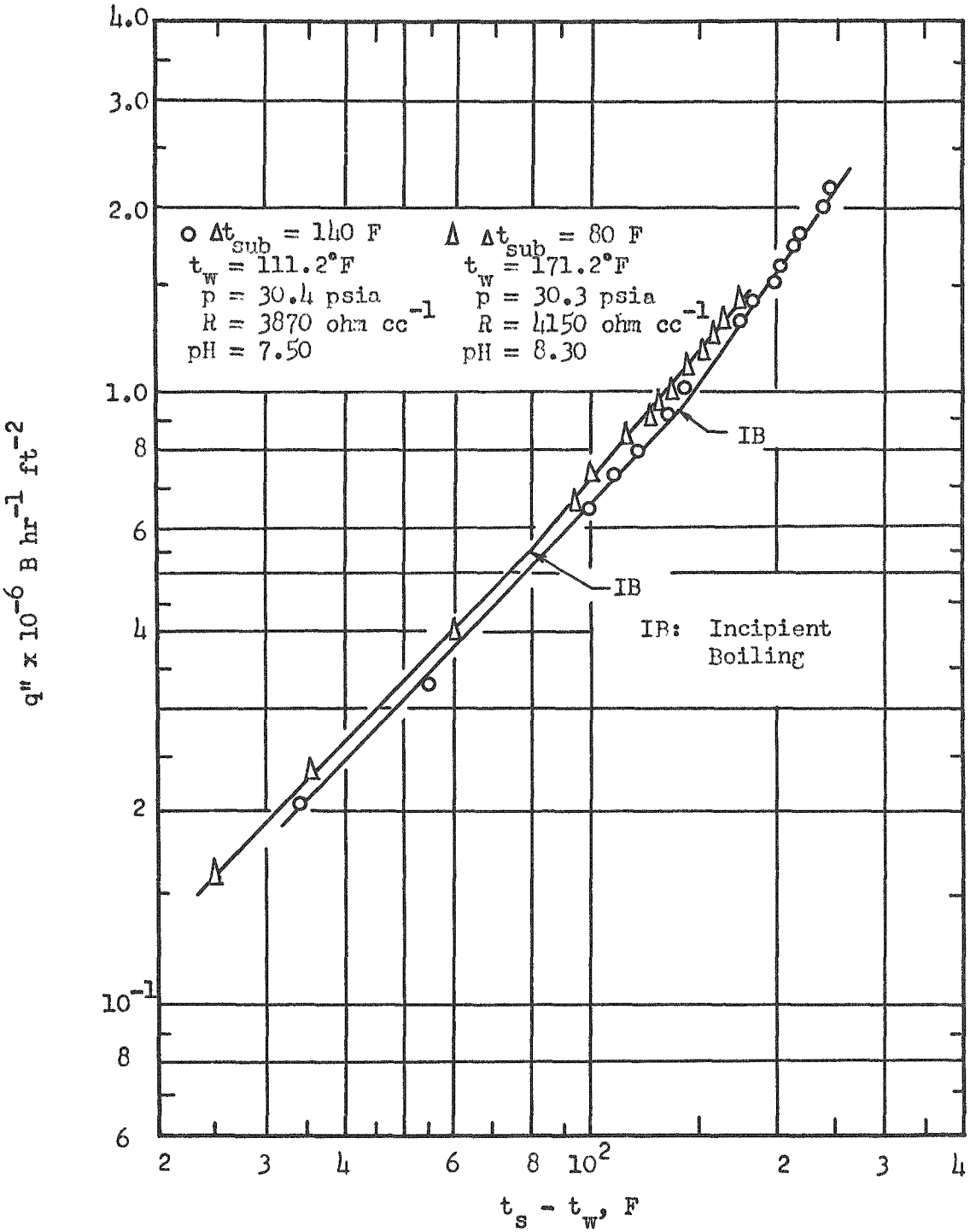

Fig. 9 Effect of Subcooling on Boiling at Velocity 6.8 ft/sec

theory and the effect of superheating at the surface does not seem pronounced, under the prevailing conditions.

Figures 10 and 11 show the effect of velocity on boiling at values of subcooling of 140 F and 80 F, respectively. For the same subcooling, boiling commences at higher heat flux density as velocity becomes higher. All boiling curves tend to merge together as heat flux increases.

Figure 12 is a plot of heat flux density versus temperature excess for velocities ranging from 1 to 6.8 ft/sec, and subcooling of 140 F and 80 F. All twelve curves tend to converge to a zone where boiling is vigorous, or fully established. In this zone the temperature excess $(t_s - t_{sat})$ is comparatively insensitive to heat flux density, velocity and the degree of subcooling.

Burnout

A summary of the results of the burnout experiments are shown in Table 2. Owing to the lack of complete and detailed understanding of various factors involved and the role they play at burnout conditions, such as the effect of surface condition, the role of fluid properties and other variables, the burnout results are correlated in a dimensional equation. This correlation, carried out by first plotting the heat flux density at burnout q''_{BO} against degrees of subcooling Δt_{sub} and then drawing correlating lines through each set of data representing a given mainstream velocity, yielded slopes of approximately 0.78. When heat flux densities q''_{BO} were plotted against mass flow rates given by $G/10^6$ lines at a slope of approximately 0.18 were found to represent the data.

A somewhat better correlation was found as heat flux at burnout q''_{BO} varying with $(\frac{G}{10^6})^{0.2} (\Delta t_{sub})^{0.8}$. The results were finally correlated

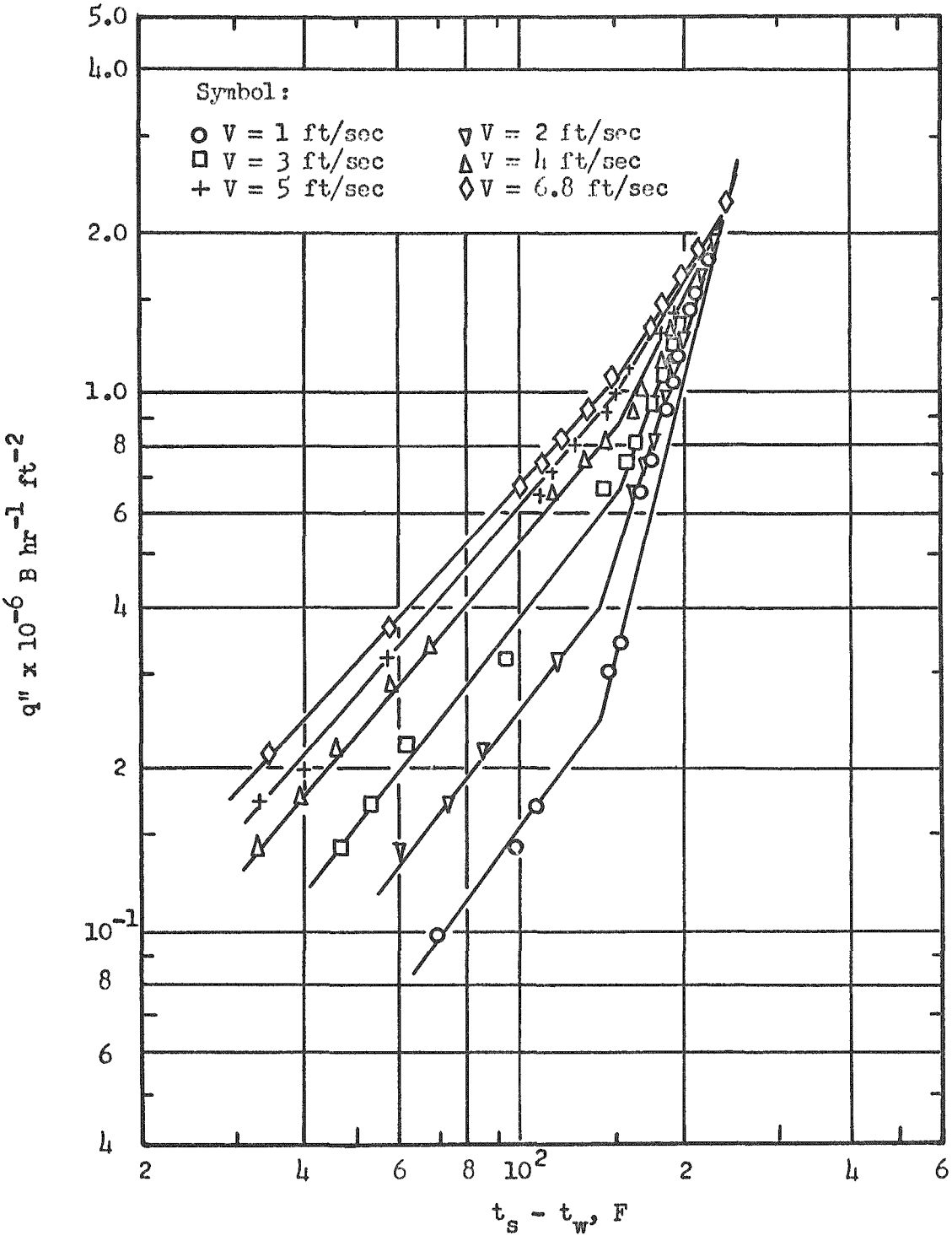

Fig. 10 Effect of Velocity on Boiling at Degree of Subcooling 140 F

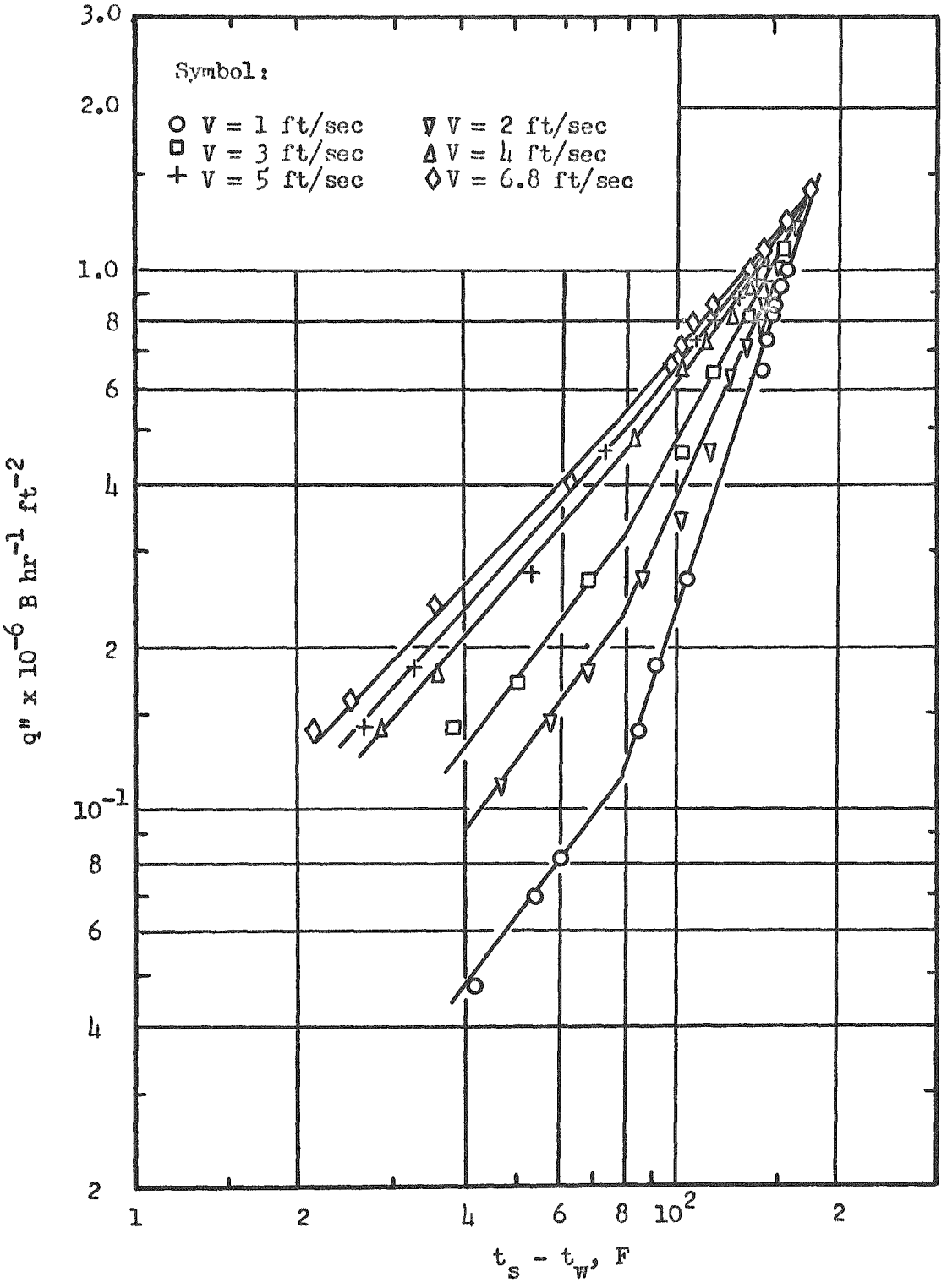

Fig. 11 Effect of Velocity on Boiling at Degree of Subcooling 80 F

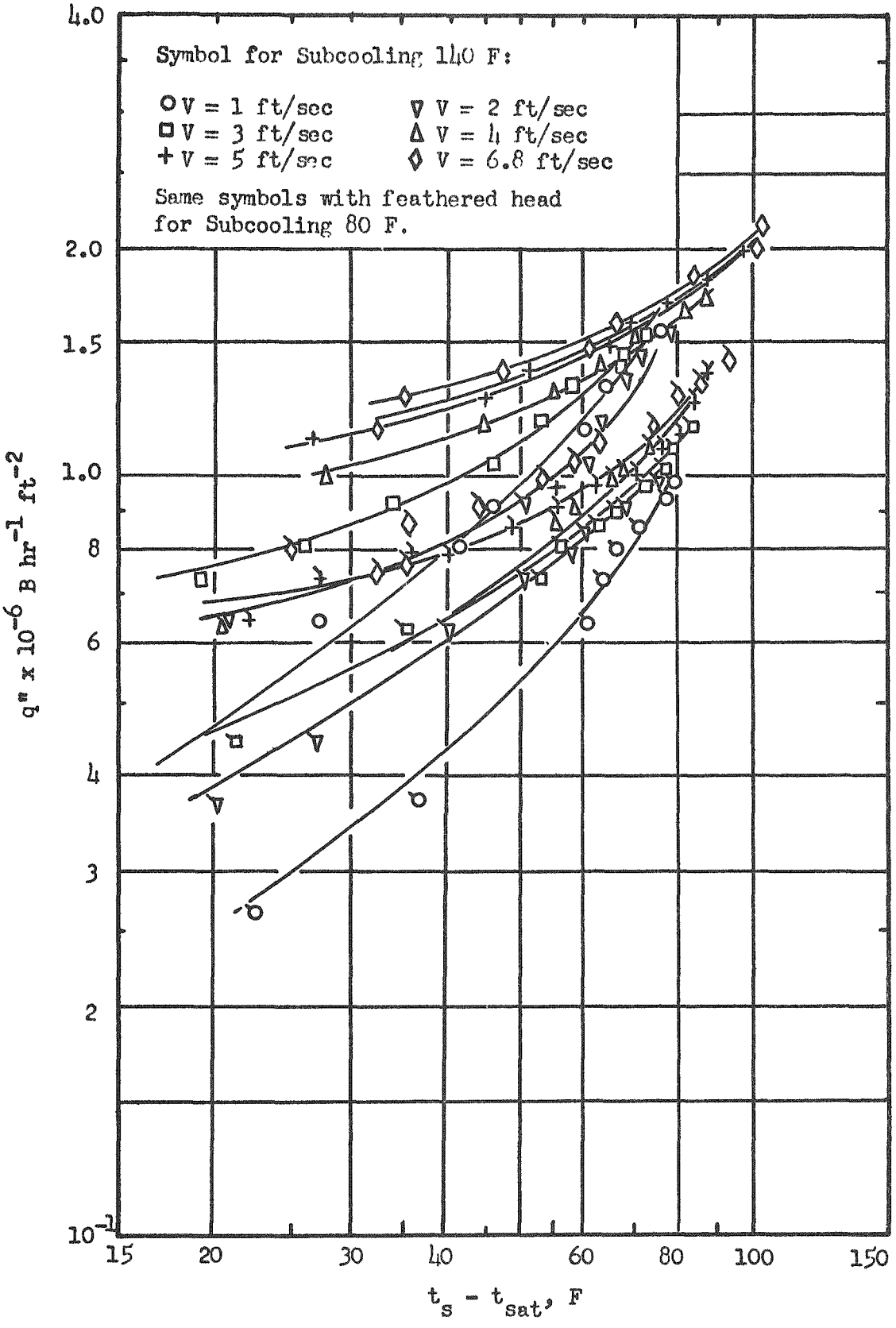

Fig. 12 Heat Flux Density q" versus Temperature Excess $(t_s - t_{sat})$

Table 2 Burnout Test Results

Run No.	Velocity V ft/sec	p_{abs} in.Hg	t_w °F	Δt_{sub} F	G x 10^{-6} $\frac{lb_m}{hr\ ft^2}$	$(q''_{BO})_{exp}$ x 10^{-6} $\frac{B}{hr\ ft^2}$	$(q''_{BO})_{cal}$ x 10^{-6} $\frac{B}{hr\ ft^2}$	Deviation (based on experiment)
1	1	36.19	110.0	112.0	0.2229	1.9083	1.7206	- 9.8
2	2	38.79	109.0	116.5	0.4459	2.0307	2.0421	+ 0.5
3	2	39.03	109.9	116.1	0.4459	2.0309	2.0420	+ 0.5
4	3	42.58	110.8	119.2	0.6685	2.1339	2.2512	+ 5.5
5	4	47.76	112.7	123.8	0.8914	2.2107	2.4602	+11.2
6	5	54.76	97.0	147.5	1.1178	2.6009	2.9587	+13.6
7	6.8	60.78	127.9	122.1	1.5113	2.8071	2.7068	- 3.5
8	1	36.15	61.1	160.9	0.2247	2.5387	2.3262	- 9.3
9	2	38.40	57.0	168.0	0.4496	2.7577	2.7604	+ 0.1
10	3	42.12	56.5	173.2	0.6745	2.8386	3.0766	+ 8.6
11	4	47.74	64.1	172.2	0.8986	2.9320	3.2428	+10.6
12	5	53.73	69.2	173.7	1.1245	3.1161	3.3929	+ 8.9
13	6.8	61.60	52.1	198.9	1.5317	3.7502	4.0254	+ 7.8
14	1	35.53	141.3	79.7	0.2207	1.4227	1.3186	- 7.3
15	2	37.96	143.6	80.8	0.4414	1.5953	1.5383	- 3.5
16	3	41.42	140.2	88.5	0.6620	1.7429	1.7795	+ 2.1
17	4	46.78	146.0	89.3	0.8820	1.9571	1.8921	- 3.3
18	5	53.47	148.0	94.7	1.1016	2.0433	2.0797	+ 1.7
19	6.8	60.26	145.4	104.2	1.5028	2.2490	2.3852	+ 6.0
20	1	36.03	179.0	42.5	0.2190	0.8449	0.8737	+ 3.4
21	2	37.88	179.2	45.3	0.4359	0.9976	0.9594	- 3.8
22	3	41.25	173.5	55.2	0.6556	1.1585	1.2114	+ 4.5
23	4	46.65	175.5	59.7	0.8471	1.3460	1.3561	+ 0.7
24	5	52.70	178.1	64.1	1.0908	1.6028	1.5329	- 4.3
25	6	60.27	174.0	76.7	1.4859	1.8612	1.8546	- 0.3
26*	1	36.15	85.0	136.7	0.2239	1.8536	2.0261	+ 9.3
27*	3	41.85	85.0	144.4	0.6718	2.7440	2.6639	- 2.9
28*	5	54.44	85.0	158.8	1.1196	3.2864	3.1785	- 3.3
29**	2	38.32	85.0	139.8	0.4478	2.3851	2.3744	- 0.4
30**	4	47.66	85.0	151.3	0.8957	2.9222	2.9105	- 0.4
31**	6.8	61.40	85.0	165.5	1.5227	3.5404	3.4894	- 1.4
							Average	4.8

*Data were taken from simple matrices with Chromax wires as vertical elements (see Appendix B).

**Data were taken from simple matrices with Teflon rods as vertical elements (see Appendix B).

by the method of averages (22) with a maximum deviation of 13.6 per cent and an average deviation of 4.8 per cent and are expressed by the following equation:

$$q''_{BO} \times 10^{-6} = 0.0536 \left(\frac{G}{10^6}\right)^{0.2} (\Delta t_{sub})^{0.8} \qquad (10)$$

The experimental results and the correlating equation given above are shown in Fig. 13. Sample wires after burnout are shown in Fig. 14.

Table 3 shows the comparison of correlations of burnout proposed by investigators who employed different flow systems, heating surfaces, and ranges of variables.

The position of wire burnout along the length of the test wire is shown in Fig. 15 in which location is plotted for different mean flow velocities. The zero position on the abscissa represents the center of the test wire. Four individual burnouts are shown for each mean velocity, except for a velocity of 2 ft/sec where seven burnout runs were made. The randomness of the burnout position is evident, considering also the velocity distribution across the test section (ahead of the test wires) shown in Fig. 16.

Photographic Results

Employing a Fastax high-speed camera, fifteen reels of 16mm Kodak film were taken to record surface boiling phenomena at different heat flux densities and flow conditions. Representative pictures of typical bubble formation are shown in Fig. 17-A through -D.

Figures 17-A and 17-B are sequences of high-speed photographs taken under identical flow velocities of 4 ft/sec and for approximately the same heat fluxes, but with the degree of subcooling decreased from 160 F in

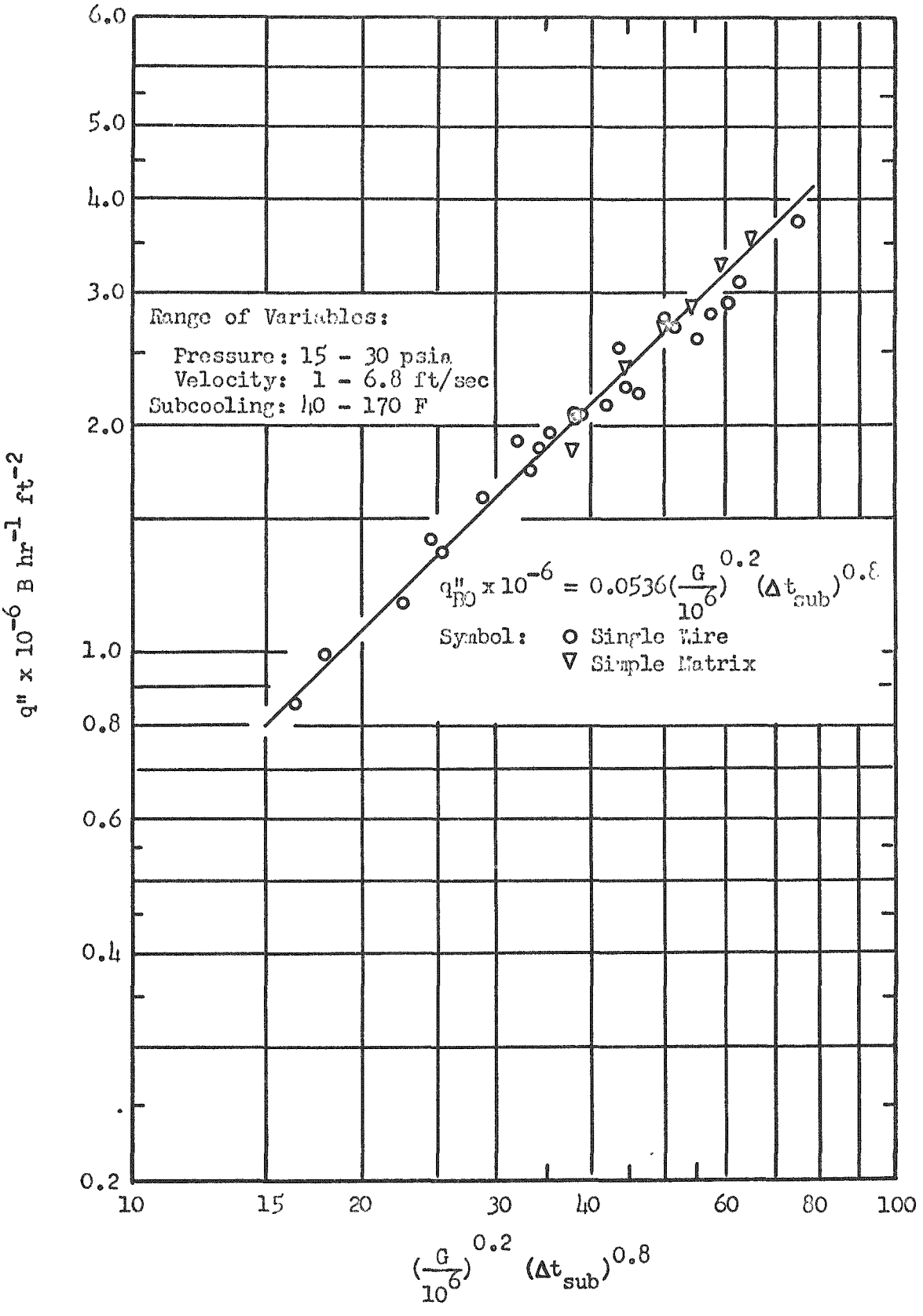

Fig. 13 Correlation of Burnout Data

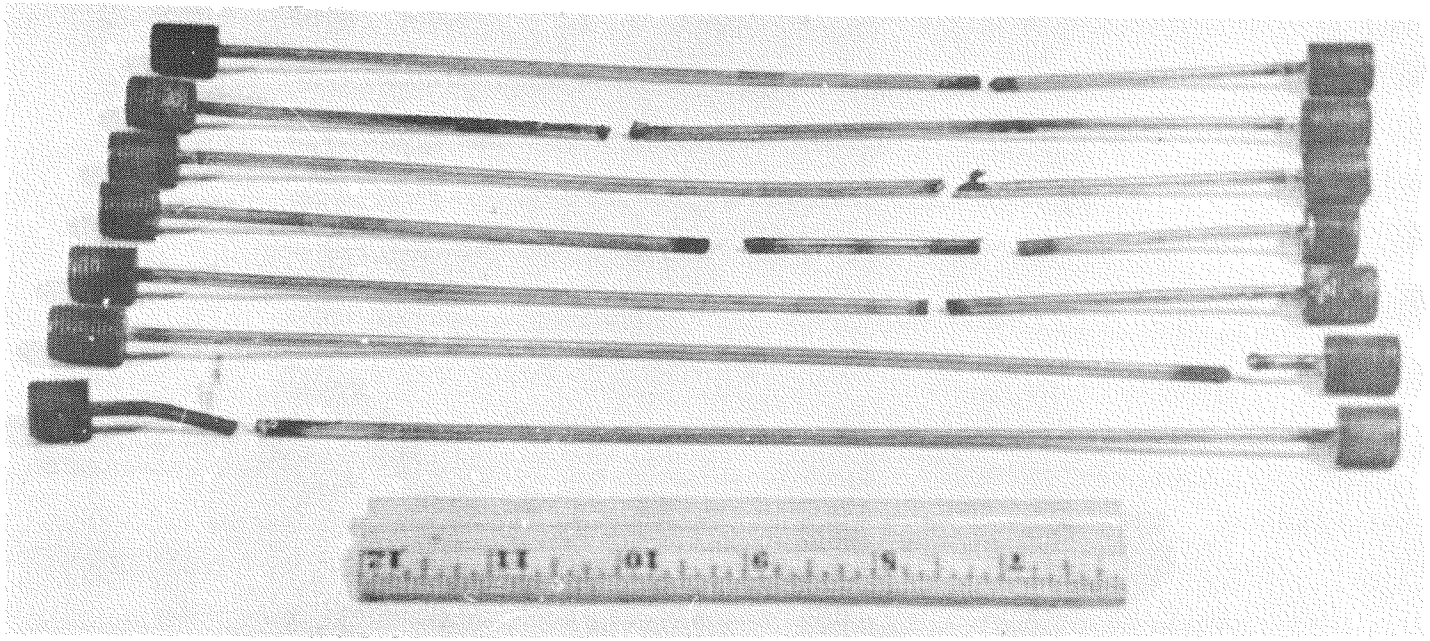

Fig. 14 Typical Wires after Burnout

Table 3 Comparison of Correlations of Forced-Convection Burnout

Equation	Source	Heated Surface	System of Flow	Range of Variables
1. $q''_{BO} \times 10^{-6} = 0.0536 \left(\frac{G}{10^6}\right)^{0.2} (\Delta t_{sub})^{0.8}$	Present Study	Chromax	Cross (Outside tube)	V: 1-6.8 ft/sec P: 15-30 psia Δt_{sub}: 40-170°F
2. $q''_{BO} = (400{,}000 + 4800\,\Delta t_{sub})\, V^{1/3}$	McAdams (12)	SS Tube	Annular	V: 1-12 ft/sec P: 30-90 psia Δt_{sub}: 20-100 F
3. $q''_{BO} = 7000\, V^{1/2}\, (\Delta t_{sub})$	Gunther (15)	Metal Strip	Channel	V: 5-30 ft/sec P: 500-2000 psia Δt_{sub}: 3-600 F
4. $q''_{BO} = 520\, G^{1/2}\, (\Delta t_{sub})^{0.2}$	Buchberg (16)	SS Tube	Inside Tube	V: 5-30 ft/sec P: 500-2000 psia Δt_{sub}: 3-600 F
5. $q''_{BO} \times 10^{6} = C \left(\frac{G}{10^6}\right)^{m} (\Delta t_{sub})^{0.22}$	Jens (19)	SS and Nickel Tube	Inside Tube	V: 5-30 ft/sec P: 500-2000 psia Δt_{sub}: 3-600 F

where C and m are constant depending on pressure P, as:

P psia	m	C
500	0.16	0.817
1000	0.28	0.626
2000	0.50	0.445

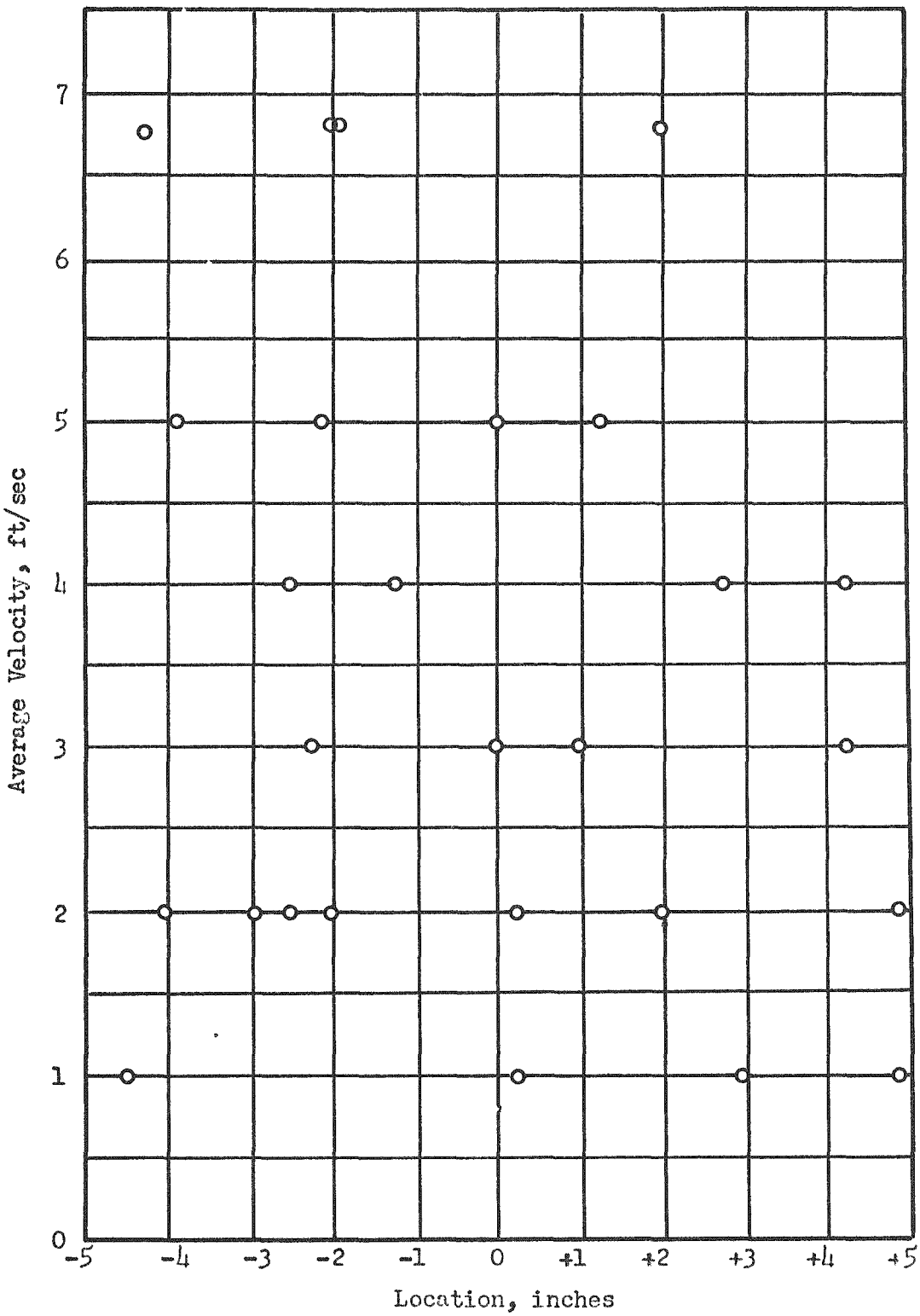

Fig. 15 Locations of Burnout

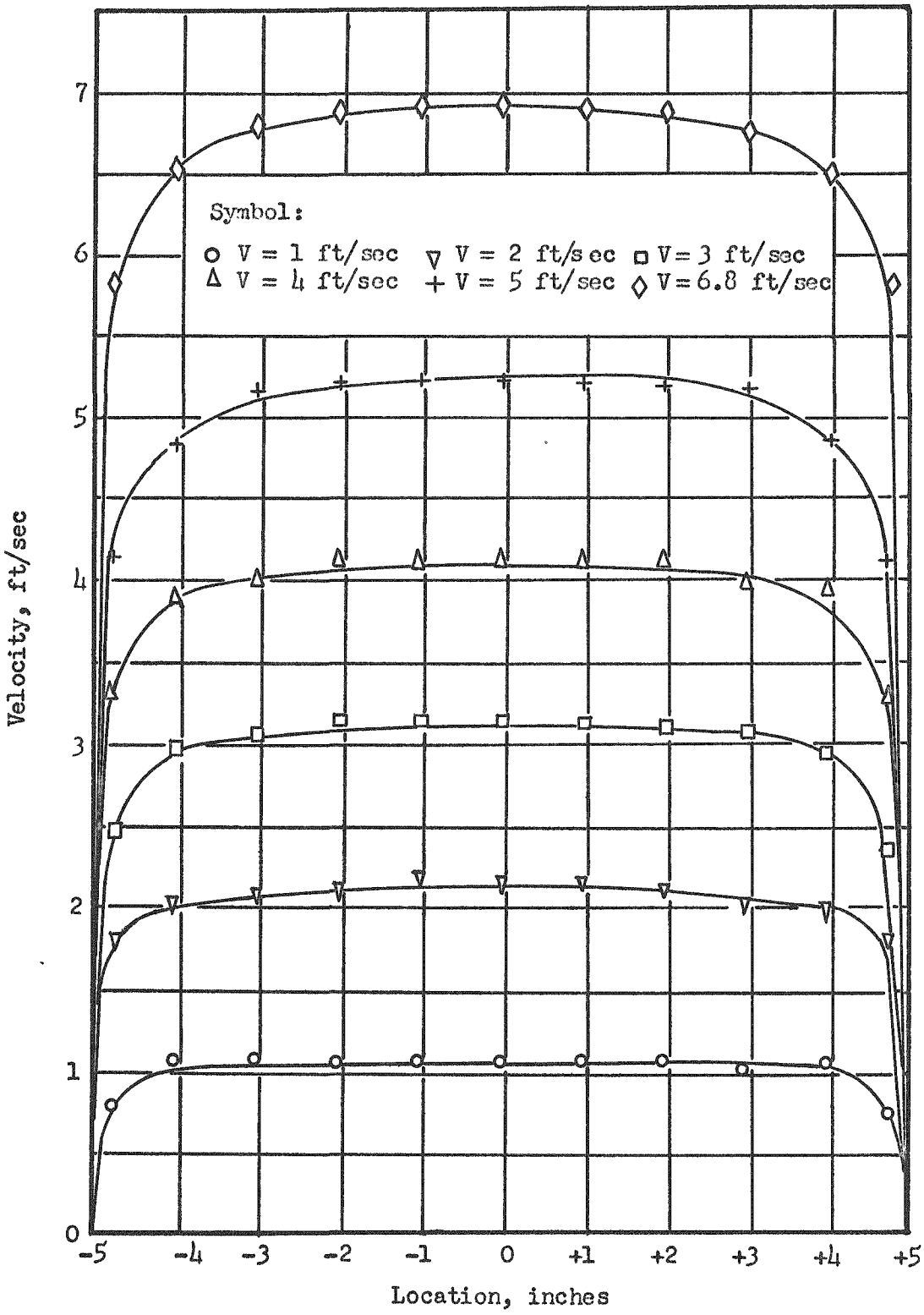

Fig. 16 Velocity Distribution across Test Section with 40-mesh Screen Upstream

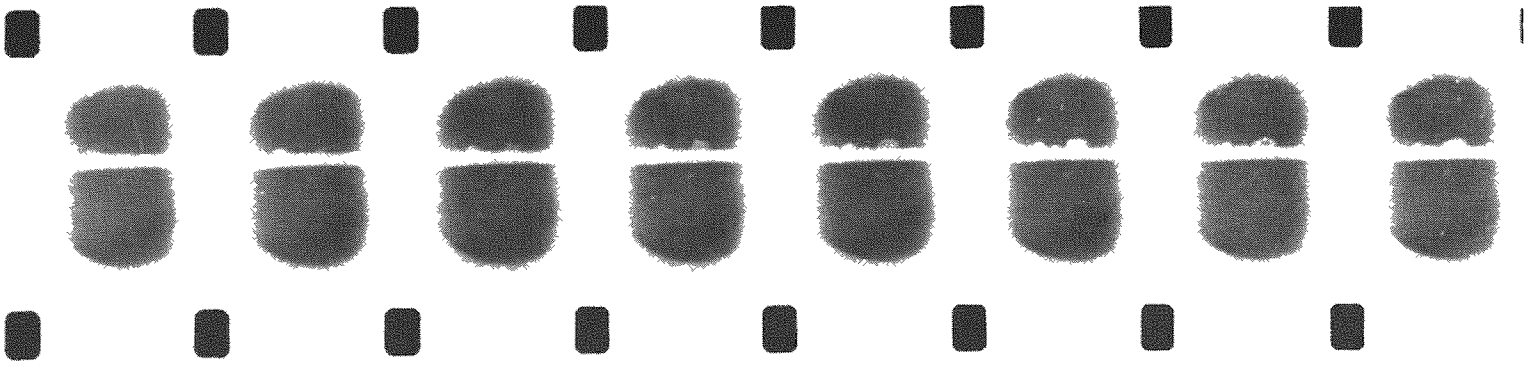

(A) Velocity: 4 ft/sec
Degree of Subcooling: 16OF

Heat Flux: 2.7 x 10^6 B/hr ft^2
Water Temperature 77° F

17-A

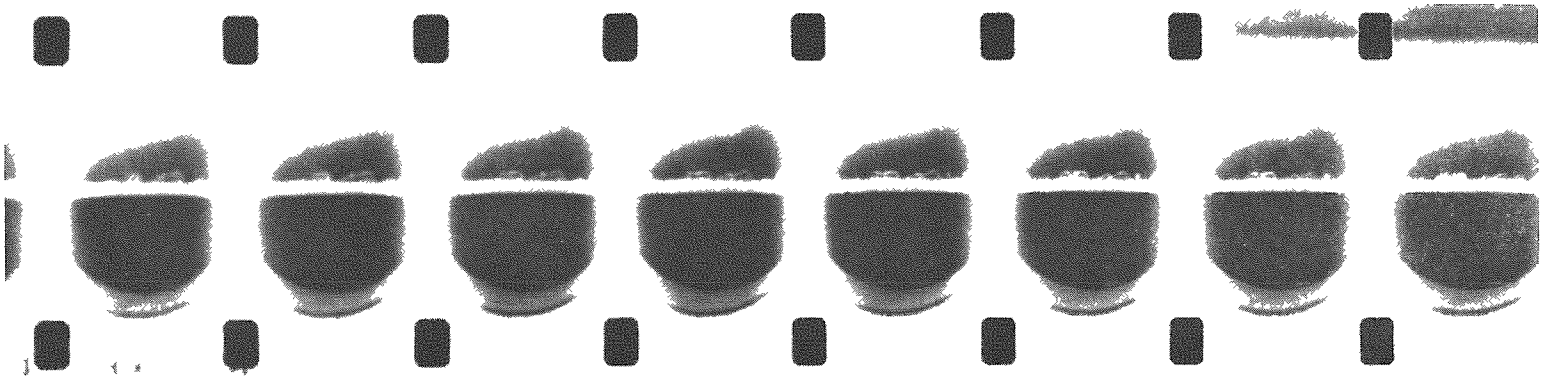

(B) Velocity: 4 ft/sec
Degree of Subcooling: 114 F

Heat Flux: 2.1x10^6 B/hr ft^2
Water Temperature: 120° F

17-B

Flow ↑ Direction

Fig. 17 (A&B) Typical Formation of Bubbles

Film Speed: 3250 frames/sec Film Sequence: From Left to Right

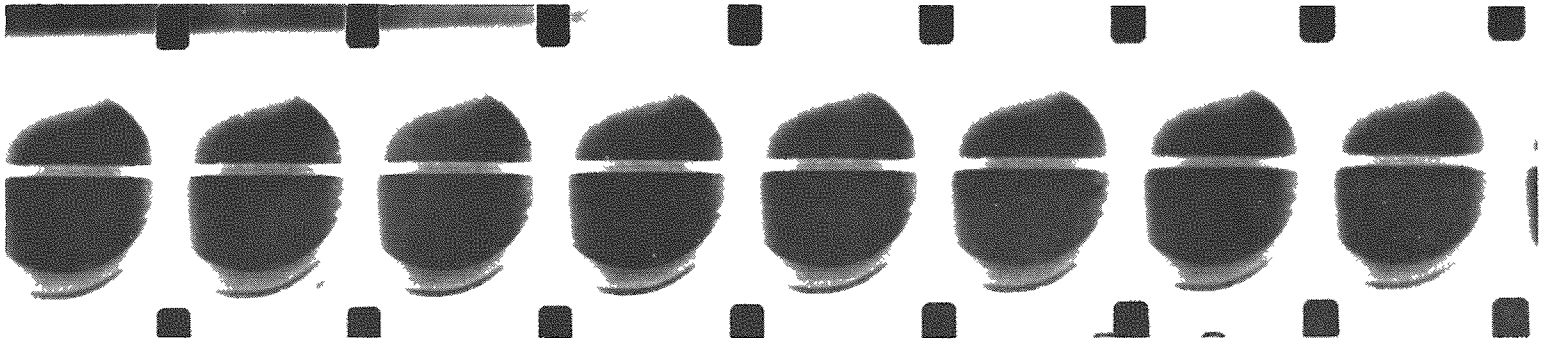

(C) Velocity: 4 ft/sec
Degree of Subcooling: 114 F

Heat Flux: 1.5×10^6 B/hr ft^2
Water Temperature: 120° F

17-C

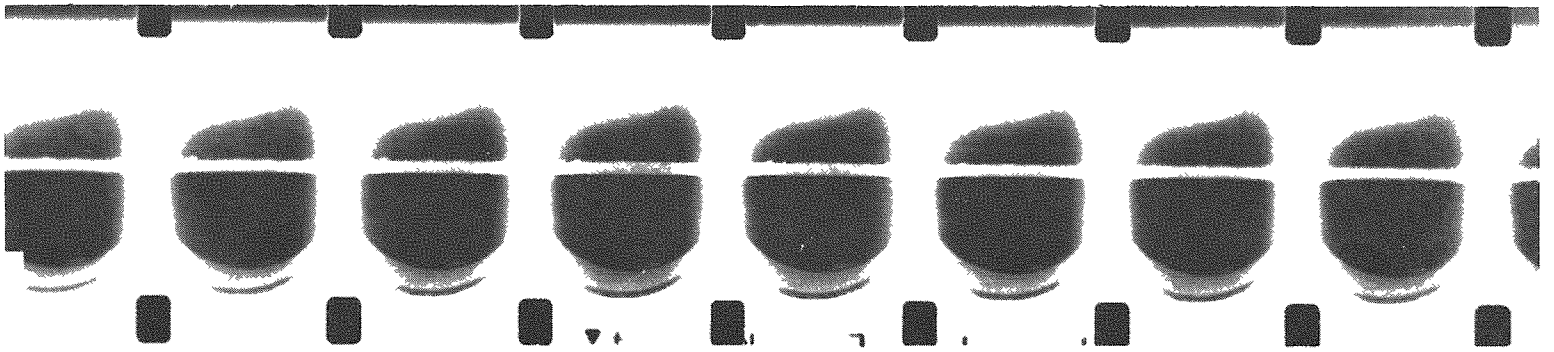

(D) Velocity: 6.8 ft/sec
Degree of Subcooling: 114F

Heat Flux: 2.1×10^6 B/hr ft^2
Water Temperature: 137° F

17-D

Flow ↑ Direction

Fig. 17 (C&D) Typical Formation of Bubbles

Film Speed: 3250 frames/sec Film Sequence: From Left to Right

sequence 17-A to 114 F in sequence 17-B; here, a film speed of 3250 frames per second was used. Comparison of Fig. 17-A and 17-B shows clearly the larger bubble population on the wire exposed to the water stream having the smallest degree of subcooling (17-B, the water closest to its saturation temperature), even though the heat flux in the second case is some 20 per cent less than that for the wire shown in Fig. 17-A.

The sequences shown in Fig. 17-C and 17-D, also taken at a film speed of 3250 frames per second, are presented to allow further comparison of the boiling phenomenon. Figure 17-C is a sequence taken for the same conditions as Fig. 17-B, namely, a velocity of 4 ft/sec and 114 F degrees of subcooling; here, however, the heat flux has been reduced materially (from 2.1×10^6 to 1.5×10^6 B hr^{-1} ft^{-2}). The sequence of Fig. 17-D represents conditions identical with those of Fig. 17-B, namely, degree of subcooling 114 F and heat flux of 2.1×10^6 B hr^{-1} ft^{-2}, except that the velocity has been increased to 8.6 ft/sec.

Comparing Fig. 17-B and 17-C shows a marked decrease in the quantity (and size) of the bubbles brought about by the sharp decrease in heat flux; only a few small bubbles can be seen in Fig. 17-C.

Comparison between Fig. 17-B and 17-D shows that, at the same heat flux and degree of subcooling, bubbles less in number and smaller in size were formed under conditions of higher flow velocity. Although the absolute pressure in the run at the velocity of 6.8 ft/sec was 30.4 psia and that at the velocity of 4 ft/sec was 23.2 psia, it is not expected that the pressure difference influences the result significantly.

In all of the photographs it is seen that the bubble formation occurs at the rear portion of the wire for the conditions involved; only at very

high heat fluxes did the bubble formation advance to include the forward portions of the test wire. This is to be expected, considering the combination of the lower pressure area downstream from the forward stagnation region and the sweeping action of the flow.

Under certain conditions bubble growth and collapse occurred at the wire surface, particularly for large bubbles, while in other cases the bubbles would separate from the surface and degenerate in the downwash.

To obtain quantitative information from the film sequences available would be extremely difficult, if at all possible, because the test apparatus was not specifically designed with such research in mind and, furthermore, the technique would have to be improved considerably.

CHAPTER III

EXPERIMENTAL APPARATUS

General

Figure 18 is a schematic diagram of the experimental apparatus showing the main flow system and its auxiliaries, as well as the test section and wiring diagram for the electrically heated test wire. The major components of the test apparatus include the following: the main loop of schedule 5, Type 304, stainless-steel pipe with a stainless-steel test section (rectangular shape 7 in. high and 10 in. wide), storage tank with auxiliary heaters, and circulating pump of stainless steel; an auxiliary cooling system consisting of a heat exchanger to remove heat from the main system, a cooling tower to dissipate the heat to the atmosphere, and pump, sump, and piping; a special power transformer to supply electrical power to heat the Chromax test wires; and instrumentation for measuring water flow rate, water pressure and temperature, surface temperature of the test wires, and electric power output of the transformer.

All parts of the main flow system are constructed of either Type 304 or Type 316 stainless steel.

Figures 19 and 20 are photographs of the experimental apparatus showing the main components. In Fig. 19 the main loop is shown; the supply tank and pump (with by-pass loop) can be seen at the upper center, while the test section can be seen in the horizontal branch at the left. Control valves for the main loop and those for the auxiliary heat exchanger (visible just below the foreground branch) can also be seen.

Figure 20 shows the power transformer at the right (behind which a portion of the test section is visible) and the control panel at the left.

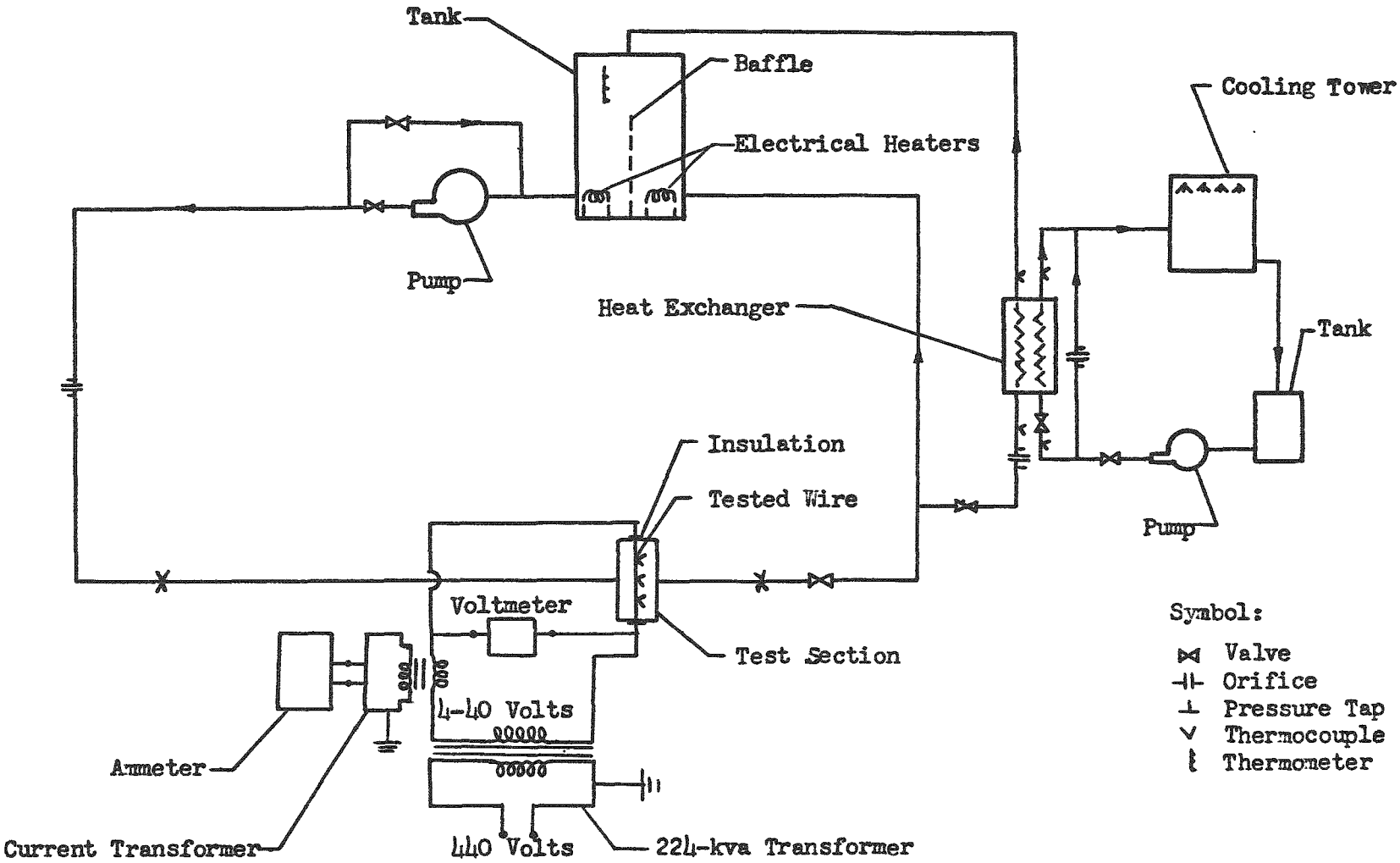

Fig. 18 Flow and Wiring Diagram

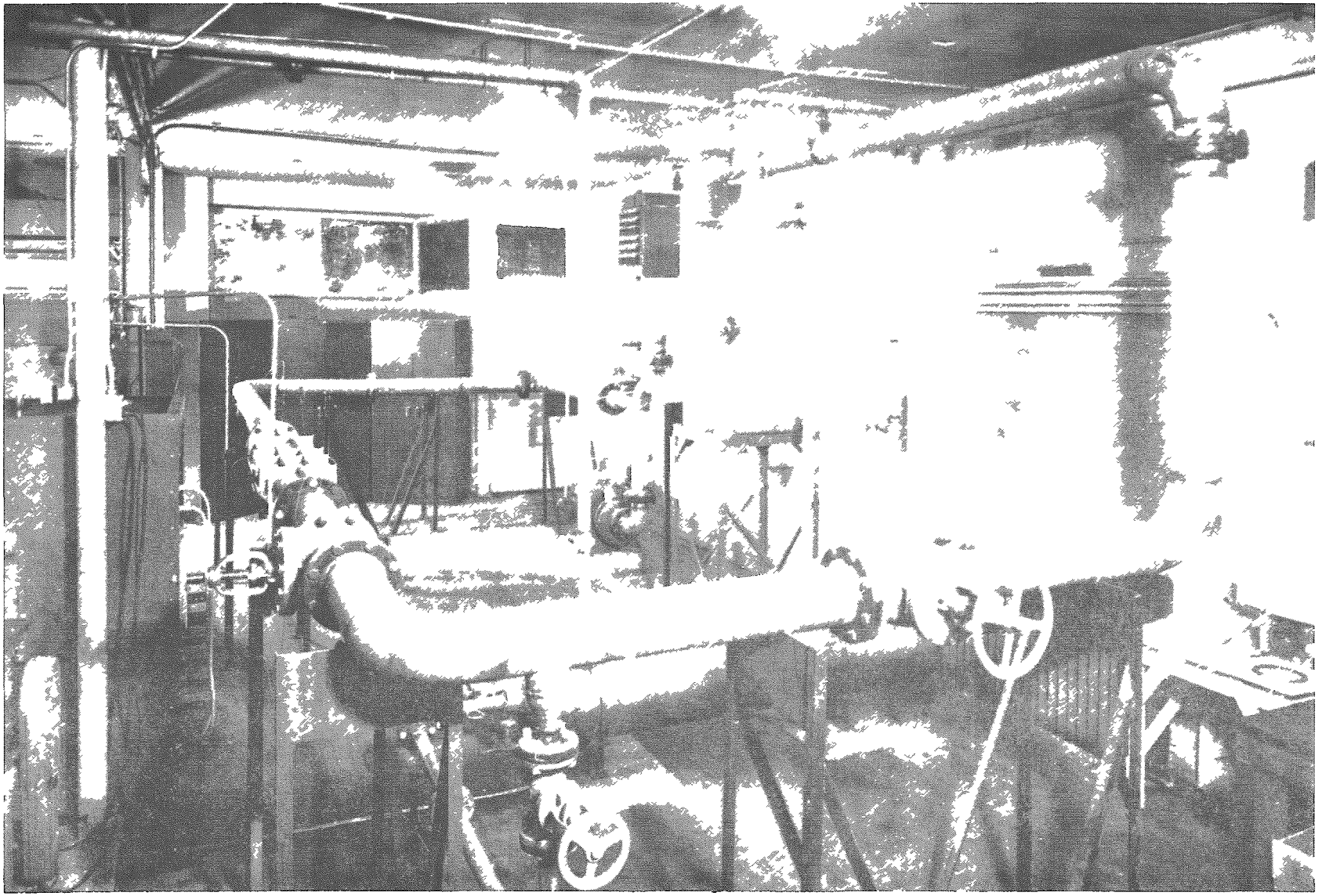

Fig. 19 General View of Test Loop

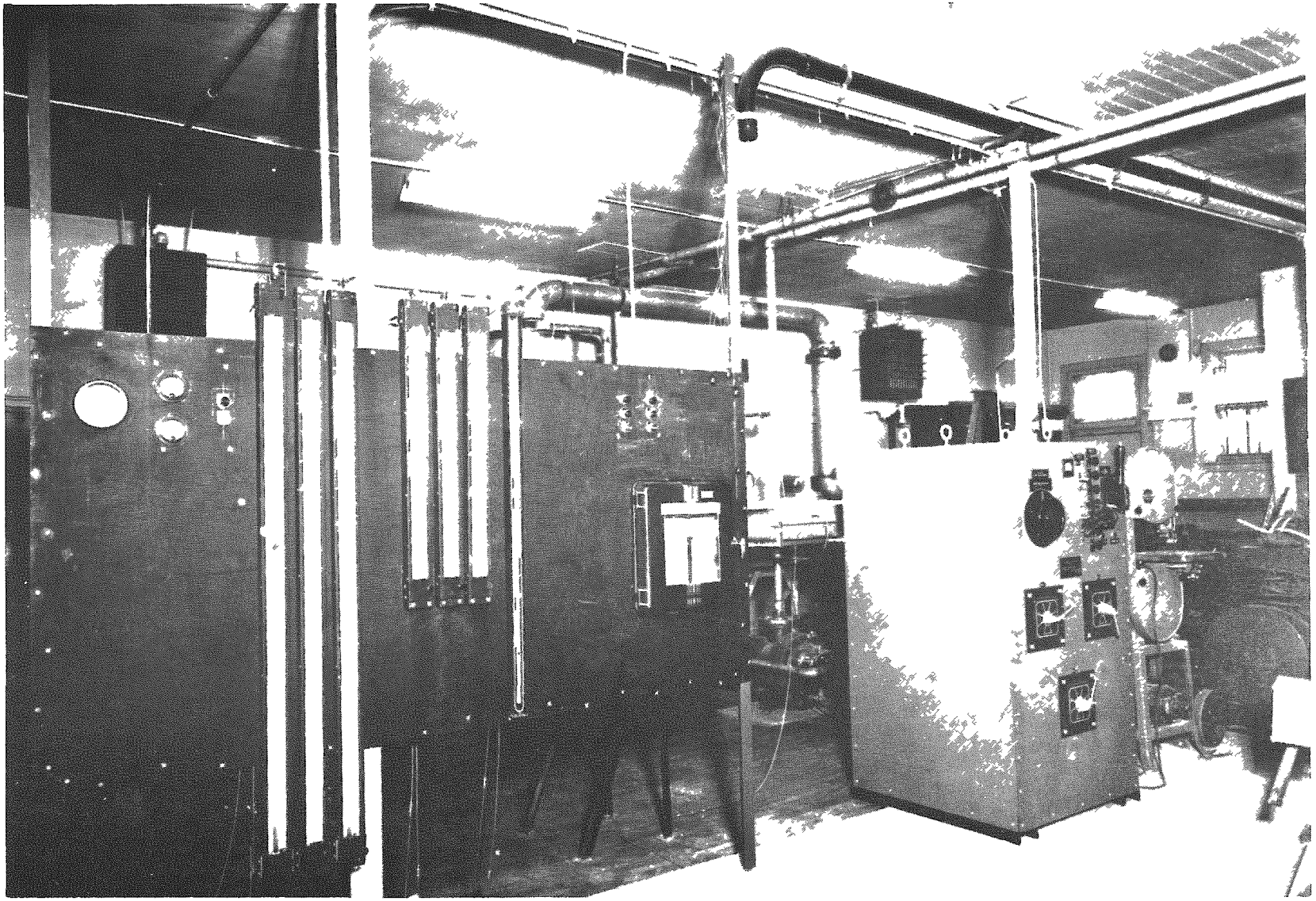

Fig. 20 Control Panel and Transformer

Main Flow System

Before tap water leaves the open supply tank, its temperature level and, therefore, the degree of subcooling, can be adjusted by two 480-volt single-phase 2-kw immersion heaters (Chromalox TLS-220) located in the tank and manually controlled by means of toggle switches located at the instrument panel.

Water flows from the supply tank into the 950-gpm, 60-ft, single-stage, centrifugal pump (Allis-Chalmers Model 5x4 SSN) which is driven by a 20-hp, 1750-rpm, three-phase induction motor. The pump body and impeller are of Type 316 stainless steel construction. The pump discharges through a gate valve into a 4-in. pipeline which is branched off into a 6-in. main line and a 4-in. by-pass. The latter serves as a means for flow control by returning a part of the water to the suction side of the pump. Downstream of the pump the water passes through a 40-mesh stainless steel wire screen before it comes to a calibrated orifice. This screen serves to standardize the flow turbulence and to produce a more uniform flow approaching the orifice, which is located downstream of the first 90-degree bend after the pump.

After leaving the orifice, the water flows along a short straight section and then passes through a 90-degree elbow where it enters a straight section 23 pipe diameters in length. The test duct, made of 16-gage Type 304 stainless steel, is connected to the end of the long straight pipe.

The test duct consists of a round-to-rectangular transition section followed by a short rectangular section, the rectangular test section, another short straight section, and finally a rectangular-to-round transition section. Both of the transition sections are 19 in. long with a

diffusing angle of 6 degrees; one transforms the 6-5/8 in. circular section into a 6-5/8-in. by 10-in. rectangular section, whereas the other (downstream) transforms the flow back to a circular section. One straightening section 19 in. long (the longer of the two) is assembled upstream of the test section, while the 12-in. long straight section is fitted to the downstream side; both are 6-5/8 in. high and 10 in. wide. The test section is of the same cross section, 9 in. long. A piezometer ring connecting three pressure taps located at the midplane (lengthwise) of the upstream straight section is connected to a 60-in. Merriam well-type mercury manometer for measuring absolute pressure.

A 40-mesh stainless steel wire screen is fitted between the divergent transition section and the straight section to standardize turbulence in the flow and to assist in producing smooth and reasonably flat velocity profiles.

Downstream of the test section the flow passes through a 6-in. control valve and, after leaving this control valve, the major part of the water returns to the supply tank for recirculation. The other part is branched off to a 2-in. pipeline leading to a 144-tube, 4-pass stainless steel heat exchanger (Bell and Gossett Type WU-147-45) where it is cooled before it returns directly to the supply tank for mixing. The amount of water passing through the heat exchanger can be manually controlled by a 6-in. globe valve in the mainline and by 2-in. and 4-in. globe valves in the by-passes. An orifice is installed in the 2-in. pipeline and two pressure taps, one 2 pipe diameters upstream and the other 4-1/2 pipe diameters downstream (of the orifice) are provided, and they are connected to a 50-in. Trimount stainless steel U-tube manometer filled with

chlorinated naphthalene;[1] this instrumentation allows for measurement of the flow through the heat exchanger.

Flow control is accomplished by manually operating the 4-in. globe valve in the by-pass line of the circulating pump in conjunction with the 6-in. globe valve located downstream of the test section.

The temperature of water upstream of the test section is measured by three radially moving thermocouples; they are 120 degrees apart and located upstream of the long calming pipe. Three thermocouples of the same construction are located downstream of the transition section. Temperatures of water inlet and outlet of the heat exchanger are also measured by thermocouples placed in thermometer wells already provided. All thermocouples are connected to a recording potentiometer (Leeds and Northrup Micromax Model S40000).

Orifice for Main Flow Measurement

The orifice, 4.500 in. in diameter, was machined and assembled in the manner described in reference (24), except that the central portion of the front face of the orifice was recessed by 1/32 in. to protect its sharp edge during assembly into the flanges. Another orifice, 2.500 in. in diameter, of the same construction, but for lower flow measurement, is also provided. One piexometer ring connecting three pressure taps which are 90 degrees apart is located 2 pipe diameters upstream of the orifice; the other ring of the same construction is located 4-1/2 pipe diameters downstream as specified (24).

---

[1] Commercially known as "green" indicating fluid; it has a specific gravity of 1.25.

Figure 21, a plot of discharge coefficient of the orifice C_d as a function of the Reynolds number, shows the results of the calibration, which was carried out on a full-scale basis[1] with the orifice as installed in the final set-up.[2] Also shown on Fig. 21 are the standard calibration curves, normally accepted under the proviso that all installation conditions specified by the standards are met.

It is apparent from the comparison of the actual and standard calibration curves in Fig. 21 that the location of the orifice less than 15 pipe diameters downstream of a 90-degree elbow influences the calibration appreciably.

Cooling System

Water stored in a supply tank is induced into a 100-gpm, 90-ft, single-stage centrifugal pump (Ingersoll-Rand 1-1/2-KRVS-3) which is driven by a 3-hp, 3450-rpm, three-phase induction motor. The pump of cast iron casing and bronze impeller discharges into a 2-in. galvanized steel pipeline leading to the shell side of the heat exchanger. A manually operated 2-in. globe valve is located at the inlet of the heat exchanger and a by-pass is provided across the pipelines of the inlet and outlet of the heat exchanger. Through this arrangement flow inlet to the heat exchanger can be regulated.

---

[1]Facilities of the Hydrodynamics Laboratory of IIT's Civil Engineering Department were placed at our disposal for the calibration; further calibration was carried out after final assembly using a 10-point traverse along the pipe diameter.

[2]The minimum amount of straight section of pipe on the upstream side of the orifice as specified by the standards (24) could not be provided, according to the space available; therefore, calibration had to be carried out on an "as-installed" basis. Results of the calibration clearly show the necessity of this procedure.

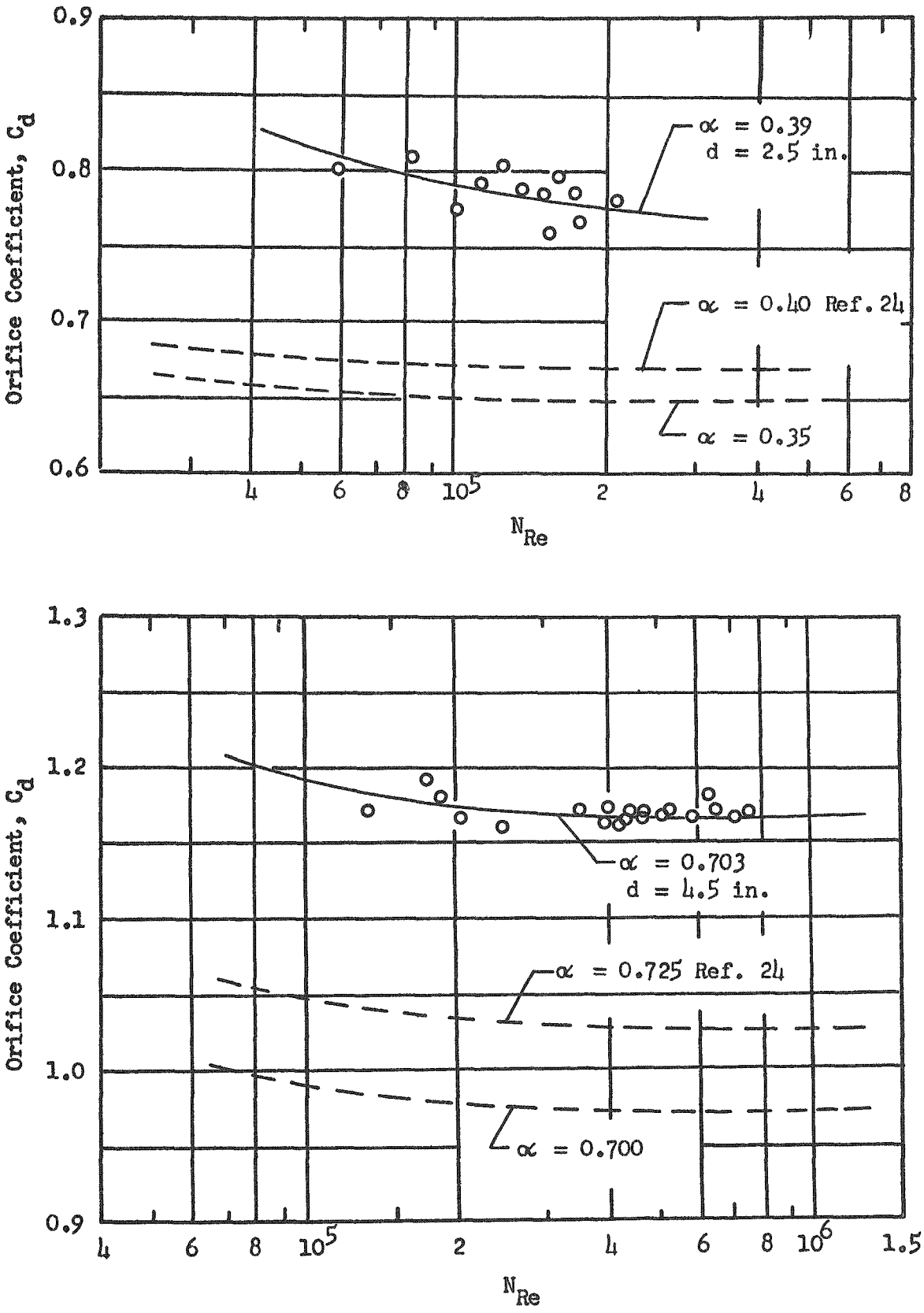

Fig. 21 Calibration Curves for 2.5- and 4.5-inch Orifices

After the water leaves the exchanger it flows to a 30-ton blower-type cooling tower (Binks 3B11-A) where it is sprayed through nozzles downward against a counter-flow air current forced into the bottom of the tower by a centrifugal blower. After passing through wooden eliminators, water accumulates at the bottom of the tower and returns through a 3-in. pipe to the supply tank for recirculation.

Water flow is metered by two orifices of the same construction as previously described. One orifice is located in the supply line and the other in the by-pass. Two pressure taps from the supply line are connected to a 30-in. Merriam well-type stainless steel manometer filled with mercury; the other pressure taps from the by-pass are connected to another 30-in. manometer filled with acetylene tetrabromide.[1]

Temperatures of supply and return water are measured by well-type thermocouples connected to a K-2 potentiometer (Leeds and Northrup No. 2430) through a selector switch.

Test Section

The test section, made of 16-gage Type 304 stainless steel, is 6-5/8 in. by 10 in. in cross-section and 9 in. in length with flanged ends of 1/8-in. stock. Figure 22 is a frontal photograph of the test section showing an installed test wire with three surface thermocouples in place.

Details of the mounting of the test rod are shown in Fig. 23, and a description of the assembly is as follows: At the center of each side wall a 1-in. hole was drilled to provide for installation of the electrodes.

---

[1] Commercially known as "red" indicating fluid; it has a specific gravity of 2.94.

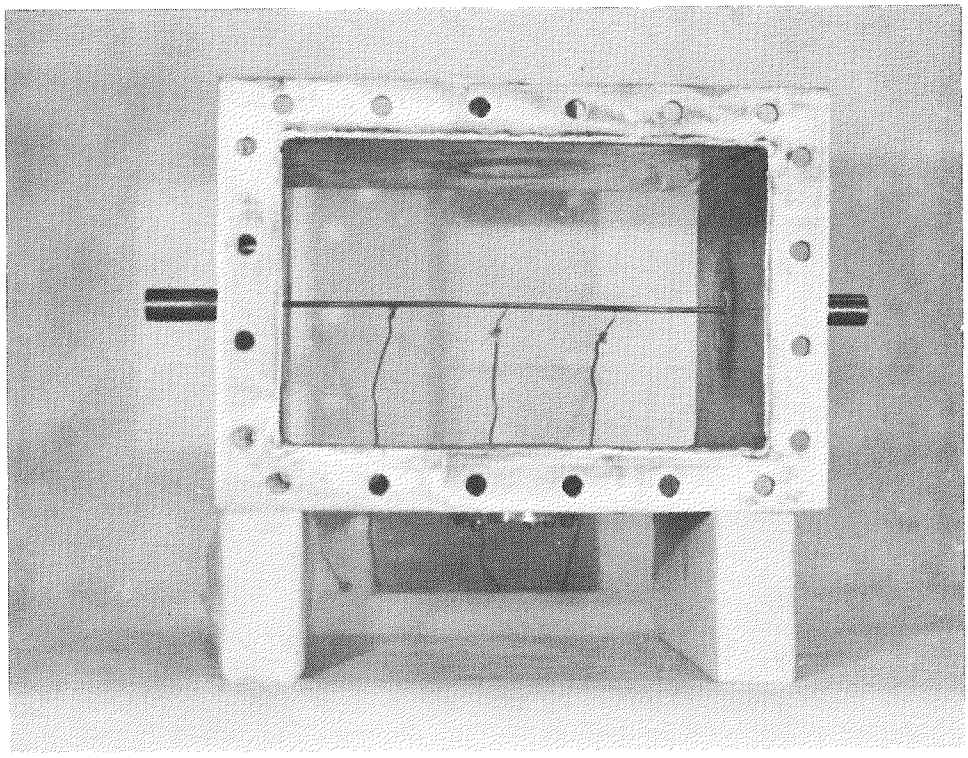

Fig. 22 Typical Assembly of Test Wire

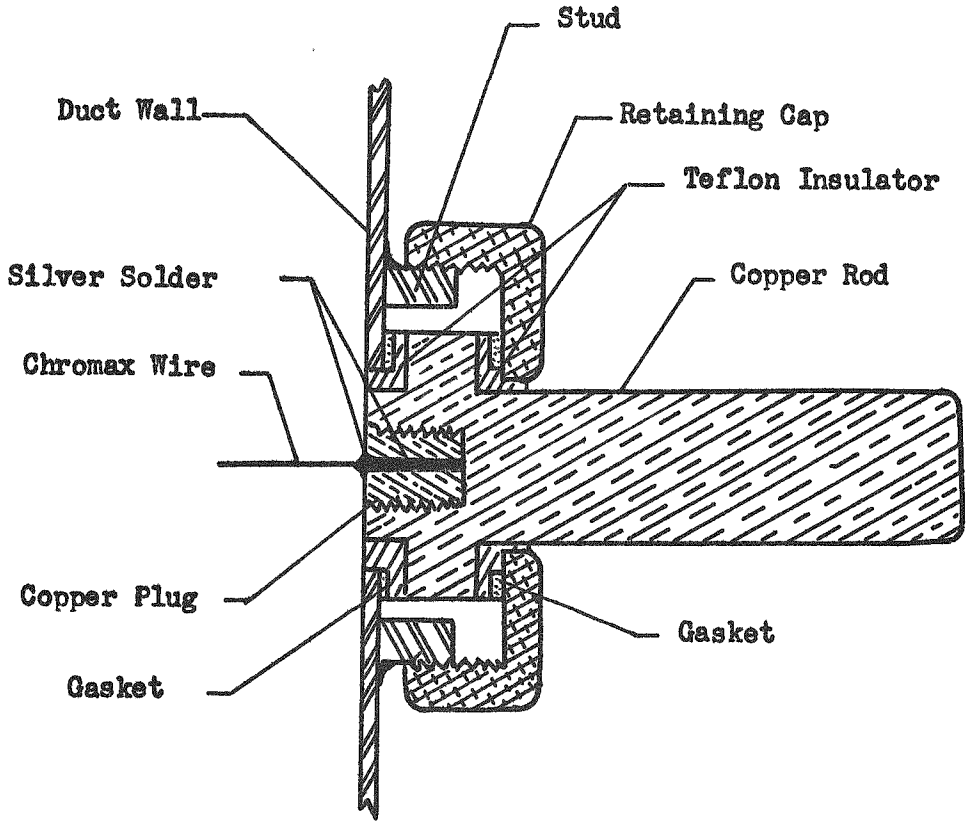

Fig. 23 Assembly of Electrode

Machined from 2-in. diameter copper rod, each electrode is 2-1/2 in. long and 3/4 in. in diameter, except that a portion 3/16 in. away from the inside end is 1/2 in. long and 1-1/2 in. in diameter. This larger portion of the electrode is provided to allow clamping and sealing of the whole assembly. On one end of the electrode a 1/2-in. hole is tapped, so that the Chromax wire, which has already been silver-soldered to a threaded 1/2-in. diameter copper connector, can be connected through its two threaded ends. For electrical insulation from the pipeline two 1/8-in. thick Teflon insulators with sleeves are inserted against each surface of the larger portion of the electrode, one surface against the metal wall and the other against the face of the aluminum retaining cap which holds the electrode in position. Neoprene ring-type gaskets are provided between the Teflon insulators and the duct as seals.

At the middle of each electrode a lead is provided for measuring potential drop across the heated wire. The heated length of the test wire was defined as the distance between the inner face of the two threaded copper connectors.

Electric power is supplied through copper bus bars protruding through the back of the transformer and the other end is fastened to a Bundy connector which was, in turn, firmly clamped to the electrode.

As a safety precaution the entire duct system was completely grounded.

For visual observation two 1-1/2-in. holes opposite each other were drilled at the center of the top and the bottom of the test section. On the outer surface of each hole is welded a 1/4-in. thick stainless steel ring for reinforcement. A 2-in. thick Plexiglas window is inserted into each ring. Between the Plexiglas window and the ring there is a 1/16-in.

Neoprene gasket. Six No. 8 screws hold the Plexiglas plug to the ring and keep it watertight. The inner surfaces of the Plexiglas are flush with the inner surfaces of the test section so that the flow would not be disturbed (see inside of duct at top in Fig. 22). A mirror is installed directly above the top Plexiglas window so that the boiling can be observed from the side of the duct; a light source was placed below the bottom Plexiglas window to aid the visual observations.

Transformer

The transformer, enclosed in a metal housing 60 in. high and 24 in. by 30 in. at the base, can be seen at the right of the photo, Fig. 20. It operates from a 440-volt, 60-cycle, single-phase current. The secondary connections, composed of equal windings, are brought out in the form of 1/2-in. by 1-in. bus bars protruding through the back panel. Each secondary was designed to deliver 800 amperes maximum at 40 volts. The transformer is equipped with a special current transformer, mounted on its front panel, used as an indicating instrument to adjust current during a run. On the front panel of the unit there is an amber pilot light to indicate that power is available at the main transformer switch. A red pilot light is also provided to indicate when the main transformer switch is closed and power is flowing in the windings.

For power control there are 15 taps on the primary, terminating in two 8-point rotary switches connected in series. Beyond the adjustment range of these switches there is a 15-kva powerstat (Superior Model 1256L25B) in series with the primary of a buck-boost transformer, of which the secondary is connected in series with the primary of the main transformer. This set-up results in voltage steps of 1/2 volt in each secondary of the

main transformer between 4 and 40 volts. There are also 8 dividing taps between the start of the primary winding and the first coarse tap. These are vernier taps and they terminate in an 8-position rotary switch on the front panel. The purpose of these taps is to shift upward or downward in small increments whatever secondary condition has been produced by pre-arrangement of the other two rotary switches.

Using the three 8-point switches and the vernier, infinite step control is provided on the output side in the range 4 to 40 volts and for 0 to 800 per secondary.

Seven telephone jacks are provided on the front panel for the purpose of connecting ammeters to read current in the secondary windings. When the meter plug is not inserted, these jacks short circuit so that the secondary winding of each current transformer does not burn out. When the meter plug is inserted in a jack, the load of the meter is placed across the winding before the short-circuit disconnection is made. This occurs automatically. Adjacent to the row of jacks a flexible cord and a plug are brought out of the panel. This is connected in series with an a-c ammeter (Weston Model 476) with a full-scale accuracy of 2 per cent and a range of 0 to 5 amperes. This panel ammeter only indicates the approximate current in the secondary windings.

Another loose plug is also provided for connection to an electro-dynamometer type, a-c and d-c ammeter (Weston Model 370) with a full-scale accuracy of 0.25 per cent and a range of 0 to 5/2.5 amperes. This precision ammeter is not mounted on the front panel, but is placed on a table in front of the unit. The arrangement described above makes it possible to read one or more secondary windings depending upon the number of circuits to be used.

During the early period of operation of the transformer, it was discovered that it did not function in accordance with its predicted performance; consequently, all the seven secondaries were connected in parallel to give the power required.

Temperature Measurements

(A) Measurement of Surface Temperature of the Heated Wires

One of the most difficult tasks in experimental heat transfer studies is the determination of the temperature of the heat-transfer surface. In this study much thought and effort were given to employ the heated wire as a resistance thermometer in estimating the surface temperature. At the outset of the work it was planned to obtain the surface temperature by calculation, assuming that the heat transfer coefficient is uniform around the wire and applying the theory of non-uniform development of heat inside of a cylinder (25) when it is heated electrically. This method requires a precise knowledge of the electrical and thermal properties of the wire and the precise measurement of the current and voltage drops.

As a first step, the electrical resistivity versus temperature relationship was obtained by direct calibration, as described in Appendix D. The thermal conductivity of the wire was provided by the manufacturer. With voltage drop and current known from measurements, one can, by employing Eq. (17), Appendix D, calculate the mean temperature difference. Based on the measured resistance, one can also obtain the mean temperature using the resistance temperature calibration. Hence, surface temperature can be determined.

It was experienced in the early stages of the work that values of electrical resistance of the operating wire could not be obtained with the desired degree of precision originally sought; a slight inaccuracy in determining the electrical resistance will yield a fairly high inaccuracy in mean temperature. Because of these difficulties, the use of directly attached surface thermocouples was finally decided upon.

The thermocouples finally employed were made of AWG No. 28 Chromel-Alumel wires. Three thermocouples were carefully silver-soldered to each test wire at 2-1/2 in. equal spacing with one at the center and one at each side. The soldering was made as small a fillet as possible. Any excessive solder or soldering flux around the thermocouples and between the wire of thermocouples was removed by carefully scraping and filing.[1] They were then tested by submerging the wire in a tank of water at uniform temperature to check their indication. After assembly in the test section, inspection of the thermocouples was again made with the test wire heated with very low current and no water flow.

Each thermocouple had an independent circuit. The cold junctions were inserted in separate glass tubes and immersed in an ice-water mixture in a Dewar flask. Leads were then connected to a 10-point switch (Leeds and Northrup Type 8240).

The thermal electromotive force was measured by a Leeds and Northrup K-2 potentiometer connected to a d-c galvanometer (Leeds and Northrup Type No. 2430), a standard cell (Eppley No. 524184) and a 2-volt Willare storage battery. The potentiometer, in the range used, reads

---

[1]This was done under a magnifying glass having a magnification factor of five.

microvolts directly; a reading can be estimated to a tenth of a microvolt, which corresponds to about 0.004°F. This indication is much better than the reproducibility of the thermocouple and the potential leads. The potentiometer accuracy, under the test condition, is 0.1 per cent, or better, of the reading. The galvanometer sensitivity is 0.45 microvolt per millimeter on scale.

The Chromel-Alumel thermocouple wires employed were calibrated in an electric furnace (Sentry Model V #7) against a 24-in. platinum-platinum plus 10 per cent rhodium thermocouple (Leeds and Northrup Model 8702) which was certified by the Bureau of Standards with corrections of -0.1°F at 300°F and -1.0°F at 800°F. The results obtained were +0.2°F at 245°F and 0°F at 766°F.

(B) Measurement of Water Temperatures

In measuring water temperatures all thermocouples were made from the same batch of Leeds and Northrup varnished and cotton-insulated AWG No. 30 copper-constantan wires. Each junction was formed by soft soldering with a bead approximately 1/32-in. diameter.

Each thermocouple was inserted into a 1/8-in. OD stainless steel tube with its junction protruding out of one end about 1/16 in. This end was sealed with a mixture of Kadon liquid and powder, a dental plastic. The other end of the tube was sealed with Paxalloy. Two thermocouples from the same batch of wires were calibrated simultaneously in a hypsometer at the steam point. The average deviation from a standard table was found less than 0.1°F; consequently, no correction was made.

To measure the water temperature in the main flow, the three radially movable thermocouples located upstream of the long straight

section and the other three located downstream of the test section are used, as already mentioned. Each is inserted into an individual adapter silver-soldered to the periphery of the pipe. Each adapter is provided with a rubber O-ring, a spacer and a locking nut, comprising a sealed holder for the movable thermocouples. All of them were connected to a Leeds and Northrup Micromax (Model S 40000) to detect the radial temperature variations.

In order to record water temperature accurately, one of the three radially movable thermocouples upstream of the calming section and one of the three downstream were connected to the K-2 potentiometer through a selector switch. Another of the aforementioned thermocouples was connected to a Leeds and Northrup Type G speedomax, and this was used to maintain constant water temperature while the system was in operation.

To measure the temperatures of water in the cooling system, two thermocouples were provided. Each of them was installed in a 1/8-in. stainless steel tube which was then slipped into a pre-drilled hole in a 1/8-in. steel pipe plug and soft-soldered. They were then assembled with their junctions approximately in the midstream of the supply and return lines. They were also connected to the Micromax for recording.

Temperatures at the inlet and outlet of the heat exchanger were also obtained using copper-constantan thermocouples.

Even if the system were insulated, it would be difficult, if possible at all, to perform a meaningful energy balance.

Pressure Measurement

Instrumentation is provided for measuring orifice pressure differentials and gage pressure upstream of the test section. To measure orifice

pressure differentials upstream taps are located 2 pipe diameters from the orifice and downstream taps at 4-1/2 pipe diameters away were used.

In the main flow system, every pressure tap was prepared by first drilling a 1/8-in. radial hole through the stainless steel pipe wall (0.109-in. thick) and then installing and silver-soldering in place the 1/8-in. tube of a stainless steel adapter, cut to a length equal to the thickness of the pipe wall. After soldering, the hole was once again cleaned out with a drill and polished with emery cloth. All burrs were eliminated and the inside of the pipe was polished smooth with emery cloth.

Three radial pressure taps, each at 90 degrees apart in the plane perpendicular to the flow direction at 2 pipe diameters upstream of the main orifice and another three similar pressure taps at 4-1/2 pipe diameters downstream, are connected through piezometer rings to a 60-in. Merriam well-type manometer filled with acetylene tetrabromide (specific gravity 2.94). As already mentioned, the location and construction of this orifice is not exactly in accordance with the standards (24), so that a calibration was made (see Fig. 21).

Three pressure taps, 14-in. just upstream of the test section, were also connected through a piezometer ring to a 60-in. Merriam manometer filled with mercury for measuring the absolute pressure (in conjunction with a barometer).

Two pressure taps, one at 2 pipe diameters upstream and one at 4-1/2 pipe diameters downstream of the orifice in the 2-in. by-pass to the heat exchanger, were directly connected to a 50-in. Trimount U-tube manometer filled with chlorinated naphthalene (specific gravity 1.25).

All connections were made with 1/8-in. stainless steel tubing.

In the cooling system, consisting of schedule 40 galvanized steel pipes, the same care used in constructing taps in the main flow system was taken in the preparation of pressure taps, except that the 1/4-in. brass fittings were first screwed to the pipe and then brazed into place. The 30-in. Merriam manometer for measuring pressure differentials in the coolant-supply at the rate of 100-gpm was filled with mercury and that for coolant through by-pass was filled with acetylene tetrabromide.

All manometers have divisions of 0.1 in. and readings can be estimated to 0.02 in.

Electrical Power Measurement

For rough indications and settings the ammeter (Weston Model 476) mounted on the front panel can be used to read the current in the secondary windings. However, for accurate measurements a precision voltmeter and a precision ammeter coupled with a current transformer were employed.

Potential leads were provided at the middle of the copper electrodes which held the Chromax test wire. A Weston Model 341 voltmeter with a full-scale accuracy of 0.25 per cent and a range of 0 to 75/30 volts was employed to record voltage drops above 15 volts, and a Westinghouse Type G voltmeter with a full-scale accuracy of 0.5 per cent and a range of 0 to 75/15/3 was used to measure voltage drops below 15 volts.

On account of the difficulties encountered in installation, voltage drops were measured by potential leads tapped at the copper electrodes instead of the Chromax wire itself. That this is an acceptable procedure can be seen from examination and comparison of the electrical properties and geometry of the Chromax wire and copper electrode.

	Chromax wire	Copper electrode
Electrical resistivity, ohm/cir mil/ft at 70°F	600	10.6
Dimensions	1/8-in. OD by 10-in. long	3/4-in. OD by 1-1/2 in. long

Since the electrical resistance of a conductor is directly proportional to its resistivity and length and inversely proportional to its cross-sectional area, it is observed from the above values that the resistance of the copper electrode is negligible compared to that of the Chromax wire.[1]

To measure the current three current transformers were employed. They were used in conjunction with a Weston Model 370 ammeter having a full-scale accuracy of 0.25 per cent and a range of 0 to 5/2.5 amperes. The current transformers are listed as follows:

Make	Accuracy	Ratio	Range Employed
Westinghouse Style 29798	0.25 per cent	400:5	below 400 amperes
Weston Model 461, Type 1	0.25 per cent	800:5	below 800 amperes
Weston Model 461, Type 2	0.25 per cent	1000:5	above 1000 amperes

The current transformers were located around the main bus bar leading to one of the test-section electrodes.

---

[1]This assumes that the contact resistance between the threaded portions of the copper connector and the copper electrode (see Fig. 23) is also negligible. To check this some runs were made with potential taps on the inside of the test section and results obtained in this way were compared to the potential drops measured in the manner described above; differences could not be found within the accuracy of the measuring instruments.

In order to determine the effective power output of the transformer from the measurements of voltage drop and current, the power factor must be known. The calibration of power factor versus load was obtained using a Weston Model 310 wattmeter with an accuracy of 0.25 per cent together with a voltmeter, an ammeter and the current transformers. The calibration curve is shown in Fig. 24.

Determination of Water Conditions

The electrical resistance of the tested water was measured with a Leeds and Northrup conductivity bridge (Serial No. 1041256) with approximately 3 per cent accuracy. The pH value was determined with a Bechman Model G glass electrode pH meter with an accuracy of $\pm$ 0.2.

High-Speed Movie Camera and Its Accessories

The high-speed movie camera used is a 16mm Fastax camera manufactured by Wollensak Optical Company of New York. The camera employs a continuous moving film with a rotating prism positioned between the lens and film. The prism rotates synchronously with the film, creating successive and properly spaced images traveling with the film. Thus, a continuous sequence of still photographs is obtained.

This camera can be operated with a d-c source for film speed below 1000 frames per second. For speed above 1000 and up to 7000 frames per second an a-c source must be used. The camera has two 1/4-hp, 120-volt universal motors, one driving the film take-up spindle, and the other driving the film sprocket and rotating prism. Although the motors are designed to operate at full initial impact up to 130 volts without requiring

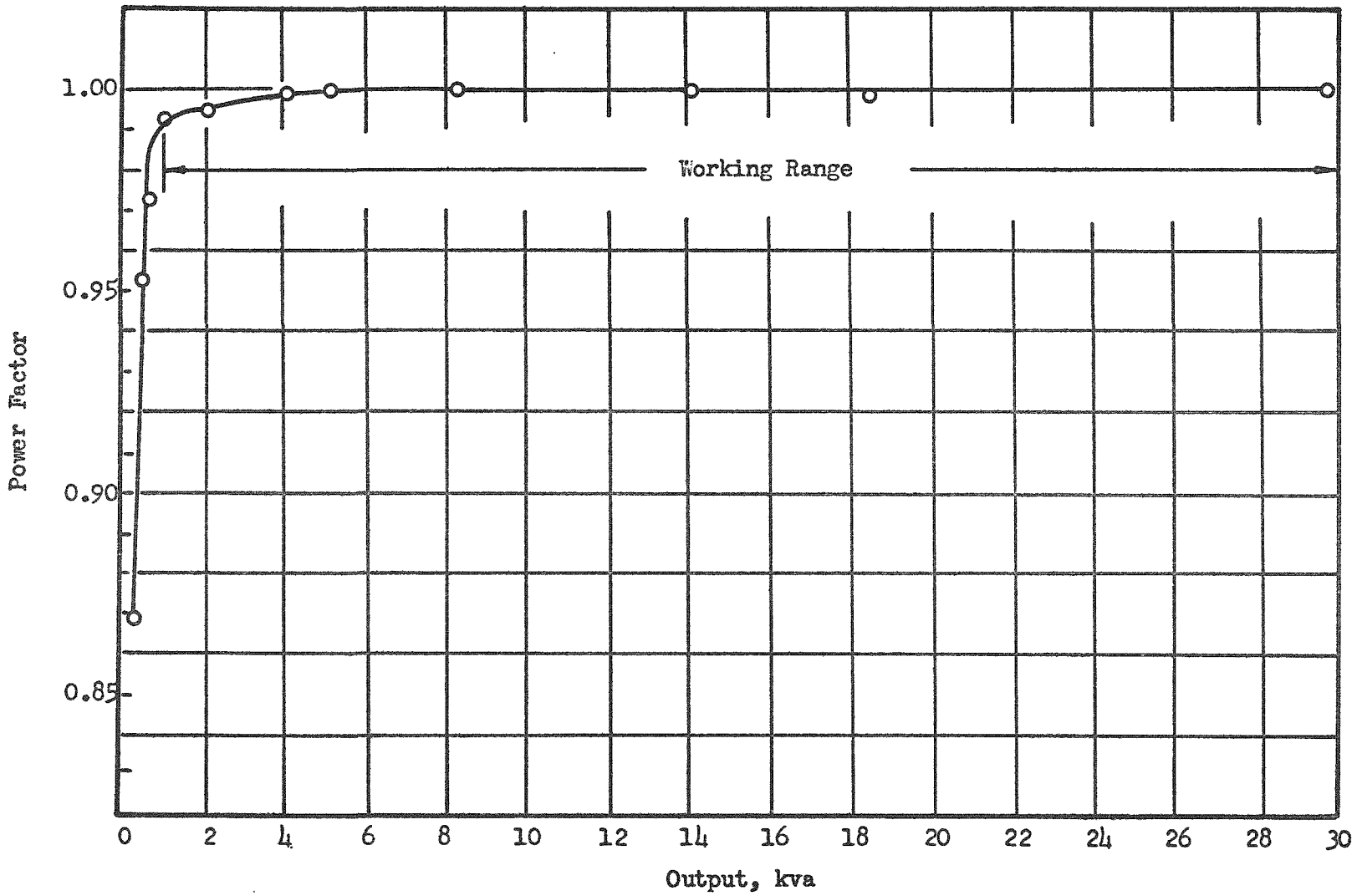

Fig. 24 Calibration of Power Factor of Transformer

accelerating equipment, a control unit[1] is used to control acceleration characteristics and speed. Coupled with this control unit, a film speed at 7000 frames per second can be obtained.

Various combinations of lens and extension tubes, both provided with the camera, enable one to choose the most suitable size of camera field and the image. For this study the pictures were taken using the 154.5mm - f:6.5 lens plus a 1-in. extension tube.

A neon glow lamp timer is mounted inside the camera. The lamp normally operates from a 115-volt 60-cycle a-c supply and gives 120 pulses of light per second. Using timing marks on the edge of the film, the average time elapsed between two consecutive frames can be calculated.

On account of the inadequate space for back lighting, the flow channel was turned 90 degrees, that is, the tested wire was in a vertical position. Two General Electric Model 750-R spotlights were placed facing the front window and one facing the rear through a vellum paper for diffusing the light. The setting for camera speed and lighting condition was obtained by a Weston electric light meter and a calculator. The film used throughout this study was Kodak XX (black and white).

---

[1] Trade-named "Goose".

CHAPTER IV

EXPERIMENTAL PROCEDURE

Before any run was made the temperatures indicated by the three thermocouples silver-soldered on the surface of the tested wire were checked against themselves and the water temperature indicated by one of the thermocouples in the main flow circuit. This was done mainly to provide a check of the continuity of the surface thermocouple circuits, considering that damage to the rather delicate junctions could occur during assembly of the test wire into the test section. After this initial check, the transformer circuit was closed allowing a low power input to the test wire; the power supplied was at approximately 20 amperes at approximately 4 volts, corresponding to a heat flux of about 1000 B/hr ft^2. At this power input another check of the surface thermocouples was made. The transformer circuit was then opened and the run was started.

To start the run the flow rate and, hence, the flow speed at the test section was set at the desired value using the control valves. Then, with the circulating pump of the cooling system and the cooling-tower fan turned on, the amount of cooling water to the heat exchanger was regulated. Depending upon the desired temperature level of operation, the temperature level in the main line was controlled by using either or both of the 2-kw electric heaters immersed in the reservoir tank and/or by diverting part of the flow to the heat exchanger.[1]

---

[1] At the highest operating temperatures, which represent the lowest degrees of subcooling, the auxiliary heaters would be turned on several hours prior to the run and, in some instances, had to be left on through the previous night to raise and keep the relatively large bulk of water at high temperature.

After the water temperature was brought to the desired temperature and maintained at that fixed level, under the preset flow conditions for at least 20 minutes, experiments were started by closing the transformer circuit and setting the level of the power to the test wire by changing tap positions and adjusting the powerstat control. It was observed from the temperature measurements at the surface that a steady state condition was achieved within two to three minutes after the taps were initially set. For comparatively minor adjustments in power level the time required to reach steady state was even less. Even so, final data were usually not recorded until steady conditions held for at least five minutes beyond this time, except, of course, for runs in which the burnout point was approached in which case the data were recorded frequently until burnout occurred.

During the course of the experiments the water temperature would tend to increase because of the additional heat introduced by the test wire.[1] When this increase approached 2 F the transformer was cut off and the amount of coolant to the heat exchanger was increased accordingly. Experiments were resumed after the water temperature was held constant over a five-minute interval. Nevertheless, the water temperature during any experiment was kept constant within $\pm$ 2 F.

The main data recorded for each run include values of current and voltage to the test wire, the emf's of the surface thermocouples, emf of water temperature, thermocouples, and pressures (manometer readings).

---

[1] The energy input of the pump (and any other fixed energy input) is compensated by the initial adjustment of the by-passed water coupled with the adjustment of the flow rate of the coolant to the heat exchanger.

Two persons were required to operate the apparatus and to record the data.

At the end of each experiment, the tested wire was taken out for inspection and cleaning. It was sometimes found that the wire was coated with an extremely thin layer of white scale, discernible only from the change of surface finish. This layer was rubbed off before a new test was undertaken.

Whenever a new wire assembly was installed, the checking of the surface thermocouples was repeated before new experiments were performed.

When boiling was violent and large clumps of bubbles appeared as the burnout point was approached, the power input was increased very slowly and carefully, and data were repeatedly recorded up to the moment of burnout.

To facilitate the photographic work, the test section was rotated on its axis through 90 degrees so that the viewing ports were at the sides instead of at the top and bottom. This arrangement allowed the high-speed camera to be used in a horizontal position in its usual tripod mount and it allowed for the introduction of at least the minimum lighting required to carry out the photography.

The resistivity and pH value of the water were determined at the Physical Chemistry Laboratory of the Institute.

CHAPTER V

DISCUSSION

Reproducibility of the Surface Thermocouples

As a check on the uniformity of the mounting technique of the surface thermocouples, tests were carried out using different instrumented wire assemblies. The results of auxiliary tests, reported as Test No. 17 (A and B) in Appendix E, are compared with results obtained with different assemblies during the course of the main forced-convection boiling experimentation; in particular, temperature indications observed in Test No. 17A (comprising 13 runs) are compared with those of main Test No. 8, both at a velocity of 4 ft/sec, and those of Test No. 17B (comprising 14 runs) are compared with those of main Test No. 10, both at a velocity of 5 ft/sec.

The results are compared on the basis of surface temperature indication t_{ind} plotted against heat flux, and they are shown in Fig. 25. Conditions for each comparison are identical for all practical purposes.[1] The maximum difference in both Fig. 25A and 25B comes close to $6^{\circ}F$, and this occurs at a heat flux of about 0.9×10^{6} B/hr ft^2. At lower and higher values of heat flux the agreement is even better for both comparisons, amounting to $3^{\circ}F$ or less.

The reproducibility is considered excellent in view of the difficult and delicate technique involved in properly attaching the surface thermocouples.

---

[1] For example, conditions of Test No. 8 were identical with Test No. 17A in the essential features: velocity 4 ft/sec (same); degree of subcooling $\Delta t_{sub} = 140^{\circ}F$ (same); absolute pressure 47.77 in. Hg compared with 47.47 in. Hg; water temperature $96.5^{\circ}F$ compared with $96.3^{\circ}F$. Likewise, conditions of Test No. 10 and Test No. 17B are practically identical as can be seen from the data.

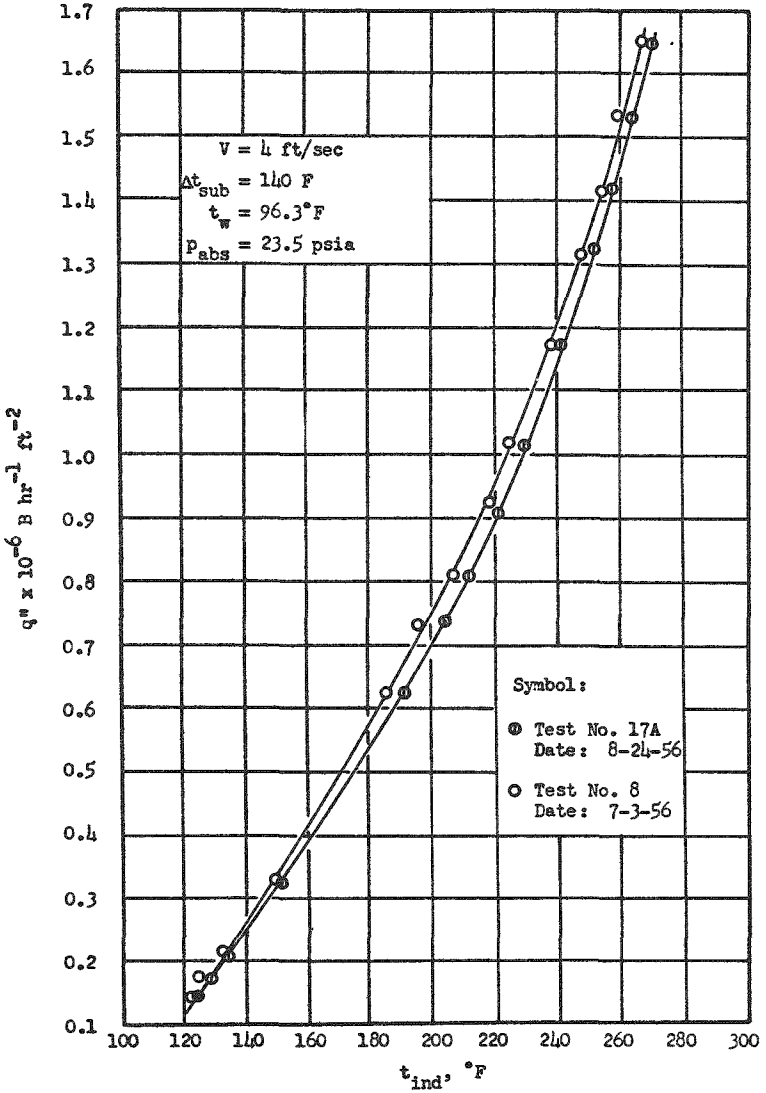

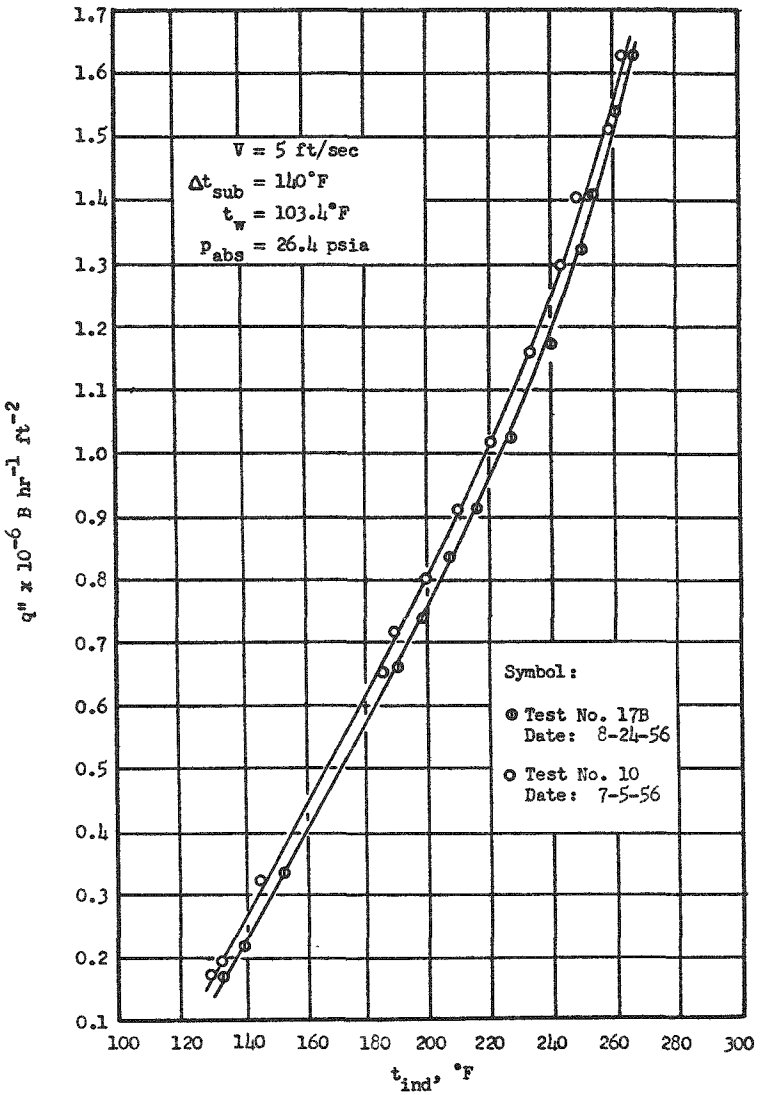

Fig. 25 Comparison of Temperature Indications of Different Surface Thermocouple Assemblies

An estimation of experimental errors is presented in Appendix A.

Non-Boiling Heat Transfer Results

It may be observed that the correlating lines shown in Fig. 1, which is a log-log plot of heat flux q" as a function of temperature difference $(t_s - t_w)$, have slopes ranging from about 1.06 for the highest water velocity of 6.8 ft/sec to a value of approximately 1.25 for the lowest velocity of 1 ft/sec. The slopes increase progressively, although slightly, as the fluid velocity decreases; the change is systematic, and it shows an increasing dependence on the convective heat-transfer coefficient on the temperature difference between surface and bulk fluid, slight at first, but becoming more pronounced at the lowest velocities. While some dependence of the heat-transfer coefficient on temperature difference may be expected,[1] the proportionality between the convective heat-transfer coefficient to nearly the one-fourth power of the temperature difference, shown by the data for the lowest flow velocities of 1 and 2 ft/sec, appears too large to be accounted for by property changes alone. In fact, the dependence of the heat transfer on the 1.25 power of temperature difference falls in the range of what normally is expected for free convection alone. On this basis it is probable that, as the lower velocities are reached, free convection effects begin to play some role.

To check the possible influence of free convection, an approximate theoretical computation was carried out, considering the action of the

[1] Mainly as a result of temperature influence on properties in the laminar boundary layer existing over the forward portion of the wire.

buoyant forces involved to result in an upward acceleration of the fluid to a final velocity of V_f. Physically, one may consider the average buoyant force acting through a vertical distance which characterizes the system (in this case through a vertical distance equal to the diameter of the wire D) to result in a certain amount of work done on the fluid itself; the work done shows up as an increase in kinetic energy of the fluid in the direction of the force. Such an analysis[1] -- assuming the density of the fluid ρ evaluated at an average temperature -- results in the relationship $V_m^2 = g\beta(t_s - t_w) \cdot D$, where β is the coefficient of thermal expansion of the fluid.[2]

Considering the surface temperature at $t_s = 195.7°F$ and a water temperature $t_w = 85°F$ (highest heat flux run at 1 ft/sec flow speed in Run 13 of Test No. 1, shown in Appendix E) the value of β is found from steam table data to be 2.93×10^{-4}; herewith, taking $D = \frac{1}{8}$ in. $= \frac{1}{96}$ ft and the acceleration of gravity $g = (32.2 \times 12.96 \times 10^6)$ ft/hr^2, we find $V_f = 377$ ft/hr or 0.105 ft/sec, which is just over one-tenth of the forced flow velocity in the system.

While the above computation shows that influence of free convection at the lowest flow speed of 1 ft/sec is not at all decisive, its magnitude of the upward velocity component is such as to suggest some bearing on the results obtained at this lowest speed. As the speed increases, however, the influence of buoyant forces would rapidly become less important, per-

---

[1] See, for example, Brown and Marco (32), p. 132; Jakob (25), p. 493, shows a related analysis.

[2] Defined in terms of the specific volume by $v_s = v_w[1 + \beta(t_s - t_w)]$, where subscript s refers to surface and subscript w refers to bulk water.

centagewise, and even smaller in magnitude because of the decreasing surface temperature of the wire.

The systematic nature of the shift in the slope of the correlating lines, then, may be the result of a second order effect in the nature of the surface temperature correction applied. At least this possibility exists and, considering the character of the results at low speed and high heat flux rates, it offers at first hand a reasonable explanation of the shift. For example, an error in corrected surface temperature of 10 F (too low)[1] at the highest heat flux rate of 0.178×10^6 shown for $V = 2$ ft/sec line would bring the slope into better agreement with the higher speed curves. But, on the other hand, the existing slope for the 1 ft/sec velocity agrees very closely with that found for the data obtained using a tube instead of a solid wire rod, in which case the surface temperature was obtained in an entirely different way. (Figure 1 and Fig. 30 of Appendix C may be compared to check this.) For the case of the tube, the outer surface temperature was calculated from a measured value of inside wall temperature (adiabatic) and the internal heat production within the tube (see Appendix C).

Nevertheless, the dimensionless correlation of these data, obtained for the range $1500 \leq N_{Re,f} \leq 11{,}000$ and shown in Fig. 2, is consistent within itself, and it agrees reasonably well with an extrapolation of the correlation recommended by McAdams (23) which is based on results of previous investigators who employed liquids flowing normal to wires and tubes in the range $0.1 \leq N_{Re,f} \leq 250$. It is clear from Fig. 3 that the extra-

---

[1] This would mean a 30 per cent error in the correction at this point, which is not very likely.

polation, a risky enterprise to pursue in general, appears to be well substantiated both by the order of magnitude and by the trend of another general correlation obtained by modifying the specific correlation available from the plentiful data for air in cross flow over cylinders. In this instance, the air results, also available from McAdams (23), have been reduced to include all fluids; they are also plotted on Fig. 3 and, in fact, they are in very close agreement with the results of the present study.

If one assumes that McAdams' correlation for liquids alone is correct, and that it is valid over its extrapolated range above a Reynolds number of 250, then it would mean that the heat-transfer coefficients found in the present work are somewhat low. This implies that the surface temperatures used in the present study are too high, which does not seem likely in view of the probable magnitude and direction of the error involved in determining the surface temperature.

Save for the two low points, which represent data from the 1-ft/sec run, the results are in excellent agreement with the general correlation obtained from the air data.

Surface Boiling Heat-Transfer Results

Slope of the Boiling Curve. The lines representing the data obtained under conditions of change of phase at the wire surface, plotted in the form of heat flux q'' versus the temperature difference $(t_s - t_s)$ and shown in Fig. 4 through 9, indicate at sharp upward inflection just as boiling commences. It may be observed from Fig. 4 through 9 that the heat flux increases practically linearly as the temperature difference between the wire surface and the bulk water until the surface temperature reaches

the saturation temperature of the water, at which point boiling commences. In the boiling region a relatively minor increase in temperature results in a proportionately larger increase in heat flux than for non-boiling.

This behavior may be attributed to the fact that the whole mechanism of heat transfer from a solid surface to a flowing liquid changes as the temperature of the solid surface exceeds the saturation temperature. When boiling occurs, the thermal resistance is greatly reduced; it is postulated that this reduction in thermal resistance results from the growth and collapse of bubbles formed at the liquid-solid interface, thus increasing the heat transfer rate with relatively small temperature increase. In this regard it must also be considered that the violent action of bubble formation effectively reduces and to a great extent destroys the boundary layer which comprises the main resistance to the heat flow. Hence, cooler liquid comes into contact with the surfaces and brings about a large increase in the effective heat transfer.

The figures also show that the degree of increase of the slope of the boiling curve over that for non-boiling, under the same conditions of water velocity and temperature, becomes less pronounced as the bulk velocity is increased (see, for instance, Fig. 9). This can be understood in terms of the comparatively thinner boundary layer, and the attendant larger heat-transfer coefficient, already existent over the forward portion of the wire surface at the higher velocities; therefore, the increase in heat flux per unit increase in temperature difference is proportionately less than at the lower velocities.

Onset of Boiling. It is important to note that the transition from non-boiling to boiling is not abrupt or instantaneous as is indicated by

the sharp break in the correlating lines of Fig. 4 through 11; instead, it occurs as a more or less rapid transition from the initial slope for non-boiling to the steeper one evident under boiling. Nevertheless, the location of the sharp break shown in each case, which was obtained by extending the lines for each of the two heat-transfer regimes to their point of intersection, corresponds to a wire surface temperature very nearly equal to the saturation temperature of the water -- a condition which must prevail before change of phase can take place.

Referring to the figures, it can be seen that for lower bulk water temperature (higher subcooling), incipient boiling occurs at a correspondingly higher value of heat flux and, of course, of $(t_s - t_w)$.

Effect of Subcooling. Figures 4 through 9 show that, at the same velocity, the heat transfer is greater for the case of lower subcooling (higher bulk water temperature), but the slope of the boiling curves is steeper at higher subcooling (lower bulk water temperature).

That the heat transfer would be higher for lower subcooling can be understood from the higher surface temperatures involved, which, comparatively speaking, are much higher than the saturation temperature of the water, and this results in a more vigorous boiling with attendant higher coefficients of heat transfer. This can be seen readily by comparing any two boiling curves (for fixed velocity) at a given value of $(t_s - t_w)$.

The differences in slope of the boiling curves at fixed velocity may be explained in terms of the bubble formation. Lower water temperature favors the formation of smaller bubbles with higher frequency of formation and collapse, compared with lower frequency and larger size for lower

subcooling, and the greater frequency apparently acts in the direction of more vigorous agitation of the fluid in the boundary layer thereby promoting better heat transfer. Thus, a higher rate of heat transfer will be associated with a smaller temperature increase; consequently, the slope of the boiling curve becomes steeper with higher subcooling. At higher heat flux the curves tend to merge, which may be attributed to the fact that at high heat flux the surface temperatures in both cases have far exceeded the saturation temperature of the water producing vigorous boiling in which case the subcooling, or, more specifically, the bulk water temperature plays a role of much less importance.

Effect of Velocity. In the case of non-boiling heat transfer the boundary layer established on the forward portion of the wire comprises the main thermal resistance. The thickness of the boundary layer decreases as velocity increases, and this results in a decrease of the thermal resistance. For surface-boiling heat transfer the boundary layer breaks down due to the agitation created by the growth and collapse of bubbles; moreover, cooler fluid comes in contact with the heated surface. Hence, the thermal resistance is greatly reduced. The influence of velocity on resistance is, in this case, mainly confined to a sweeping action of the bubbles. Curves plotted in Fig. 10 and 11, each for a given value of subcooling, show that the effect of velocity on the heat transfer is not great once surface boiling commences, and it diminishes proportionately as the vigorousness of boiling increases.

Domain of Vigorous Boiling. Inspection of Fig. 12 reveals that as boiling becomes vigorous at a higher heat flux q'' and a higher tempera-

ture excess $(t_s - t_{sat})$ the curves appear to merge regardless of velocities and subcooling. This clearly indicates that once the boiling is vigorous or fully established at high heat flux, the effect of agitation of the liquid on heat transfer becomes dominant and effects of velocity and subcooling become much less pronounced.

Comparison with other Results. While it appears that no previous data exist for boiling in normal flow to cylinders, a comparison is made with some of the data obtained in another investigation in which a basically different configuration was employed, in order to get an idea of the comparative range of the data with respect to variables other than the geometry and to allow for some general remarks about boiling. For this purpose boiling data obtained by Buchberg and co-workers (16B) for flow of water through an annulus have been used. They are shown in Fig. 26 together with results obtained from the present study. The three sets of data compared were obtained at the same main-flow velocity, degree of subcooling and absolute pressure, but for different configurations and for different amounts of dissolved air in the water.

Certain important characteristics of the curves compared in Fig.26, such as the heat flux and associated surface temperature at incipient boiling, as well as with the slopes of the boiling curves, are listed in Table 4.

As indicated in Fig. 26 and Table 4 the data of Buchberg et al, obtained for an annular-flow system with forced upward flow, were found using two different types of tube materials, namely, stainless steel and nickel. From Table 4 it is seen that the surface temperature of the stainless steel tube at incipient boiling is 280°F while that for the nickel tube, under

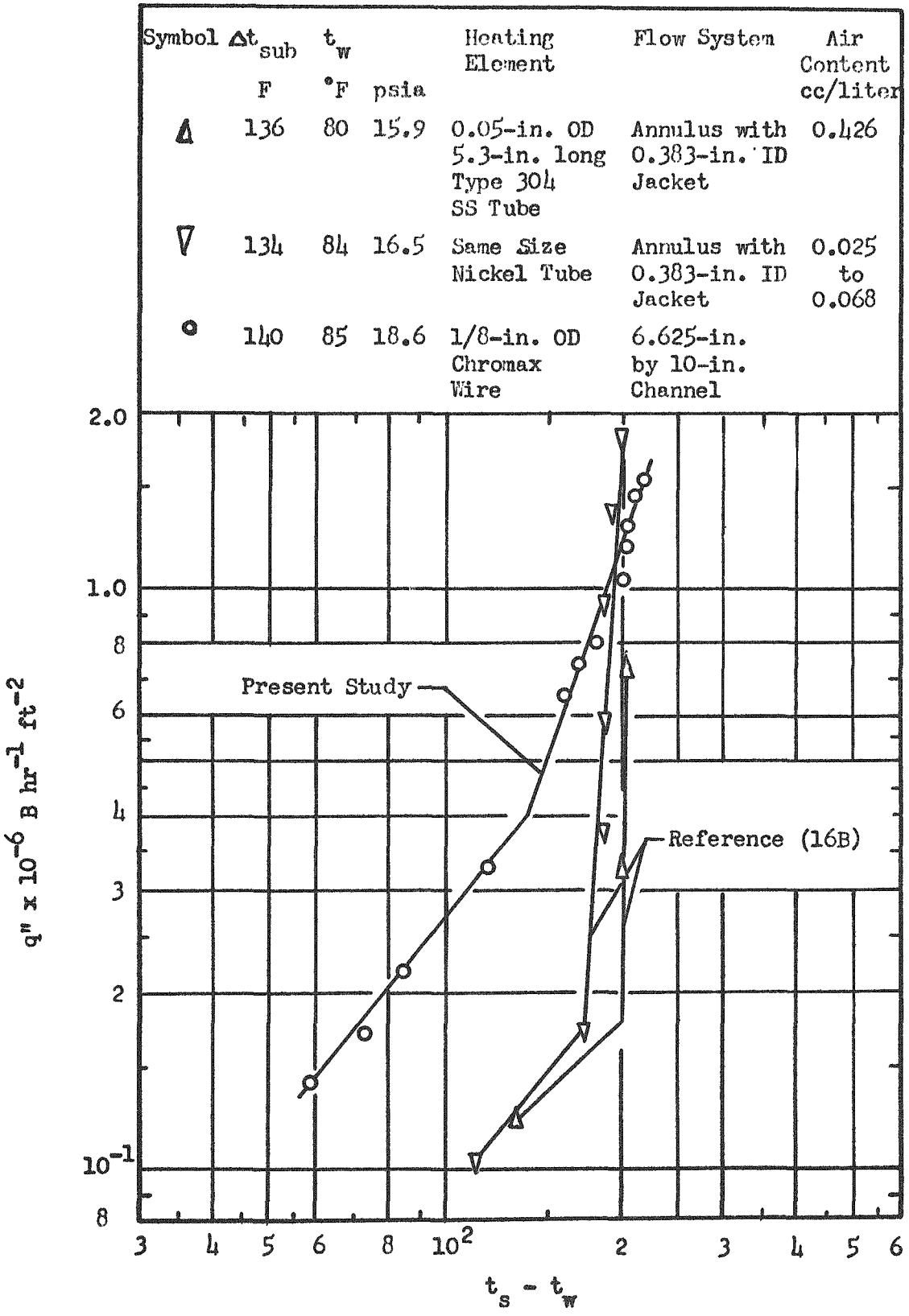

Fig. 26 Comparison of Boiling Data at Velocity 2 ft/sec

identical conditions, was found to be 256°F. At first hand, two variables offer possible explanations for this difference; they are the dissolved air content of the water and the nature of the surface at which boiling occurs.

Table 4. Characteristic Features of the Data Compared in Figure 26.

Heat Flux $\times 10^{-6}$ $\frac{B}{hr\ ft^2}$	Surface Temperature °F	Slope of Boiling Curve	Heated Surface	Source
0.180	280	Vertical	S.S. Tube	Ref. (16B)
0.172	256	19	Nickel Tube	Ref. (16B)
0.420	235	3	Chromax Wire	(Present Study)

Regarding the influence of dissolved gases, it is generally believed that higher gas content of the water facilitates earlier boiling and increased heat transfer, thus lowering the surface temperature at the incipient boiling point. While basically different configurations are compared herein, the effect of configuration on the point of incipient boiling is probably not too great and, therefore, the much lower surface temperature at incipient boiling exhibited by the present data in Fig. 26 is quite likely the result of higher dissolved gas content.[1] This argument is supported by the experimental work of McAdams and co-workers (12) who obtained some limited data for forced flow through an annulus showing that 69cc of dissolved air per liter have a pronounced effect on the initiation of boiling.

[1] No analysis of the air content was made in this study, but, using information from the report of Kreith and Summerfield (13), it is estimated that roughly 20 cc of air were dissolved per liter of water, considering that the water was in equilibrium with atmospheric air on the suction side of the pump.

In view of this, the difference in surface temperature at incipient boiling exhibited by the data of Buchberg and co-workers (see Fig. 26) cannot be attributed to differences in air content because in the case of the stainless steel tube the air content was higher than in the case of the nickel tube. It is most likely that, in the same flow system, different surface temperatures for different points of incipient boiling are attributable to the different surface conditions. Different solid-liquid interfaces usually have different spots favoring the formation of bubbles, in the sense that comparatively lower temperature would allow an earlier initiation of bubbles on one solid surface than on another and comparatively lower temperature difference would allow transfer of heat at a higher rate from one surface than the other. Thus, different solid-liquid interfaces would have different surface temperatures and rates of heat transfer at incipient boiling and would assume different boiling curves. At very high heat flux rates the role of the nature of the surface is less pronounced. This is supported, for example, by the experimental results of Farber and Scorah(9). They studied free-convection boiling heat transfer from four different metals, namely, Chromel A and C, nickel and tungsten to water in a pool under atmospheric and elevated pressures and found that under the same pressure different metals assume different boiling curves.

Furthermore, it is probable that the flow system may also affect (to a certain extent) the surface temperature, at which boiling initiates, as well as the slope of the boiling curve. In an upward annular flow system, bubbles form on the tube wall and rise in the relatively narrow space, interfering with the motion of one another as they progress toward the top. The fluid changes in density and properties as it flows through the

tube. In an open cross flow system, on the other hand, some of the bubbles formed at the front and on the upper and lower surfaces of the wire slide along the surface and most of them are swept away into the water stream and collapse therein. Since the sliding path is very short, the mutual interference would not be as pronounced as that in the case of an annular flow, if important at all.

Comparison of Results of the Present Study obtained using Different Heating Surfaces and Different Techniques of Temperature Measurement. Results obtained in the same flow system and at the same velocity and degree of subcooling, but using different solid-liquid interface and different technique of temperature measurement, are compared herein. The data shown in Fig. 4, obtained from a Chromax wire with thermocouples attached to the surface for measuring the surface temperatures, are compared with the data shown in Fig. 30, Appendix C, obtained using a Type 304 stainless steel tube with outer surface temperatures determined from the measured temperature of the inner wall and the calculated temperature drops across the wall.[1] In both cases the velocity was 1 ft/sec. Table 5 summarizes the main points of comparison.

As pointed out previously, the difference in heat fluxes at incipient boiling and slope of the boiling curves may be attributed to the surface conditions. As can be seen, they are, nevertheless, in the same order of magnitude and show satisfactory agreement, considering that the prevailing conditions, although very close, are not identical.

[1]The auxiliary experiments carried out using a 1/8-in. OD tube are described in Appendix C; the computation of surface temperature of the tube, using the inside wall temperature and the internal heat production in the tube, is also shown there.

Table 5. Comparison of Boiling Data from a Heated Wire with that from a Heated Tube (both present study).

Subcooling F	Incipient Boiling: Heat Flux $q'' \times 10^{-6}$ $\frac{B}{hr\ ft^2}$	Incipient Boiling: Surface Temperature (Approximate) °F	Slope of Boiling Curve	Heated Surface
140.0	0.25	224.0	4.5	Chromax Wire
144.7	0.29	225.0	3.0	S. S. Tube
80.0	0.12	222.5	3.0	Chromax Wire
82.6	0.17	222.6	2.0	S. S. Tube

Burnout

As a check on the reproducibility of data on burnout, which are quite consistent within themselves, a duplicate run was performed at the practically identical conditions of 2-ft/sec velocity and 116.5°F and 116.1°F degrees of subcooling, respectively.[1] The heat flux densities obtained at burnout are 2.030×10^6 B/hr ft^2 and 2.039×10^6 B/hr ft^2, respectively. The deviation amounts to 0.4 per cent.

The locations where burnouts occurred, shown in Fig. 15, should be considered along with the velocity distribution across the test section (under test condition) shown in Fig. 16. Since the velocity in the vicinity of the duct wall is generally lower than that in the mainstream, burnout may be expected to occur in the neighborhood of the duct wall. This was not the case at all; inspection of Fig. 15 shows that only two burnouts occurred near the duct wall and, moreover, no particular spots

[1] See Runs No. 2 and 3 of Test No. 14, Appendix E.

are favored. No doubt the cooling effect at the ends of the wire[1] resulting from the fairly heavy copper electrodes into which the wires are set[2] counteracts the possible effects from lower velocity at the wall. As can be seen, the location of burnout is completely random.

Visual Observations

Visual Observations with Unaided Eyes. The boiling phenomenon could be observed through the Plexiglas window while experimentation was in progress. At moderate heat input, more or less spherical bubbles were formed on the wire surface along the leading edge and trailing edge. (On account of limitations in orienting the lighting, the boiling action on the top surface could not be observed clearly.) Some of the bubbles departed into the main water stream and collapsed faster than the others. Because of the dynamic force of the water, some were pushed along the surface and finally collapsed. As heat flux increased, the size of bubbles became smaller.[3] As heat flux further increased, a fine spray of bubbles would issue from the surface into the flowing water, and audible noise could be heard. As heat flux again increased, a big clump of bubbles would grow and cover a very small portion of the wire at a favored spot along the trailing edge. That portion of the wire located under the clump of bubbles was over-heated and could be seen glowing red. Up to a certain size, the relatively large bubble clump would collapse (condense) as the water pressure overcame the vapor pressure within it, under the condition

---

[1] Outside of the central test zone.

[2] See Fig. 23.

[3] The formation of large bubbles at the early stages is apparently caused by the presence of the dissolved air.

of the net heat transfer prevailing. When the bubble collapsed, the surface momentarily cooled and the brightness of the overheated spot disappeared. In a matter of a few microseconds, the clump of bubbles reappeared over the same spot, and so did the brightness. After a few repetitions the bright spot would extend forward (upstream) to the center of the wire and then burnout occurred instantly. The ability of the wire to withstand the repeated overheating may be attributed to its relatively large heat capacity, which may not be sensitive to the onset of film boiling.

Visual Observations of High-Speed Motion Pictures. From the high-speed motion pictures taken it was observed that a decrease in water velocity increased the bubble number, size, and lifetime; a decrease in subcooling had a similar effect. Due to the presence of dissolved gases, some small and apparently permanent[1] bubbles were carried out from the heated surfaces into the water stream. The pictures also showed that the bubbles formed cyclically.

A reel of high-speed film, from which Fig. 17B was reproduced, was taken at velocity 4 ft/sec, degree of subcooling 114 F and heat flux 2.1×10^6 B/hr ft^2. It was very near burnout condition, and it could be seen that the whole wire was almost covered with big clumps of bubbles swaying around its trailing edge.

---

[1] They had a very slow rate of collapse, unlike the steam bubbles.

CHAPTER VI

SUMMARY AND CONCLUSIONS

Forced-convection heat transfer from an electrically heated Chromax wire oriented normal to a subcooled water flow was experimentally investigated with and without change of phase. Experiments were carried out up to the limit of burnout, and photographic observations were also made. The variables employed in this study range: velocity from 1 to 6.8 ft/sec; subcooling in the range 140 to 80 F; and heat flux density up to 3.5×10^6 B/hr ft^2. Pressures at the test section ranged from 15 to 30 psia.

The following items cover the results and conclusions:

1. The results of the forced-convection non-boiling heat transfer can be correlated with a maximum deviation of 7.6 per cent and an average deviation of 1.9 per cent in the Reynolds number range between 1500 and 11,000 by the following equation:

$$N_{Nu,f} \Big/ N_{Pr,f}^{0.3} = 0.145\, N_{Re,f}^{0.66} \quad . \tag{8}$$

This correlation gives heat-transfer coefficients in good agreement but somewhat lower than would be obtained from an extrapolation of a correlation for liquids presented by McAdams, assuming that McAdams' correlation can be extended beyond Reynolds number 250. The results are in very close agreement with a generalized representation of existing and well-established data for air in normal flow against a cylinder, except for two experimental points at about Reynolds number 2000, which are low.

2. Results obtained in the boiling regime are presented in tabular form (Appendix E) and they are shown in graphical form as Fig. 4 through 12

in which correlating lines are shown.

3. Surface boiling commences when the surface temperature of the heated wire slightly esceeds the saturation temperature of the flowing water at the prevailing pressure (Fig. 4 through 9). The effect of superheat on the initiation of boiling in the cross flow system employed was found not to be pronounced. In this study the point of incipient boiling was obtained as the point of interception of the non-boiling and boiling curves. This implies sudden and sharp change from the non-boiling to the boiling regimes; in reality, the transition is not abrupt, but the assumption that it is results in surface temperatures corresponding closely to the saturation temperature of the water.

4. Once surface boiling begins, the heat transfer mechanism changes. The agitation created by the growth and collapse of bubbles causes a breakdown and virtual destruction of the boundary layer. Thus, thermal resistance is greatly reduced and a very much higher rate of heat transfer results from a relatively small increase in surface temperature; the comparatively low thermal resistance explains the extremely steep slopes of the boiling curves in contrast to those for non-boiling.

5. High degree of subcooling in boiling favors the formation of bubbles of small size with higher frequency of bubble formation and, in view of item (4) above, the thermal resistance is reduced over that for a lower degree of subcooling (all other conditions remaining the same) and a higher heat transfer results. Such an effect, shown clearly by the experimental results in Fig. 4 through 9, becomes less important as the velocity increases, although it is still clearly present at the highest velocity reached, that of 6.8 ft/sec.

6. The influence of the velocity on boiling in the range studied, shown in Fig. 10 and 11, is large at first -- at incipient boiling, however, as the bubble field at the surface becomes better established it diminishes until, at large rates of heat flux (near burnout), it plays a minor role. The decrease of thermal resistance as velocity increases is apparently mainly confined to the sweeping action of the bubbles; when the agitation caused by the bubbles is great (high heat flux) the velocity influence, or sweeping action, becomes relatively unimportant.

7. For vigorous boiling the relationship between heat flux q'' and the temperature difference $(t_s - t_{sat})$ apparently tends toward a fixed limit (before burnout) for a given water temperature. This trend can be seen in Fig. 12, and it represents the change in character of the thermal resistance as the bubble populations become so great that the wire is effectively covered with a blanket of vapor. At higher degree of subcooling (cooler water temperature) the limit of q'' and of $(t_s - t_{sat})$ are higher; whether or not a definite trend is involved cannot be stated conclusively from the data on hand.

8. The results at burnout are correlated with an average deviation of 4.8 per cent by the following equation:

$$q''_{BO} \times 10^{-6} = 0.536 \left(\frac{G}{10^6}\right)^{0.2} (\Delta t_{sub})^{0.8} \qquad (10)$$

in which G is the average mass velocity at the test section in pounds per hour per square foot. The maximum deviation of any experimental point from the above equation was 13.6 per cent.

9. The location of burnout along the wire was found to be random, indicating essentially no effect of the velocity profile on the position of burnout. This is not an unexpected result, considering that the profile is essentially flat over the central 6 inches of the test wire and that the conduction of a small amount of heat from the ends of the wire by the main electrodes counteracts the tendency toward burnout in the vicinity of the wall where lower velocities exist. In general, conditions at the surface favoring the growth of relatively large bubbles bring about burnout at a particular spot.

10. Auxiliary experiments (Appendix B) were conducted for the burnout of Chromax wires comprising the active wire in a simple crossed-wire matrix, in which the horizontal heated wire was arranged between three vertical elements of the same diameter and made of either Teflon or Chromax. The purpose of these tests was to learn whether or not the points of cross over in the simple array are favorable burnout positions. At mainstream velocities ranging between 1 and 6.8 ft/sec, for six separate wire arrays, all burnout positions fell outside of the "cross-over" locations. This result is not considered entirely conclusive, however, because four of the six burnouts occurred within one inch from the wall of the test section, representing a higher frequency of occurrence near the wall than found in the main burnout studies. This is the direct effect of a different and less flat velocity profile employed in these auxiliary studies. Additional experimentation using a screen upstream (as was done in the main tests) is required before more decisive results can be obtained. However, neither of the two burnouts which did occur within the central 6 inches of the test took place at or near the cross over positions. At all events, if the

conditions at the cross-over points strongly favor burnout, it is likely that some evidence would have been found to this effect even within the limited experiments carried out; this was not the case, and more refined experimentation is needed to see whether there is any favoring at all of the crossing points.

11. Some auxiliary experiments were performed at 1 ft/sec using a 1/8-in. OD stainless-steel tube in place of the solid Chromax wire employed in the main tests; in this case the surface temperature was calculated from the internal heat developed and the measured adiabatic wall temperature at the inside surface of the tube. The results of these tests, reported in Appendix C and discussed in Chapter V where they are compared with the main results, show that the surface temperature at which boiling commences agrees closely with that found with the Chromax rods, although the slopes of the boiling curves are somewhat less.

12. High-speed motion pictures show the formation and condensation of the bubbles on the wire surface takes place in a cyclic manner apparently not, however, related to the frequency of the 60-cycle current used. The pictures also show that an increase in the degree of subcooling results in a decrease in size, population, and lifetime of the bubbles; an increase in velocity has a similar effect although much less pronounced. At or near burnout the whole surface was blanketed with bubbles and clumps of bubbles.

13. The use of the heated wire as a sort of resistance thermometer whose surface temperature would be tractable from the measured mean resistance coupled with the theory of non-uniform development of heat within

a rod appears promising. The experimental program was started with the planned use of this method, but, after considerable investigation and effort, difficulties in obtaining the desired degree of accuracy (see Appendix D) forced abandonment of this technique and adoption of the direct surface temperature measurement with necessary corrections. The technique requires a precise knowledge of the thermal and electrical properties of the wire and precise instrumentation; while the properties of Chromax were rather accurately known and the instrumentation was quite precise by research standards, the temperature coefficient of resistance (found indirectly from the resistivity-temperature measurements carried out in our laboratory) was found to be lower than originally anticipated and therefore the method could not be used with accuracy. Only the lack of availability of a reasonably low-cost material having a somewhat higher temperature coefficient of resistance than does Chromax limits use of this method in this application.

APPENDIX A

ANALYSIS OF DATA AND ESTIMATION OF EXPERIMENTAL ERRORS

Analysis of Data

Evaluation of Heat Flux Density. The heat flux density, or the rate of heat transfer from the heated wire to the flowing water was calculated from the following equation:

$$q'' = \frac{3.412\ EI\ (P.F.)}{A_s} \quad . \tag{11}$$

where P.F. is the power factor of the transformer. The calibration of P.F. versus kva has already been shown in Fig. 24. Using Fig. 24 one can obtain the power factor from the output kva, which, in turn, is found from the measurement of voltage and amperage. A_s is the heat transfer area.

Correction of Surface Temperature. Because of difficulties encountered in accurately determining and reproducing the measured resistance of the heated wire, the early idea of using the heated wire as a resistance thermometer was abandoned in favor of the use of the Chromel-Alumel thermocouple wires directly attached to the surface. These thermocouples, silver-soldered to the surface of the wire and protruded out into the flowing water, are subject to thermal conduction through the leads and convection from the leads and to the water,[1] thus decreasing the temperature of the wire at the thermocouple junction. The temperature indicated by the thermocouple, therefore, will not be the true temperature of the surface, that is, the temperature at the spot if the thermocouple were

[1] So-called conduction error.

absent. Although there are other sources of error, such as the error due to imperfect attachment, these are of secondary importance compared to the conduction error. Hence, only correction of the error due to conduction is made.

Boelter and co-workers (26) considered the case of a thermocouple protruding from one surface of a flat plate of which both sides are exposed to flowing fluids. Assuming that the section of the plate occupied by the junction is circular and at an uniform temperature, and that the heat transfer coefficients of the fluids are uniform, they obtained an equation and its simplified solution for temperature corrections as:

$$\frac{t_s - t_{ind}}{t_s - t_w} = \frac{1}{1 + \frac{2\pi r_s}{\gamma} b k_p \sqrt{\beta} \frac{K_1(\sqrt{\beta} r_s)}{K_o(\sqrt{\beta} r_s)}} \qquad (12)$$

where $\gamma = 2\pi r_{tc} \sqrt{2 h_{tc} k_{yc} r_{tc}}$

$$\beta = \frac{h_{p1} + h_{p2}}{b k_p}$$

$$r_s = 2\sqrt{r_{tc}} \quad .$$

The subscript tc refers to thermocouple.

Boelter and Lockhart (27) experimentally verified the above equation and they reported that the results are in fairly good agreement with the theory.

In this study, Eq. (12), after modification, was employed to estimate the temperature correction due to thermal conduction. To approximate the system, the vertical, diametral plane of the wire is assumed to be an insulated plane, and the wire immersed in one fluid is "transformed" into a

rectangular plate of which the cross-sectional area is equivalent to that of the wire and which has a length equal to the wire diameter as its one side. Hence, the thickness of this "transformed" plate is:

$$b = r^2/2r = r/2 = 0.00818 \text{ ft}.$$

The radius and thermal conductivity of AWG No. 28 Alumel-Chromel thermocouple wires obtained from Ref. (27) are respectively:

$$r_{tc} = 0.0126 \text{ in.} = 0.00105 \text{ ft}$$

$$k_{tc} = 16 \text{ B/hr ft F}$$

and the thermal conductivity of Chromax wires obtained from Ref. (30) is:

$$k_p = 7 \text{ B/hr ft F} .$$

Substituting the above numerical values into Eq. (12) gives the working equation,

$$\frac{t_s - t_{ind}}{t_s - t_w} = \frac{1}{1 + 1.86\sqrt{\frac{h^*}{h_{tc}}}\ \frac{K_1(\sqrt{\beta}\, r_s)}{K_o(\sqrt{\beta}\, r_s)}} \qquad (13)$$

and $$\sqrt{\beta}\, r_s = 6.2 \times 10^{-3} \sqrt{h^*} .$$

Assuming that the thermocouple wires are normal to the flow, one may estimate h_{tc}, the heat transfer coefficient between the thermocouple wires and water from Eq. (9),[1] which is valid for Reynolds numbers between 0.1 and 250 in a cross flow system. The heat transfer coefficient between

[1] It appears as Eq. (10-7a) in Ref. (23).

the heated wire and water, h^*, can be estimated from the difference between the indicated surface temperature and the temperature of the water; its effect is discussed below.

All temperature corrections were made from Eq. (13). The values of the Bessel functions involved were obtained from Ref. (28).

It is of interest to investigate the nature of the correction. As an approximation one may consider the vertical plane passing through the axis of the wire as an insulating plane, in which case the system closely approximates that idealized by Boelter and co-workers (26). Suppose now the data of Run No. 16, Test No. 10 (Appendix E), are taken as an example, with a thermal conductivity 9 B/hr ft F selected at the indicated temperature (Fig. 33). Using Eq. (12) and choosing heat transfer coefficients 25 per cent, 50 per cent and 200 per cent of that given by the experimental data shown in Run No. 16, Test No. 10, one obtains the results (b), (c) and (d), respectively, shown in Table 6, where they are compared with a computation based on Eq. (13).

Table 6. Comparison of Temperature Correction based on Estimated Heat Transfer Coefficients.

Case	Equation Used	b	k_p	h^*	t_{ind}	t_s	Per Cent Deviation[1]
		ft $\times 10^{-3}$	$\frac{B}{hr\ ft\ F}$	$\frac{B}{hr\ ft^2\ F}$	°F	°F	
(a)	13	8.18	7	10,860	287	342.8	---
(b)	12	5.20	9	8,340	287	348.0	2.1
(c)	12	5.20	9	5,340	287	359.1	4.5
(d)	12	5.20	9	21,720	287	332.0	3.1

[1]The deviation is based on the corrected temperature 342.8°F.

Inspection of Table 6 shows that the deviation in temperature correction due to the magnitude of the estimated heat transfer coefficient, the depth of the cylindrical source and the slight variation of the thermal conductivity is not too significant. Even with the extremes chosen, it amounts to 4.5 per cent out of total correction 19 per cent at most. The example shown is a very much amplified one to illustrate the relative insensitivity of the correction to the above variables.

Experimental Errors

The measured quantities of main importance in this study are: the heat flux density, flow rate and velocity of the fluid, temperatures of water and the heated wire, absolute pressure and the condition of the water.

The nominal diameter of the Chromax wire is 0.125 in. and its variation was found to be within $\pm$ 0.0004 in., or $\pm$ 0.3 per cent. The nominal heated length of the wires is 10 in. within less than 1/32 in., that is, $\pm$ 0.3 per cent. Hence, the heat transfer area is known within $\pm$ 0.6 per cent.

The electrical power dissipated by the heated wire was obtained by measurements of current passing through it and voltage drop across it. The voltage drop was measured with either a Weston Model 341 voltmeter with a full-scale accuracy of 0.25 per cent or a Westinghouse Type G voltmeter with a full-scale accuracy of 0.5 per cent. In either case the measurements are accurate within 0.5 per cent. The contribution to voltage drop due to potential tap located at the electrode is less than 0.2 per cent. Hence, the probable error in voltage measurement is within $\pm$ 0.7 per cent. The current measurements were made with a Weston Model 370

ammeter with a full-scale accuracy of 0.25 per cent together with a current transformer either of Westinghouse Style 29798, or a Weston Model 461, Type 1 or 2. All of them have an accuracy of 0.25 per cent. Therefore, the accuracy in current measurements is estimated to be within ± 0.5 per cent. The determination of power factor of the transformer was made with a Weston Model 310 wattmeter with an accuracy of 0.25 per cent in conjunction with a voltmeter and ammeter and a current transformer as used in the determination of voltage drop and current. The accuracy of the determination of power factor is within 0.3 per cent. Consequently, the accuracy of electrical power dissipation is within ± 1.5 per cent and the accuracy of heat flux density is ± 2 per cent as a maximum, with the probable error somewhat less than this value.

The temperatures of the water, measured with calibrated copper-constantan thermocouples, are accurate to ± 0.2°F. The Chromel-Alumel thermocouple wires used to measure surface temperature were calibrated and found to be - 0.1°F at 300°F from the standard Leeds and Northrup conversion table. They were subjected to errors due to conduction, method of attachment, change of metallurgical structure of the portion of the metal, and the local turbulence at the place where silver-soldering was made; attention has only been directed to the correction of conduction error, the main source of error.

The velocity or the flow rate measurements are estimated to be in error by not more than ± 2 per cent. The manometer used has 0.1-in. divisions and can be estimated to 0.02 in., and during operation only minor fluctuations of manometer fluid were observed. Most of the error is contributed by the uncertainty of orifice calibration.

The absolute pressures were measured with a manometer with 0.1-in. divisions. The mercury column could be estimated to 0.02 in. The fluctuations sometimes were two or three times the division value. These fluctuations could cause, at most, about $\pm$ 0.5 per cent error in the runs at low flow rates, and the error will be much less at high flow rates.

The electrical resistance of the water was measured with a Leeds and Northrup conductivity bridge with about $\pm$ 3 per cent accuracy and its pH values were determined with a Bechman Model G glass electrode pH meter with an accuracy of $\pm$ 0.2. Their accuracies are believed to be within the limits of the instruments employed.

As mentioned in the main text, no attempt was made to obtain energy balance between the electrical and thermal energy. Even if the system were insulated, such a balance would be difficult, if not impossible, to achieve.

APPENDIX B

PRELIMINARY EXPERIMENTAL STUDY ON BURNOUT OF A SIMPLE MATRIX

The work presented herein is a preliminary experimental study on the location of burnout in a simple matrix made of crossed wires. Specifically, it was desired to learn whether or not the cross-over positions of the rods are favored burnout positions.

The experimental apparatus used in this study is the same as that described in Chapter III, except that the test section was modified to accommodate three vertical elements, either of Teflon or of Chromax.

The horizontal heated 1/8-in. OD Chromax wire was arranged between three vertical elements, also of 1/8-in. OD, one at the midpoint downstream of the horizontal wire, the other two located on the upstream side. All these vertical elements had a transverse pitch of 4 diameters and longitudinal pitch of 2 diameters. Each of them was slipped through pre-drilled matching holes in the upper and lower Plexiglas windows. O-rings, packing glands and brass fittings were also provided to keep the wires in position and to prevent leakage. By turning tension nuts into the threaded ends of each vertical element against the brass fitting, the element could be straightened and a good contact with the test wire would result.

Figure 27 is a photograph of the test section showing the arrangement of the simple matrix, as assembled, prior to installation. Before assembling the test section to the system, the contact points between the vertical elements and the horizontal test wire were inspected under light from an electrical lamp. After assembly, the pump was turned on and a desired flow rate was set. Power was then turned on and gradually increased until burnout occurred.

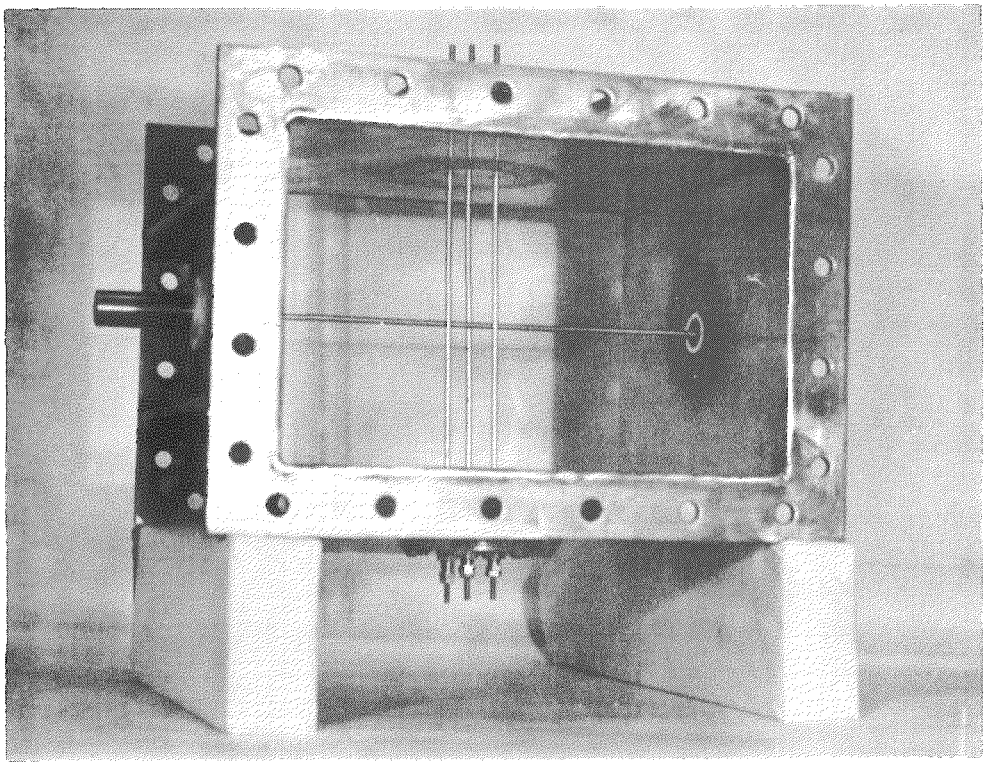

Fig. 27 Assembly of Simple Matrix

In these experiments no screen was installed upstream of the test section because it was temporarily out of service. The velocity distributions determined using a movable Prandtl tube are shown in Fig. 28.

Runs were made at mainstream velocities at 1, 3, and 5 ft/sec with Chromax wire as vertical elements; Teflon rods were used at velocities of 2, 4, and 6.8 ft/sec.

The results of location of burnout are plotted in Fig. 28. As can be seen, three burnouts occurred at about 1/2 in., one at about 7/8 in. and one at about 2 in. from the duct wall, and one at 1-1/4 in. from the center. In no case did the wire burn out at any of the crossing positions in this simple matrix. Nevertheless, one must consider the results in the light of the experimental conditions. Four of the six burnouts obtained occurred within 1 inch of the wall, and these were for the highest mean velocities. The two burnouts occurring within the central 6-inch portion of the wire were obtained at the lowest speeds in which case the velocity profiles are reasonably flat in the central regions. While it must be considered that the comparatively low velocity near the wall probably favors burnout in this vicinity, neither of the two burnouts in the central regions occurred at or even close to the matrix assembly. It would seem that if the cross-over positions were strongly favored burnout locations, some evidence would have been forthcoming even from these simple tests.

Although no burnout took place at the crossing positions, no definite conclusions can be drawn from these simple and limited tests except that the favoring, if it exists, is probably not strong, and, therefore, a more detailed and thorough investigation would be required to detect whether or not the cross-over points are favored hot spots at all. Such an investiga-

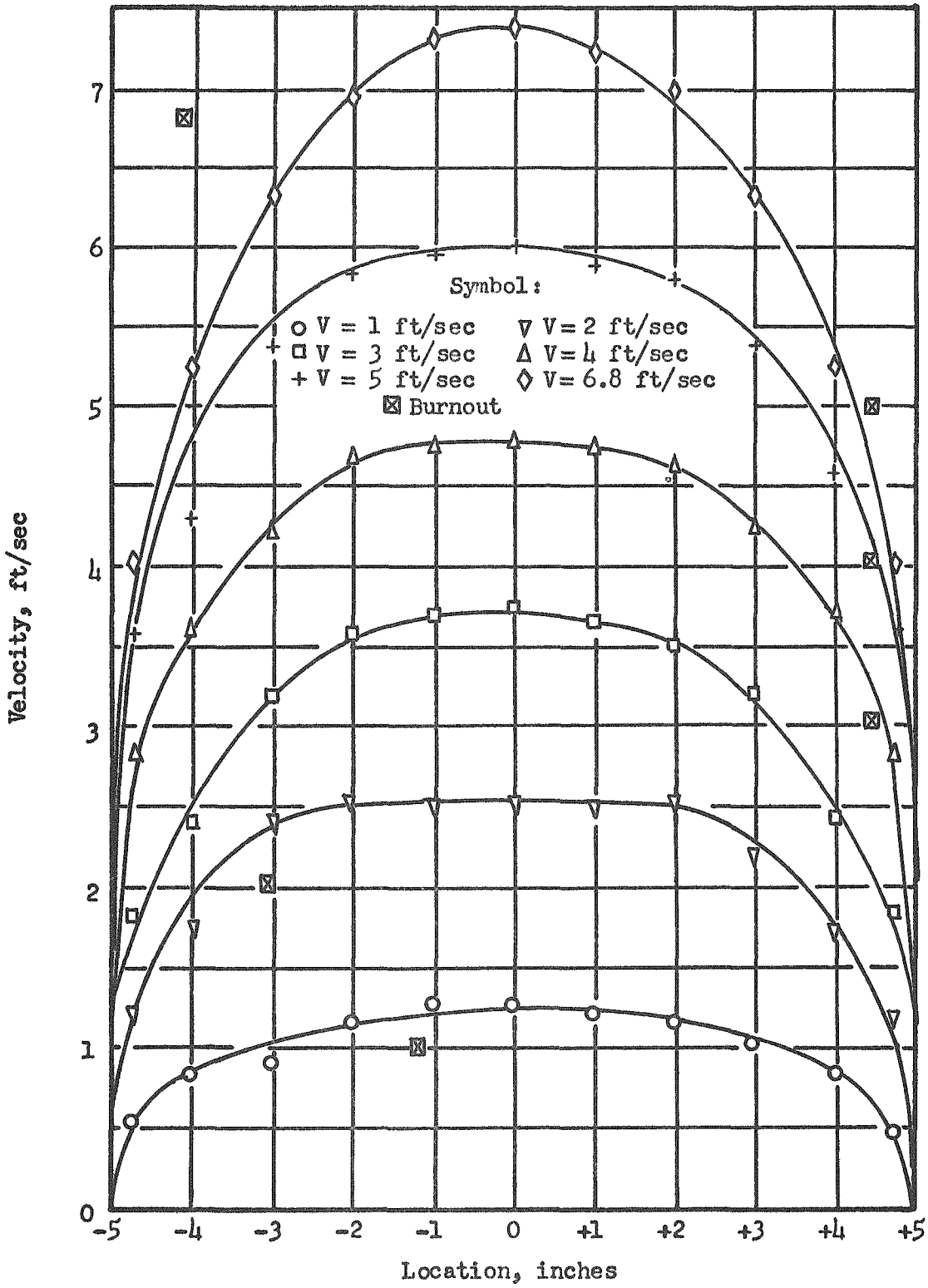

Fig. 28 Location of Burnout in a Simple Matrix and Velocity Distribution at Test Section (without upstream screen)

tion should be carried out for a complete matrix assembly using also smaller transverse and longitudinal pitch.

APPENDIX C

BOILING HEAT TRANSFER FROM A 1/8-in. OD TYPE 304 STAINLESS STEEL TUBE

The objective of experimental work reported in this Appendix was to obtain data on boiling heat transfer using a different metal as the heating element and a different technique to determine the surface temperature, so that a comparison with the main data could be made.

The experimental apparatus employed in this study are the same as those described in Chapter III, except that, instead of a wire, a 1/8-in. OD by 0.02-in. wall Type 304 stainless steel tube was used as a heating element; also, the outer surface temperature was calculated from the measured inside wall temperature and the heat developed within the tube.

Thermocouples for measuring inner wall temperatures were made from AWG No. 28 Alumel-Chromel wires with a part of their cotton insulation removed. The leads were inserted into a 1/16-in. OD, 2-hole porcelain insulator, 4 inches long; their ends were then twisted and silver-soldered with a 1/32-in. bead as a hot junction. Each heated tube had two thermocouples installed, one from each end, and each was located at 2-1/12 in. from the tube center. The end of the thermocouple was slightly bent, so that it would be in contact with the inner wall of the heated tube when inserted. The ends of the tube were separately silver-soldered to a 1/2-in. threaded copper plug for a good electrical conductor. The gaps between the porcelain and heated tubes were sealed with Paxalloy to avoid leakage.

The heated tube assembly was installed in the test section with the location of thermocouple leads facing downstream. The thermocouple leads

passed through pre-drilled holes along the axis of the electrodes and connected to a selector switch.

When runs were made, the main pump was first turned on and a desired flow rate was next set. The cooling system and electrical heaters were manually regulated so that a constant water temperature was maintained. After loads were applied, 15 minutes were allowed with fixed conditions prior to the recording of data.

The outer wall temperature was calculated from a Taylor series solution of the temperature distribution for heat conduction in an electrically heated tube with adiabatic inner wall. The working equation,[1] a simplification proposed by Rohsenow and Clark (18) wherein higher order terms are neglected and which is accurate within 5 per cent, is as follows:

$$t_i - t_o = \frac{m}{k_i \rho_i}\left[\overline{\Delta x}^2 + \frac{\overline{\Delta x}^2}{r_i} + \ldots\right] \tag{14}$$

where $$m = \frac{3.412\ I^2 \rho_m^2}{2\pi^2 (r_o^2 - r_i^2)^2}$$

In the system employed,

$$r_o = 0.0625 \text{ in.} = 0.00521 \text{ ft}$$
$$r_i = 0.0425 \text{ in.} = 0.00354 \text{ ft}$$

The working equation then becomes

$$t_i - t_o = 1.742 \times 10^3 \frac{I^2 \rho_m^2}{k_i \rho_i} \tag{15}$$

---

[1] The derivation and solution of the equation were originated by Kreith and Summerfield.

The equation allows for variations of electrical resistivity and thermal conductivity with temperature; the thermal and electrical properties were provided by the manufacturer of the heated tube (29) and they are shown in Fig. 29.

Experiments were made for runs at velocity of 1 ft/sec and degrees of subcooling of 144 F and 83 F. The outside wall temperatures were calculated from Eq.(15) and the results are shown in Fig. 30. The slope of heat flux q'' versus temperature difference $(t_s - t_w)$ curves in the nucleate boiling region is approximately 2.84 for the 144 F subcooling run and approximately 2.0 for the 83 F subcooling run. It also shows that the latter tends to merge with the former. The results are in satisfactory agreement with those obtained from boiling heat transfer from Chromax wires at the same velocity, approximately the same degree of subcooling and in the same flow system. The comparison of the results has been discussed in Chapter V.

As can be seen from Eq. (14), the temperature drop across the tube wall is inversely proportional to the thermal conductivity and electrical resistivity. Both of them are dependent on temperature. That is to say, the accuracy of the calculated outer wall temperature depends on the values of thermal conductivity and electrical resistivity. Since the chemical compositions and metallurgical structure of the stainless steel may differ slightly from heat to heat, slight variations may exist in thermal conductivity and electrical resistivity. The curves shown in Fig. 29 are only representative, average values of the metal. They may not be the exact, specific values pertaining to the tube used. For better

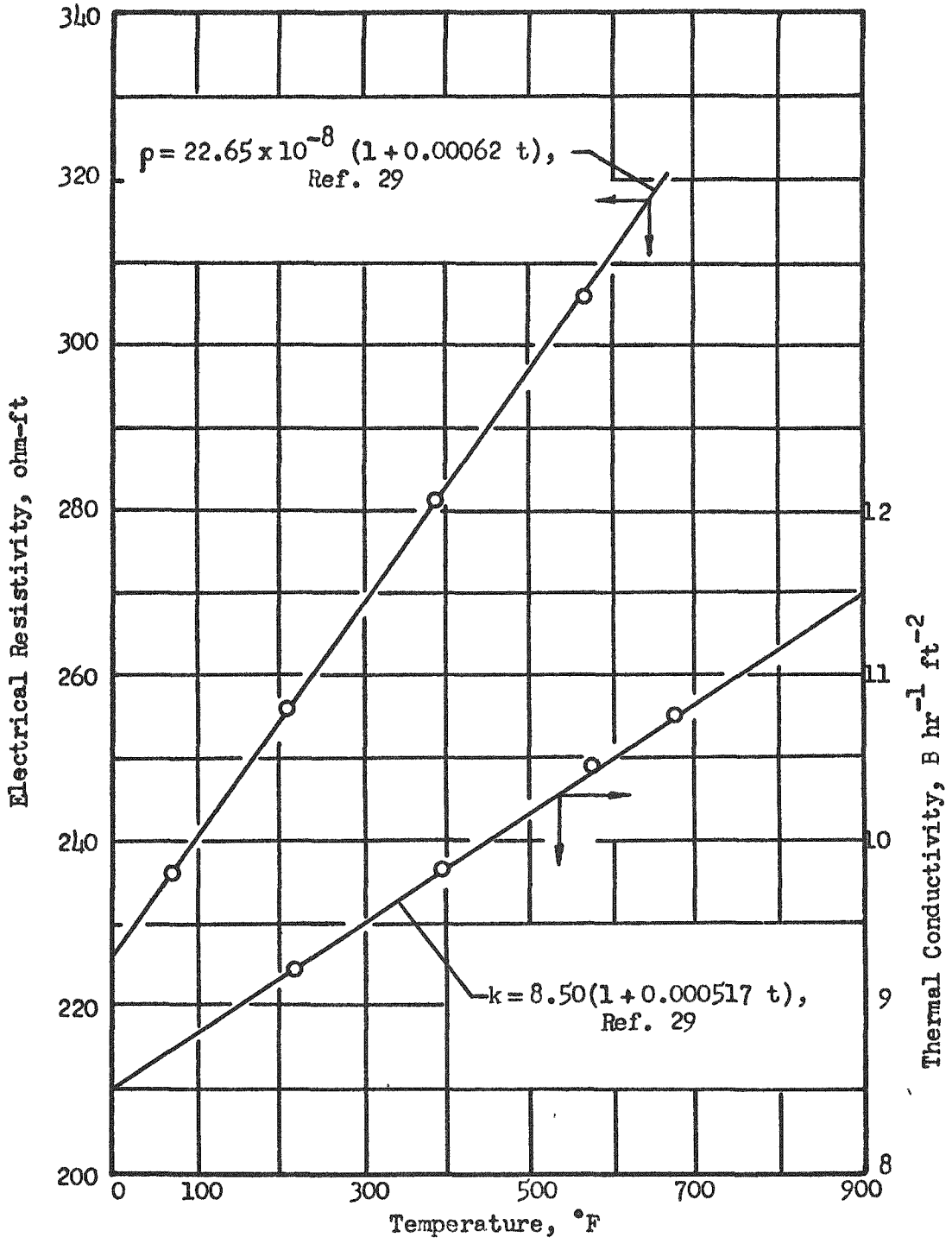

Fig. 29 Electrical Resistivity and Thermal Conductivity of Type 304 Stainless Steel

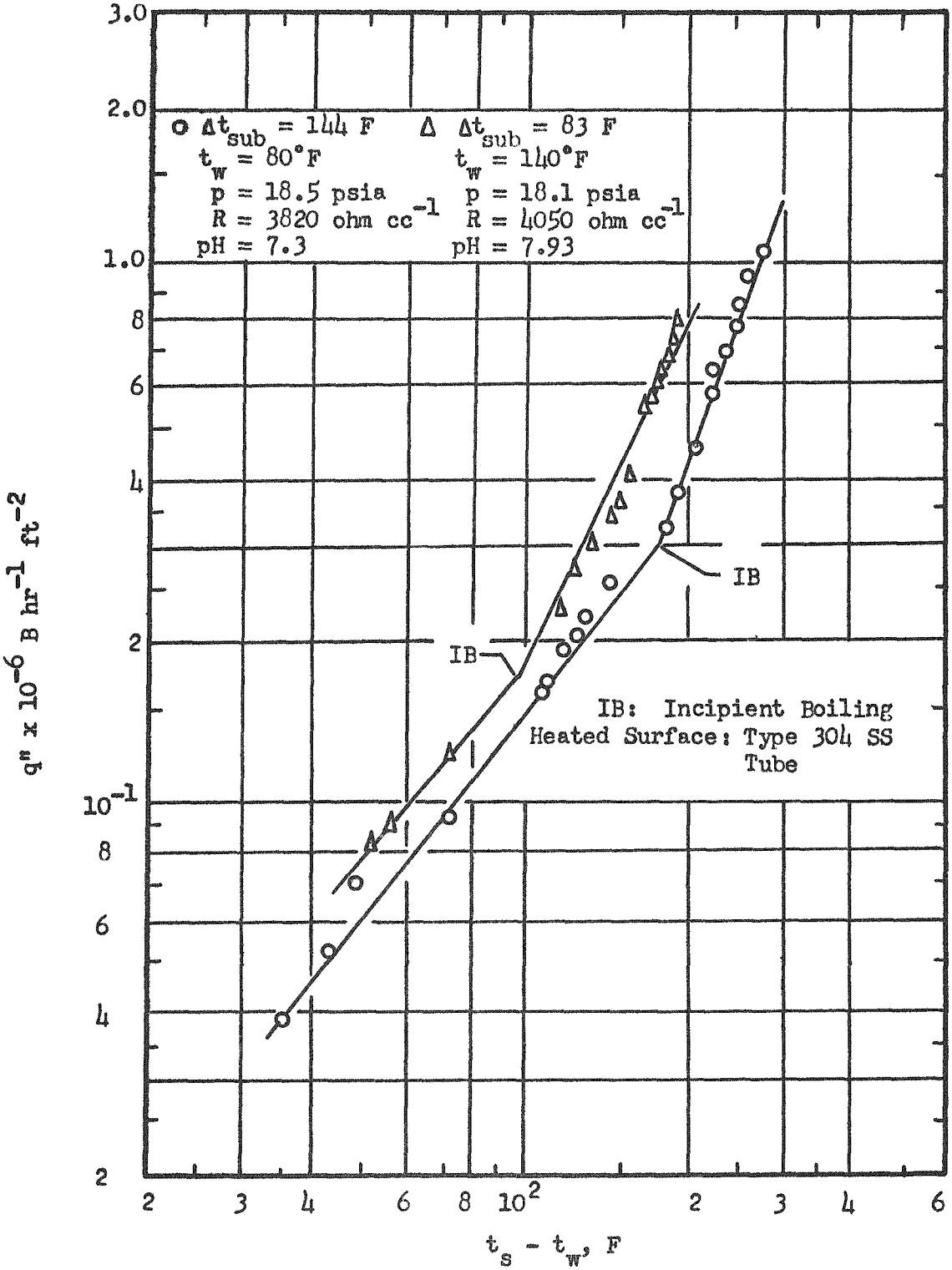

Fig. 30 Effect of Subcooling on Boiling at Velocity 1 ft/sec using a Stainless-Steel Tube

results, more precise values of thermal conductivity and electrical resistivity should be obtained by direct measurements. However, this was beyond the scope of this work.

APPENDIX D

USE OF THE HEATED WIRE AS A RESISTANCE THERMOMETER

In the present study initial attempts were made to use the Chromax wire as a heating element as well as a sort of resistance thermometer to obtain the surface temperature. This method requires a precise knowledge of the electrical and thermal properties of the wire as a function of temperature.

The report presented herein contains the calibration of the Chromax wire and the discussion on experiences with and the possibilities of employing the method.

Calibration of Wire

Figure 31 shows the wiring diagram for calibrating the electrical resistivity of the Chromax wire versus temperature, and Fig. 32 is a photograph showing the experimental apparatus.

Each Chromax wire tested, 1/8-in. diameter by 33-in. long, was threaded for about 2 in. at both ends to adapt tension nuts. Two 1/32-in. OD porcelain insulated copper wires were separately inserted and silver-soldered to two pre-drilled holes, each at 3 in. from the longitudinal center of the wire. These copper wires were used as lead wires to measure the potential drops; they were connected to the selector switch. The wire assembly was then placed inside the 2-in. ID combustion tube of the 110-volt, 60-cycle, single-phase a-c electric furnace (Sentry Model V #7). The tested wire was supported in three places with fire brick along the inside of the combustion tube. Both ends of the wire and potential leads passed through Lava plugs which closed the two ends of the combustion tube. The

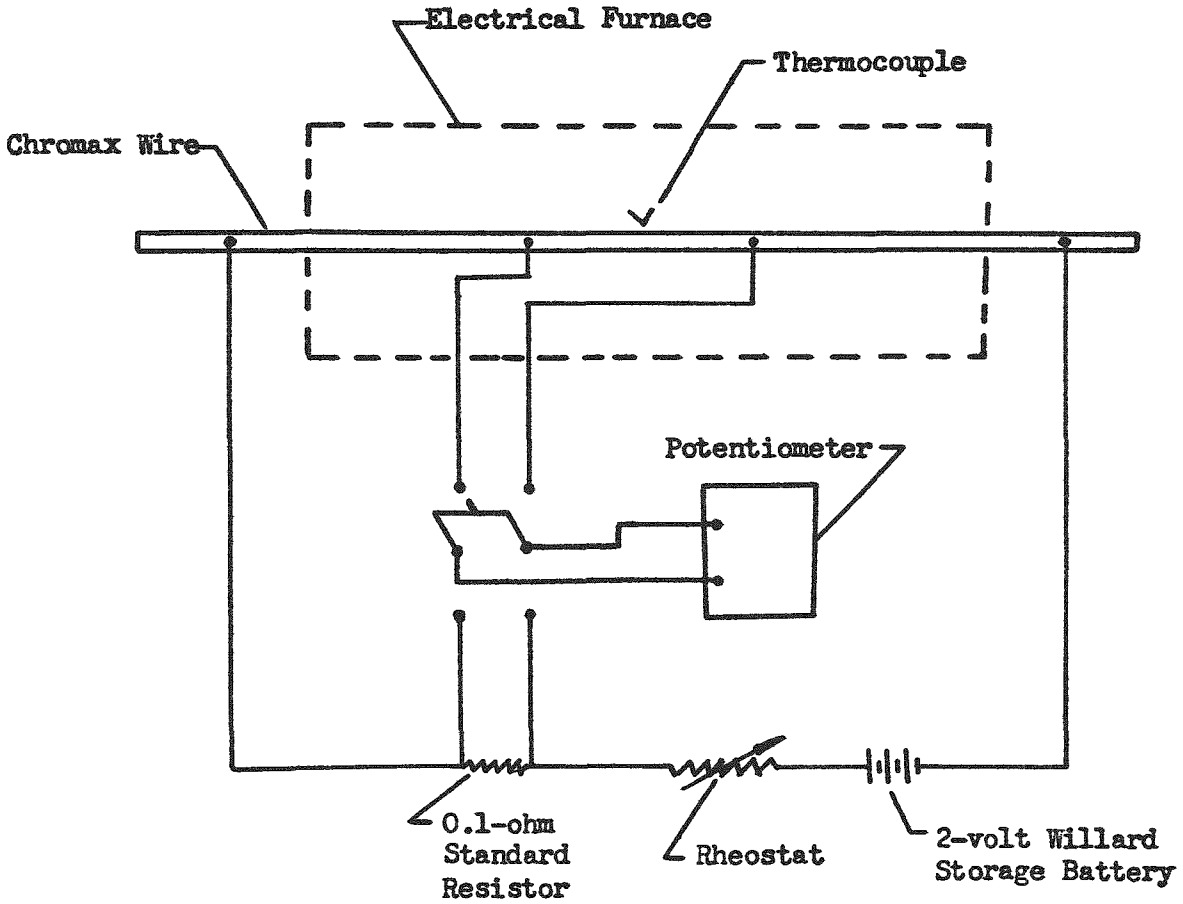

Fig. 31 Wiring Diagram for Calibration of Chromax Wires

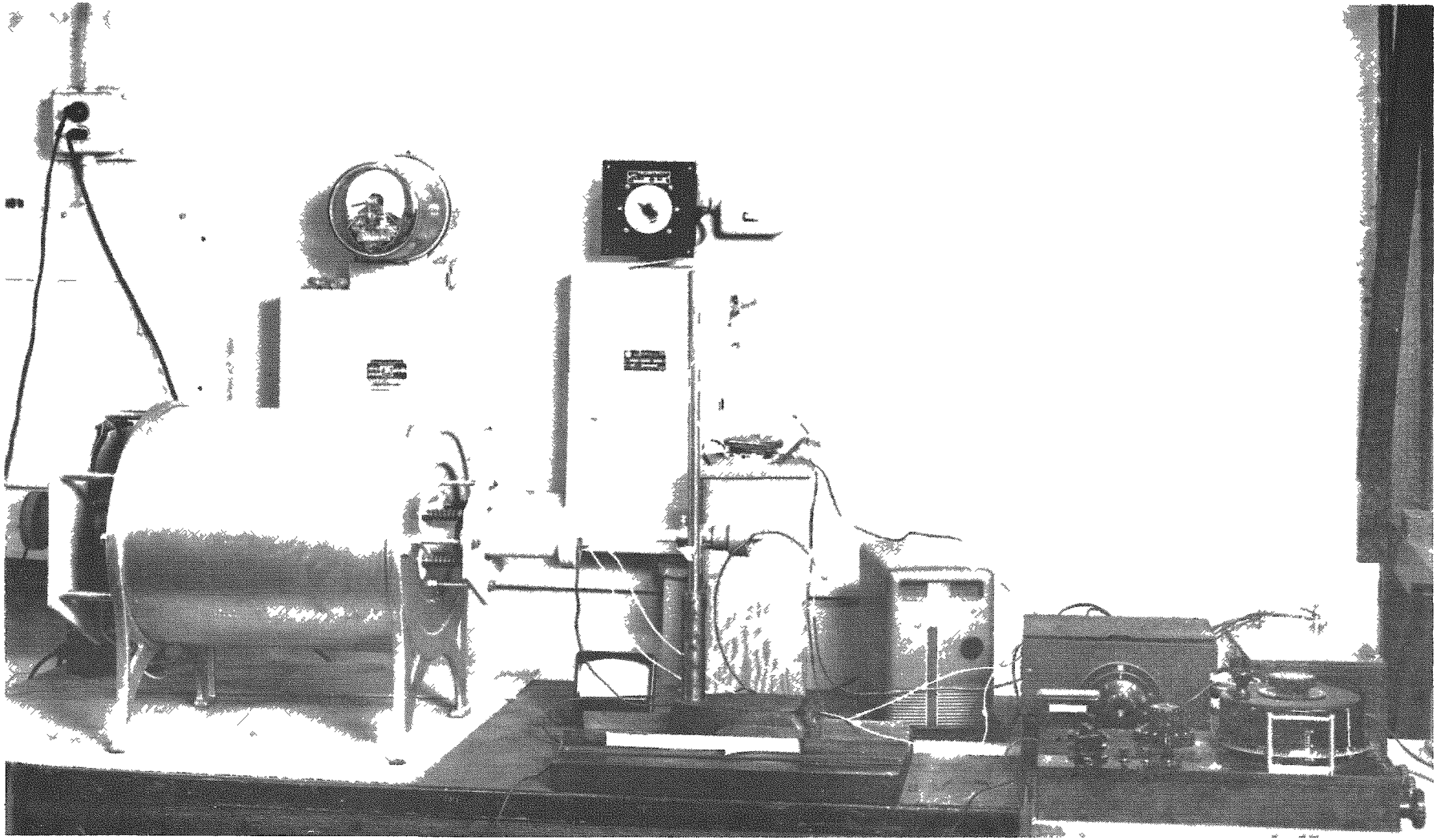

Fig. 32 Apparatus for Resistivity Calibration of Chromax Wires

sagging of the wire (under high-level heating) was diminished by turning the tension nuts against the Lava plugs; only enough tension was applied to prevent excessive sag.

For determining the temperature prevailing inside the furnace, a movable 24-in. platinum-platinum plus 10 per cent rhodium thermocouple (Leeds and Northrup Model 8702) shielded in a porcelain protection tube was used, and it was placed inside the furnace with its junction at the longitudinal center of the wire. Extension wires (Leeds and Northrup Type 16-60-1) were also used to form a cold junction and to connect to a selector switch.

Electric current for the measurement of resistance was supplied by a 2-volt Willard storage battery. In series with the rheostat was a 0.1-ohm standard resistor made of a Manganin strip and across which two potential leads were connected to the selector switch (See Fig. 31). A K-2 potentiometer was used to measure the electromotive force.

In this calibration both unannealed wires and wires annealed at 1800°F for two hours and cooled inside the electrical furnace were employed.

The resistivity of the tested wire at a measured temperature was calculated from the following equation:

$$\rho = 2 R_2 \frac{E_1}{E_2} A_c \qquad (16)$$

where R_2 is 0.1-ohm, the resistance of the standard resistor, E_2 the potential drop across the standard resistor, E_1 the potential drop across the 6-in. portion of the tested wire and A_c the cross-sectional area of the wire, 15,280 circular mils. The results of this calibration is shown in Fig. 33.

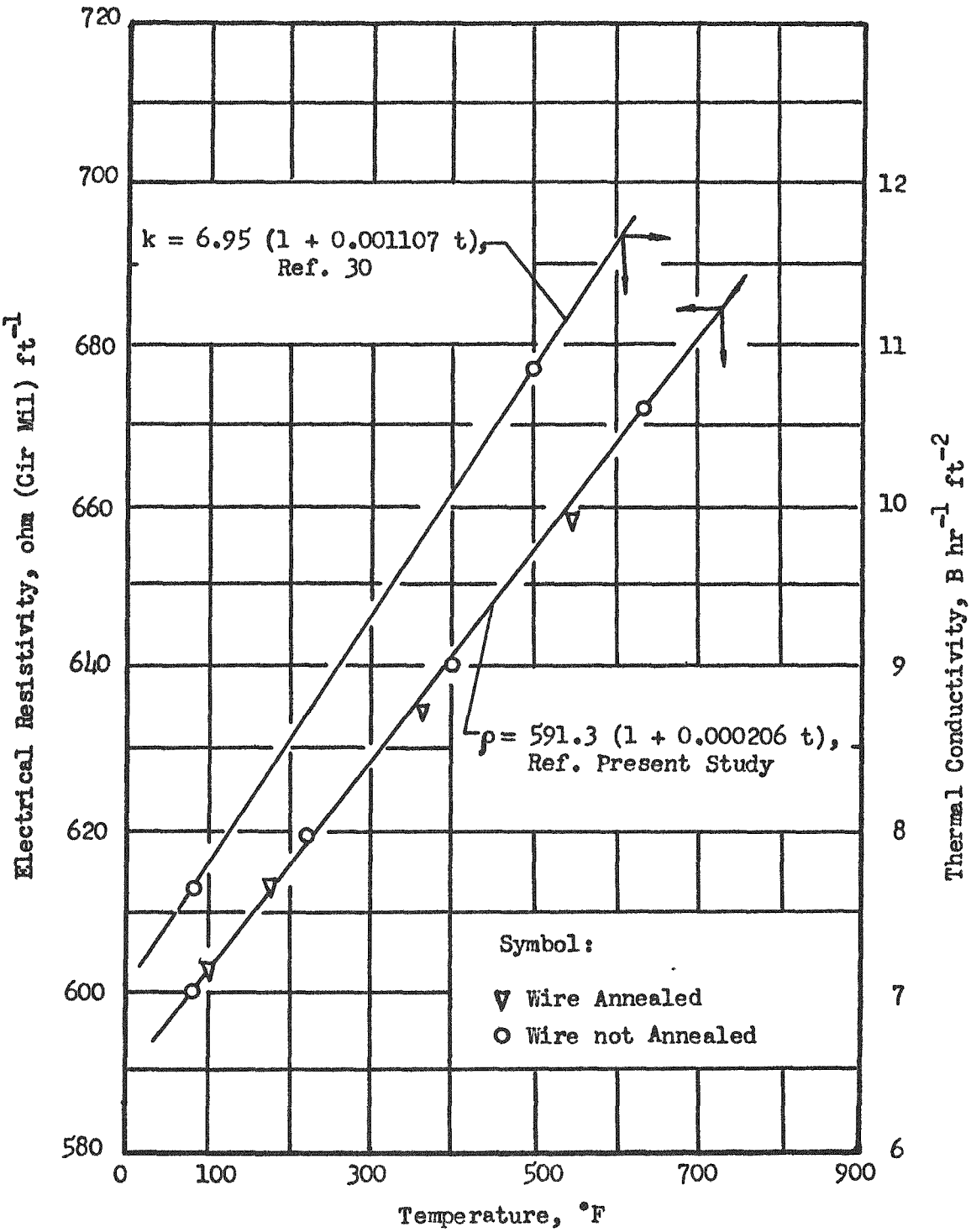

Fig. 33 Electrical Resistivity and Thermal Conductivity of Chromax Wires

According to the manufacturer of the wire, the thermal conductivity and electrical resistivity of the wire may change from heat to heat but it is claimed that the variation of thermal conductivity is not substantial. The values of the thermal conductivity shown in Fig. 33 are those supplied by the manufacturer.

Determination of Surface Temperature

Considering heat non-uniformly generated inside a cylindrical body and analyzing the temperature field within it, Jakob (24) obtained a solution for the difference between the mean temperature of the body and its surface temperature as:

$$\theta_m = \frac{1}{\epsilon}\left[\frac{2\,J_1(\sigma')}{\sigma'\,J_0(\sigma')} - 1\right] \qquad (17)$$

where $\theta_m = t_m - t_s$, F

ϵ = temperature coefficient, 1/F

$\sigma' = r\sqrt{\epsilon\, q'''_m/k}$.

Assuming that the heat transfer coefficient around the wire is uniform (that is, the surface temperature of the wire is uniform), one may apply the above equation to determine the surface temperature by employing the mean temperature of the wire, which may be accurately determined if very precise values of the current passing through and the potential drop across the wire can be obtained.

Consider, for example, Run No. 14, Test No. 2, Appendix E. For convenience, the experimental data are enumerated as follows:

Potential Volts	Current: Meter Reading	Current: Transformer Ratio	Current: Amperes	Heat Flux $q'' \times 10^{-6}$ B/hr ft^2	Surface Temperature: Indicated °F	Surface Temperature: Corrected °F
21.0	3.68	160:1	588.8	1.5518	262.3	300

The other physical and geometrical properties pertinent to the wire employed may also be given as follows: $r = 1/16$ in. $= 0.0052$ ft; $A_c = 15{,}280$ cir mil; $L = 10$ in. $= 0.834$ ft; $v = 7.08 \times 10^{-5}$ ft^3; and $\epsilon = 0.000206$ 1/F, where the temperature coefficient ϵ is obtained from the calibration curve as shown in Fig. 33 (a constant within the temperature range).

From the above data one may proceed to estimate the surface temperature. The heat generated per unit volume is:

$$q'''_m = \frac{3.412\ E\ I\ (P.F.)}{v} = \frac{3.412 \times 21 \times 588.8 \times 1}{7.08 \times 10^{-5}}$$

$$= 595.88 \times 10^6 \text{ B/hr ft}^3 .$$

The electrical resistance and resistivity at the test condition are, respectively:

$$R' = \frac{E}{I} \times \frac{12}{10} = 0.042799 \text{ ohm/ft}$$

$$\rho = R'A_c = 0.042799 \times 15280 = 653.97 \text{ ohm/cir mil/ft} .$$

Based on the above value of electrical resistivity, one can find, from Fig. 33,

$$t_m = 505°F$$

$$k = 10.9 \text{ B/hr ft F} .$$

Again,
$$\sigma = r\sqrt{\epsilon q'''_m / k} = 5.2 \times 10^{-3} \frac{2.06 \times 10^{-4} \times 595.88 \times 10^{-6}}{10.9}$$

$$= 0.5518 .$$

From table shown in Ref. (31) one gets

$$J_o(\sigma) = J_o(0.5518) = 0.927$$
$$J_1(\sigma) = J_1(0.5518) = 0.265 .$$

Substituting the pertinent values into Eq. (17) gives

$$\theta_m = \frac{1}{2.06 \times 10^{-4}} \left[\frac{2 \times 0.265}{0.5518 \times 0.927} - 1 \right] = 175.4^\circ F$$

or,

$$t_s = t_m - \theta_m = 505 - 175.4 = 329.6^\circ F .$$

This is 29.6°F, or 10 per cent, higher than the temperature measured with thermocouples and corrected for conduction error.

Discussion and Conclusions

During the main experiments a Weston Model 341 voltmeter was used to measure the voltage and a Weston Model 370 ammeter coupled with a Weston Model 461 Type 1 current transformer with a ratio 800:1 was used to measure the current flowing through the wire. All the instruments have an accuracy of 0.25 per cent. It is of interest to estimate the error in the determination of surface temperature within the accuracy limit of the instruments.

Suppose the voltage reading is on the high side and amperage on the low side. From the nominal values shown in the above example one can obtain within the limit of accuracy,

$$E = 20.95 \text{ volts}; \quad I = 590.3 \text{ amp} .$$

Hence, $R' = 0.042588$ ohm/ft and $\rho = 650.7$ ohm/cir mil/ft.

From Fig. 33 one gets,

$$t_m = 480^\circ F \quad \text{and} \quad k = 10.7 \text{ B/hr ft F} .$$

Proceeding as previously, one finds.

$$o = 0.5564; \quad J_1(o) = 0.268; \quad J_o(o) = 0.926$$

from which

$$\theta_m = 196^\circ F, \text{ and } \quad t_s = t_m - \theta_m = 480 - 196 = 284^\circ F \ .$$

This is 16°F, or 5 per cent, lower than the temperature measured by thermocouples and corrected for conduction error.

Inasmuch as the accuracy of the measured physical quantities are within the accuracy limit of the instruments employed, 0.50 per cent deviation of electrical resistivity from its nominal value would cause as much as 15 per cent, or 45.6°F, deviation of surface temperature from its nominal value. It should be pointed out that the above discussion is only concerned with the deviation within the accuracy limit of the instruments and neglects the error from other sources. If, as it unavoidably does, human error arises, for example, the reading from the ammeter with a current transformer 160:1 could have been read $\pm$ 0.01 from 3.68. This amounts to a difference in 16 amperes, or 0.3 per cent, and the temperature error thus induced would be much higher.

It may be concluded that the use of the heated wire as a resistance thermometer appears promising. In practice, it requires very precise determination of the thermal and electrical properties of the wire and precise instrumentation. It is also noted that the deviation in mean temperature or surface temperature can be reduced, provided a material with a large increase in electrical resistivity per unit temperature can be selected, but, unfortunately, excluding expensive materials such as platinum,

it appears that no such materials are readily available. In fact, Chromax was originally selected because it has the most favorable resistance-temperature relationship of a whole class of nickel-chromium alloys. It has a much larger temperature coefficient than the usual stainless steels which have been used for the most part in other boiling studies where electrical power is used as the energy source.

APPENDIX E

TABULATION OF EXPERIMENTAL DATA

This appendix comprises all experimental data, including peripheral data concerning such items as calibration.

Test No. 1, comprised of 18 runs, covers the data for non-boiling heat transfer.

Tests No. 2 through 13, representing a total of 175 runs, cover the data for surface-boiling heat transfer at different velocities and degrees of subcooling.

Test No. 14 presents the data of the burnout studies; a total of 31 runs are listed, the last six of which are taken from the burnout studies of simple matrices.

Test No. 15 presents the measurements for the velocity distribution across the test section.

Test No. 16 covers the data for surface-boiling heat transfer from the Type 304 stainless steel tube, 36 test runs in all.

Test No. 17 covers the reproducibility of the soldered-on thermocouples.

Test No. 18 presents the data for determination of power factor for the power transformer.

Test No. 19 is a presentation of data used for the determination of electric resistivity of Chromax wire as a function of temperature.

TEST NO. 1

Forced-Convection Non-Boiling Heat Transfer
at Constant Heat Fluxes

Date: 5-11-56; p_{atm} = 29.47 in. Hg; t_{rm} = 76°F; t_w = 85°F.

Run No.	V	$q'' \times 10^{-6}$	t_{ind}		Temperature Correction: h^*	h_{tc}	$\left(\frac{h^*}{h_{tc}}\right)^{1/2}$	$K_1(\sqrt{\beta}\, r_s)$	$K_0(\sqrt{\beta}\, r_s)$	t_s	h	t_f	$\left(\frac{hD}{K_f}\right)\Big/\left(\frac{c_p f}{K_f}\right)^{0.3}$	$\frac{\rho_f VD}{\mu_f}$
	ft/sec	B/hr ft^2	mv	°F	B/hr ft^2 F	B/hr ft^2 F				°F	B/hr ft^2 F	°F		
1	1	0.0860	2.603	147.3	1380	3960	0.591	4.106	1.620	169.0	1012	117.5	19.3	1655
2	2	"	2.255	132.2	1832	5650	0.570	3.513	1.487	151.1	1300	118.0	30.0	3310
3	3	"	1.882	116.2	2780	6950	0.634	2.779	1.297	128.5	1975	106.8	37.1	4550
4	4	"	1.768	110.8	3330	7950	0.647	2.500	1.215	121.4	2360	103.2	44.0	5910
5	5	"	1.705	108.2	3710	8780	0.650	2.345	1.167	117.9	2610	101.5	48.5	7180
6	6.8	"	1.595	103.5	4650	10620	0.660	2.047	1.068	111.4	3260	98.2	59.6	9300
7	1	0.1364	3.255	175.7	1510	3960	0.620	3.919	1.580	207.2	1116	146.1	22.7	2085
8	2	0.1348	2.723	152.6	1992	5650	0.595	3.357	1.449	179.3	1430	132.2	32.2	3770
9	3	"	2.256	132.3	2840	6950	0.640	2.750	1.288	150.8	2050	117.9	39.6	4970
10	4	"	2.058	123.9	3460	7950	0.660	2.460	1.203	139.2	2490	112.1	45.8	6410
11	5	0.1383	1.970	120.0	3950	8780	0.670	2.266	1.141	134.5	2800	109.8	53.2	7740
12	6.8	"	1.802	112.5	5030	10620	0.689	1.956	1.036	123.9	3560	104.5	64.8	11120
13	1	0.1786	3.725	195.7	1615	3960	0.640	3.780	1.549	231.9	(Boiling occurred)			
14	2	"	3.061	167.3	2170	5650	0.618	3.330	1.443	198.1	1574	141.6	35.6	4100
15	3	"	2.505	143.2	3070	6950	0.665	2.620	1.251	165.6	2220	125.3	39.5	5350
16	4	"	2.305	134.5	3600	7950	0.674	2.390	1.181	153.7	2600	119.4	49.7	6880
17	5	"	2.218	130.6	3910	8780	0.668	2.273	1.144	149.0	2800	117.0	53.6	8300
18	6.8	"	2.011	121.5	4890	10620	0.680	1.989	1.048	136.5	3470	110.8	66.0	10750

NOTES: 1. h^* was based on indicated surface temperature, while h was based on corrected surface temperature.

2. Corrected temperatures were calculated from Equation (13).

TEST NO. 2

Results of Forced-Convection Surface-Boiling Heat Transfer

Date: 6-27-56 p_{atm} = 29.68 in. Hg t_{rm} = 89°F Δt_{sub} = 140 F t_w = 85°F R = 3800 ohm cc^{-1} pH = 7.10

V = 1 ft/sec p_{abs} = 37.79 in. Hg t_{sat} = 224°F

Run No.	$q'' \times 10^{-6}$ B/hr ft^2	Indicated Temperature, t_{ind} Right MV	Center MV	Left MV	Mean MV	Mean °F	$t_{ind} - t_w$ F	h^* B/hr ft^2 F	h_{tc} B/hr ft^2 F	Temperature Correction $\left(\frac{h^*}{h_{tc}}\right)^{1/2}$	$K_1(\sqrt{\beta} r_s)$	$K_0(\sqrt{\beta} r_s)$	t_s °F	$t_s - t_w$ F	$t_s - t_{sat}$ F
1	0.0905	2.408	2.362	2.386	2.385	137.5	52.5	1723	3957	0.957	3.364	1.516	155.4	70.4	
2	0.1118	2.945	2.765	2.945	2.885	159.5	74.5	1900		0.696	3.441	1.470	184.2	99.2	
3	0.1656	3.100	2.880	3.120	3.033	166.1	81.1	2045		0.724	3.303	1.436	192.2	107.2	
4	0.2980	3.845	3.618	3.830	3.764	198.7	112.7	2645		0.817	3.859	1.319	231.9	146.5	7.9
5	0.3403	3.910	3.803	3.900	3.781	202.0	117.0	2910		0.860	2.702	1.275	236.4	151.4	12.4
6	0.6516	4.258	4.183	4.357	4.233	217.4	132.4	4920		1.118	1.978	1.044	251.0	166.0	27.0
7	0.7431	4.435	4.271	4.387	4.364	223.5	138.5	5370		1.168	1.881	1.009	257.5	172.5	33.5
8	0.8126	4.530	4.450	4.537	4.506	229.7	144.7	5620		1.195	1.821	0.987	265.0	180.0	41.0
9	0.9246	4.660	4.515	4.670	4.615	234.2	149.2	6180		1.253	1.717	0.948	269.5	184.5	45.5
10	1.0309	4.837	4.755	4.819	4.817	243.2	158.2	6520		1.288	1.656	0.924	280.0	195.0	56.0
11	1.1768	4.955	4.813	4.960	4.909	247.3	162.3	7240		1.355	1.552	0.883	284.0	199.0	60.0
12	1.3284	5.089	4.960	5.080	5.043	253.1	168.1	7900		1.414	1.464	0.847	290.0	205.0	64.0
13	1.4399	5.178	5.091	5.086	5.118	256.3	171.3	8400		1.455	1.406	0.822	293.3	208.3	67.3
14	1.5518	5.281	5.182	5.276	5.246	262.3	177.3	8950		1.490	1.370	0.807	300.0	215.0	76.0

NOTES: 1. h_{tc} was calculated from Equation (9) based on water temperature.

2. h^* was calculated based on indicated temperature.

TEST NO. 3

Results of Forced-Convection Surface-Boiling Heat Transfer

Date: 7-9-56 p_{atm} = 29.41 in. Hg t_{rm} = 76°F

V = 1 ft/sec p_{abs} = 36.61 in. Hg t_{sat} = 222.5°F Δt_{sub} = 80 F t_w = 142.5°F R = 4040 ohm cc^{-1} pH = 7.90

Run No.	$q'' \times 10^{-6}$ B/hr ft^2	Indicated Temperature, t_{ind} Right mV	Center mV	Left mV	Mean mV	Mean °F	$t_{ind} - t_w$ F	h^* B/hr ft^2 F	h_{tc} B/hr ft^2 F	$\left(\frac{h^*}{h_{tc}}\right)^{1/2}$	$K_1(\sqrt{\beta}\, r_s)$	$K_o(\sqrt{\beta}\, r_s)$	t_s °F	$t_s - t_w$ F	$t_s - t_{sat}$ F
1	0.469	Failure of Thermocouple	3.096	3.122	3.109	169.3	26.8	1750	4675	0.614	3.631	1.512	179.0	36.5	
2	0.0673		3.235	3.385	3.310	178.0	35.5	1900		0.638	3.446	1.469	191.0	48.5	
3	0.0802		2.437	2.503	2.470	185.0	42.5	1885		0.635	3.469	1.477	202.5	60.0	
4	0.1378		3.930	4.108	4.019	208.3	65.8	2090		0.670	3.264	1.426	225.0	82.5	2.5
5	1.1793		4.156	4.192	4.174	215.2	72.7	2470		0.726	2.977	1.351	232.0	89.5	9.5
6	0.2683		4.329	4.349	4.339	222.3	79.8	3360		0.850	2.500	1.215	244.5	102.0	22.0
7	0.3769		4.469	4.529	4.499	299.1	89.9	4350		0.965	2.133	1.097	259.0	116.5	36.5
8	0.6367			5.039	5.039	253.0	110.5	5770		1.111	1.790	0.978	282.3	139.8	59.8
9	0.7351			5.155	5.155	258.2	115.7	6370		1.170	1.682	0.934	287.0	145.2	63.2
10	0.8072			5.218	5.218	261.0	118.5	6810		1.207	1.611	0.906	290.0	147.5	65.8
11	0.8559			5.270	5.270	263.3	120.8	7080		1.231	1.575	0.892	293.1	150.6	70.6
12	0.9357			5.388	5.388	268.4	125.9	7440		1.261	1.525	0.872	299.0	156.0	76.5
13	0.9837			5.426	5.426	270.3	127.8	7700		1.285	1.489	0.857	301.0	158.5	78.5

NOTES: 1. h_{tc} was calculated from Equation (9) based on water temperature.

2. h^* was calculated based on indicated temperature.

TEST NO. 4

Results of Forced-Convection Surface-Boiling Heat Transfer

Date: 6-29-56 p_{atm} = 29.54 in. Hg t_{rm} = 80°F

V = 2 ft/sec p_{abs} = 40 in. Hg t_{sat} = 227.2°F Δt_{sub} = 140 F t_w = 87°F R = 3820 ohm cc^{-1} pH = 7.15

Run No.	$q'' \times 10^{-6}$ B/hr ft^2	Indicated Temperature, t_{ind} Right mV	Center mV	Left mV	Mean mV	Mean °F	$t_{ind} - t_w$ F	h^* B/hr ft^2 F	h_{tc} B/hr ft^2 F	Temperature Correction $\left(\frac{h^*}{h_{tc}}\right)^{1/2}$	$K_1(\sqrt{\beta}\, r_s)$	$K_o(\sqrt{\beta}\, r_s)$	t_s °F	$t_s - t_w$ F	$t_s - t_{sat}$ F
1	0.0895	1.916	1.786	1.918	1.873	115.7	28.7	3118	5640	0.746	2.594	1.243	125.6	38.6	
2	0.1108	2.306	2.048	2.300	2.216	130.5	43.5	3237		0.760	2.550	1.230	145.4	58.4	
3	0.1729	2.560	2.290	2.560	2.470	141.5	54.5	3272		0.762	2.525	1.222	160.0	73.0	
4	0.2173	2.770	2.548	2.760	2.693	151.1	64.1	3390		0.775	2.476	1.208	172.8	85.8	
5	0.3303	3.379	3.022	3.370	3.257	175.7	88.7	3724		0.815	2.337	1.164	205.0	118.0	
6	0.6587	4.148	3.968	4.140	4.085	211.2	124.2	5305		0.972	1.881	1.009	247.7	160.7	20.5
7	0.7406	4.390	4.115	4.380	4.295	220.5	133.5	5547		0.993	1.840	0.994	259.5	172.5	32.3
8	0.8153	4.560	4.328	4.560	4.449	227.3	140.3	5810		1.012	1.782	0.973	268.0	181.0	40.8
9	0.9303	4.693	4.513	4.693	4.633	235.2	148.2	6277		1.060	1.704	0.943	276.8	189.8	49.6
10	1.0313	4.877	4.711	4.877	4.822	243.8	156.6	6663		1.090	1.635	0.916	286.8	199.8	59.6
11	1.1934	4.913	4.831	4.963	4.916	247.8	160.8	7422		1.155	1.521	0.870	290.6	203.6	63.4
12	1.3608	5.065	4.950	5.065	5.027	252.4	165.4	8227		1.210	1.422	0.829	295.2	208.2	68.0
13	1.4583	5.130	5.050	5.130	5.103	255.7	168.7	8644		1.240	1.380	0.811	298.5	211.5	71.3
14	1.5519	5.260	5.123	5.260	5.217	260.8	173.8	8946		1.260	1.348	0.797	304.7	217.7	77.5

NOTES: 1. h_{tc} was calculated from Equation (9) based on water temperature.

2. h^* was calculated based on indicated temperature.

TEST NO. 5

Results of Forced-Convection Surface-Boiling Heat Transfer

Date: 7-14-56 p_{atm} = 29.54 in. Hg t_{rm} = 80°F

V = 2 ft/sec p_{abs} = 38.05 in. Hg t_{sat} = 224.5°F Δt_{sub} = 80 F t_w = 144.5°F R = 3850 ohm cc^{-1} pH = 7.50

Run No.	$q'' \times 10^{-6}$ B/hr ft^2	Indicated Temperature, t_{ind} Right MV	Center MV	Left MV	Mean MV	Mean °F	$t_{ind} - t_w$ F	h^* B/hr ft^2 F	h_{tc} B/hr ft^2 F	$\left(\frac{h^*}{h_{tc}}\right)^{1/2}$	$K_1(\sqrt{\beta}\, r_s)$	$K_o(\sqrt{\beta}\, r_s)$	t_s °F	$t_s - t_w$ F	$t_s - t_{sat}$ F
1	0.0974	3.093	3.109	3.090	3.098	169.0	24.5	3970	6640	0.775	2.252	1.137	182.8	38.3	
2	0.1371	3.282	3.306	3.278	3.289	177.0	32.5	4230		0.400	2.171	1.110	188.2	43.7	
3	0.1706	3.503	3.442	3.501	3.482	185.6	41.1	4150		0.792	2.191	1.117	199.8	55.3	
4	0.1914	3.635	3.613	3.635	3.638	191.9	47.4	4040		0.793	2.238	1.132	209.0	64.5	
5	0.2666	3.950	3.890	3.960	3.933	207.7	63.2	4230		0.800	2.171	1.110	229.4	84.7	4.9
6	0.3784	4.262	4.275	4.280	4.272	219.6	75.1	5000		0.870	1.961	1.038	244.2	99.7	19.7
7	0.4540	4.400	4.425	4.400	4.408	225.4	80.9	5630		0.920	1.821	0.987	251.0	106.5	26.5
8	0.6316	4.635	4.700	4.645	4.660	236.5	92.0	6870		1.020	1.607	0.905	263.9	119.4	39.4
9	0.7265	4.857	4.887	4.857	4.866	245.3	100.8	7260		1.048	1.548	0.881	274.8	130.3	50.3
10	0.6952	4.973	5.205	4.973	4.990	251.0	106.5	7480		1.062	1.521	0.870	281.8	137.3	57.3
11	0.8497	5.028	5.116	5.028	5.154	253.7	109.2	7740		1.080	1.481	0.854	285.0	140.5	60.5
12	0.9028	5.175	5.175	5.175	5.175	259.3	114.8	7860		1.090	1.471	0.850	292.0	147.5	67.5
13	0.9675	5.210	5.215	5.210	5.212	260.6	116.1	8320		1.120	1.446	0.839	300.0	155.5	75.5

NOTES: 1. h_{tc} was calculated from Equation (9) based on water temperature.

2. h^* was calculated based on indicated temperature.

TEST NO. 6

Results of Forced-Convection Surface-Boiling Heat Transfer

Date: 7-1-56 p_{atm} = 29.54 in. Hg t_{rm} = 80°F

V = 3 ft/sec p_{abs} = 44.60 in. Hg t_{sat} = 223°F Δt_{sub} = 140 F t_w = 93°F R = 3400 ohm cc^{-1} pH = 7.33

Run No.	$q'' \times 10^{-6}$ B/hr ft^2	Indicated Temperature, t_{ind}: Right MV	Center MV	Left MV	Mean MV	Mean °F	$t_{ind} - t_w$ F	h^* B/hr ft^2 F	h_{tc} B/hr ft^2 F	Temperature Correction: $\left(\frac{h^*}{h_{tc}}\right)^{1/2}$	$K_1(\sqrt{\beta}\, r_s)$	$K_o(\sqrt{\beta}\, r_s)$	t_s °F	$t_s - t_w$ F	$t_s - t_{sat}$ F
1	0.0914	1.839	1.792	1.840	1.824	113.5	20.5	4460	7090	0.795	2.102	1.087	120.7	27.7	
2	0.1422	2.100	2.087	2.090	2.093	125.1	32.1	4450		0.795	2.102	1.087	136.3	43.3	
3	0.1739	2.260	2.185	2.270	2.238	131.4	38.4	4540		0.803	2.077	1.078	144.7	54.7	
4	0.2203	2.452	2.386	2.390	2.412	139.1	46.1	4780		0.823	2.012	1.056	154.9	61.9	
5	0.3310	2.953	2.929	2.953	2.945	162.2	69.2	4800		0.824	2.006	1.054	186.0	93.0	
6	0.6590	3.840	3.825	3.830	3.832	200.6	107.6	6120		0.930	1.726	0.952	234.9	141.9	1.9
7	0.7405	4.135	4.120	4.146	4.134	213.5	120.5	6150		0.933	1.722	0.950	251.7	158.7	18.7
8	0.8153	4.341	4.210	4.345	4.265	219.2	126.2	6450		0.955	1.669	0.924	258.4	165.4	25.4
9	0.9303	4.445	4.393	4.430	4.423	226.1	133.1	6980		0.994	1.591	0.898	266.7	173.7	33.7
10	1.0335	4.651	4.590	4.673	4.638	235.4	142.4	7260		1.015	1.548	0.881	278.4	185.4	45.4
11	1.1800	4.814	4.761	4.816	4.794	242.2	149.2	7900		1.056	1.457	0.844	285.8	192.8	52.8
12	1.3284	4.960	4.855	4.850	4.888	246.4	153.4	8660		1.110	1.380	0.811	290.0	197.0	57.0
13	1.4207	5.107	4.980	5.110	5.066	254.3	161.3	8820		1.120	1.360	0.803	300.0	207.0	67.0
14	1.5318	5.190	5.114	5.190	5.165	258.8	165.8	9250		1.130	1.321	0.785	305.8	212.8	72.8
15	1.6544	5.245	5.185	5.260	5.230	261.5	168.5	9830		1.180	1.262	0.760	307.6	214.6	74.6

NOTES: 1. h_{tc} was calculated from Equation (9) based on water temperature.

2. h^* was calculated based on indicated temperature.

TEST NO. 7

Results of Forced-Convection Surface-Boiling Heat Transfer

Date: 7-17-56 p_{atm} = 29.40 in. Hg t_{rm} = 92°F

V = 3 ft/sec p_{abs} = 41.26 in. Hg t_{sat} = 228.5°F Δt_{sub} = 80 F t_w = 148.5°F R = 4080 ohm cc^{-1} pH = 8.00

Run No.	$q'' \times 10^{-6}$ B/hr ft^2	Indicated Temperature, t_{ind} Right MV	Center MV	Left MV	Mean MV	Mean °F	$t_{ind} - t_w$ F	h^* B/hr ft^2 F	h_{tc} B/hr ft^2 F	Temperature Correction $\left(\frac{h^*}{h_{tc}}\right)^{1/2}$	$K_1(\sqrt{\beta}\, r_s)$	$K_o(\sqrt{\beta}\, r_s)$	t_s °F	$t_s - t_s$ F	$t_s - t_{sat}$ F
1	0.1358	3.310	3.290	3.300	3.300	177.5	29.0	4680	8197	0.756	2.041	1.066	188.3	39.8	
2	0.1689	3.403	3.387	3.420	3.403	182.1	33.6	5025		0.795	1.950	1.034	144.3	45.8	
3	0.2257	3.773	3.755	3.782	3.770	198.0	49.6	5370		0.810	1.876	1.007	215.6	67.1	
4	0.3191	4.280	4.270	4.423	4.366	334.5	75.0	6025		0.860	1.745	0.958	249.2	100.7	20.7
5	0.4312	4.648	4.638	4.650	4.645	235.5	87.0	7270		0.941	1.548	0.881	263.8	115.3	35.3
6	0.7855	4.928	4.910	4.928	4.922	248.1	99.6	7270		0.941	1.548	0.881	281.6	132.1	52.1
7	0.8910	5.010	5.007	5.020	5.022	252.1	103.6	7700		0.970	1.489	0.857	285.3	136.8	56.8
8	0.9631	5.130	5.115	5.130	5.125	256.5	108.0	8000		0.990	1.453	0.841	290.5	142.0	62.0
9	0.9861	5.220	5.211	5.200	5.210	260.5	112.0	8100		0.994	1.439	0.836	295.7	147.2	67.2
10	0.9733	5.305	5.305	5.311	5.307	264.5	116.0	8100		1.015	1.406	0.822	300.4	151.9	71.9
11	1.0137	5.372	5.356	5.360	5.366	267.5	119.0	8530		1.020	1.393	0.817	304.2	155.7	75.7
12	1.0955	5.425	5.425	5.423	5.424	270.2	121.7	9850		0.042	1.348	0.797	307.2	158.7	78.7
13	1.1622	5.520	5.520	5.510	5.517	274.2	125.7	9260		1.065	1.318	0.784	312.0	163.5	83.5

NOTE: 1. h_{tc} was calculated from Equation (9) based on water temperature.

2. h^* was calculated based on indicated temperature.

TEST NO. 8

Results of Forced-Convection Surface-Boiling Heat Transfer

Date: 7-3-56 p_{atm} = 29.41 in. Hg t_{rm} = 86°F

V = 4 ft/sec p_{abs} = 47.77 in. Hg t_{sat} = 236.5°F Δt_{sub} = 140 F t_w = 96.5°F κ = 3850 ohm cc^{-1} pH = 7.50

		Indicated Temperature, t_{ind}						Temperature Correction							
Run No.	$q'' \times 10^{-6}$ B/hr ft^2	Right MV	Center MV	Left MV	Mean MV	Mean °F	$t_{ind} - t_w$ F	h^* B/hr ft^2 F	h_{tc} B/hr ft^2 F	$\left(\frac{h^*}{h_{tc}}\right)^{1/2}$	$K_1(\sqrt{\beta}\, r_s)$	$F_o(\sqrt{\beta}\, r_s)$	t_s °F	$t_s - t_w$ F	$t_s - t_{sat}$ F
1	0.0909	1.835	1.768	1.780	1.797	112.2	15.7	5790	8216	0.847	1.787	0.974	117.7	21.2	
2	0.1420	2.025	1.937	2.005	1.989	121.0	24.5	5800		0.840	1.787	0.974	129.4	32.9	
3	0.1743	2.105	2.050	2.100	2.085	124.8	28.3	6150		0.867	1.731	0.953	134.2	37.7	
4	0.2171	2.251	2.171	2.230	2.217	130.7	34.2	6350		0.881	1.682	0.934	142.3	45.8	
5	0.3270	2.660	2.530	2.610	2.600	147.3	50.8	6440		0.889	1.669	0.929	164.3	67.8	
6	0.6512	3.465	3.328	3.440	3.412	182.4	85.9	7580		0.963	1.510	0.866	210.0	113.6	
7	0.7325	3.712	3.620	3.618	3.683	194.1	97.6	7500		0.957	1.510	0.866	225.6	129.1	
8	0.8065	3.965	3.885	3.940	3.930	204.7	108.2	7450		0.954	1.521	0.870	239.5	143.0	3..
9	0.9246	4.240	4.230	4.230	4.233	217.4	120.9	7660		0.968	1.492	0.858	256.0	159.5	19.5
10	1.0173	4.385	4.360	4.370	4.372	223.8	127.3	7970		0.986	1.460	0.845	264.0	167.5	27.5
11	1.1695	4.706	4.688	4.697	4.697	237.9	141.4	8250		1.001	1.422	0.829	281.9	185.4	45.4
12	1.3167	4.890	4.820	4.872	4.861	245.0	148.5	8860		1.040	1.361	0.803	291.1	194.6	54.6
13	1.4166	5.063	5.002	5.042	5.036	252.8	156.3	9070		1.052	1.336	0.792	300.0	203.5	63.5
14	1.5360	5.190	5.120	5.172	5.161	258.5	162.0	9470		1.073	1.303	0.778	307.1	210.6	70.6
15	1.6503	5.356	5.354	5.342	5.351	267.0	170.5	9680		1.088	1.280	0.767	312.5	221.0	81.0
16	1.7201	5.420	5.498	5.402	5.440	271.0	174.5	9860		1.095	1.265	0.761	322.4	225.9	85.9

NOTES: 1. h_{tc} was calculated from Equation (9) based on water temperature.

2. h^* was calculated based on indicated temperature.

TEST NO. 9

Results of Forced-Convection Surface-Boiling Heat Transfer

Date: 7-20-56 p_{atm} = 29.46 in. Hg t_{rm} = 89°F Δt_{sub} = 80 F t_w = 150°F A = 1150 ohm cc^{-1} pH = 3.32

V = 4 ft/sec p_{abs} = 47.22 in. Hg t_{sat} = 236°F

Run No.	$q'' \times 10^{-6}$ B/hr ft^2	Indicated Temperature, t_{ind} Right MV	Center MV	Left MV	Mean MV	Mean °F	$t_{ind} - t_w$ F	h^* B/hr ft^2 F	h_{tc} B/hr ft^2 F	$\left(\frac{h^*}{h_{tc}}\right)^{1/2}$	Temperature Correction $K_1(\sqrt{\beta}\, r_s)$	Temperature Correction $K_o(\sqrt{\beta}\, r_s)$	t_s °F	$t_s - t_w$ F	$t_s - t_{sat}$ F
1	0.13[illegible]	3.276	3.280	3.279	3.278	176.6	26.6	6800	9606	0.842	1.615	0.903	181.0	31.0	
2	[illegible].1726	3.382	3.423	3.432	3.412	182.3	32.3	6550		0.829	1.648	0.921	191.[illegible]	35.9	
3	[illegible].2491	3.79[illegible]	3.812	3.822	3.811	199.5	49.5	6100		0.797	1.731	0.953	213.[illegible]	57.9	
4	0.4[illegible]	4.325	4.230	4.240	4.232	217.4	67.4	7550		0.887	1.510	0.866	23[illegible].7	82.7	2.7
5	0.646[illegible]	4.532	4.540	4.560	4.544	231.1	81.1	8720		0.954	1.370	0.807	256.2	106.2	20.2
6	0.7377	4.720	4.750	4.780	4.750	240.3	90.3	8750		0.956	1.370	0.807	260.1	112.1	32.1
7	0.8[illegible]6	4.965	4.990	5.000	4.980	250.4	100.4	8570		0.947	1.386	0.814	261.5	125.5	[illegible].5
8	[illegible].[illegible]59	5.120	5.130	5.112	5.131	257.0	107.0	8480		0.942	1.399	0.819	270.7	134.7	[illegible].7
9	0.9117	5.165	5.175	5.160	5.173	259.1	109.1	8350		0.960	1.354	0.800	283.1	137.1	[illegible].1
10	[illegible].975[illegible]	5.210	5.216	5.223	5.316	265.2	109.2	8950		0.986	1.345	0.796	301.1	145.1	[illegible].1
11	1.0134	5.390	5.382	5.376	5.383	268.1	112.1	9020		0.970	1.339	0.793	304.9	148.9	[illegible].9
12	1.0[illegible]5	5.[illegible]8	5.[illegible]0	5.450	5.[illegible]6	271.2	115.2	9100		0.990	1.303	0.776	308.5	152.5	[illegible].5
13	1.1617	5.586	5.557	5.565	5.575	276.8	120.8	9630		1.000	1.282	0.768	315.7	159.7	[illegible].7
14	1.[illegible]56	5.612	5.600	5.600	5.604	278.2	122.2	10250		1.035	1.232	0.746	316.5	160.5	[illegible].[illegible]

NOTES: 1. h_{tc} was calculated from Equation (9) based on water temperature.

2. h^* was calculated based on indicated temperature.

TEST NO. 10

Results of Forced-Convection Surface-Boiling Heat Transfer

Date: 7-5-56 p_{atm} = 29.42 in. Hg t_{rm} = 90°F

V = 5 ft/sec p_{abs} = 53.78 in. Hg t_{sat} = 243.4°F Δt_{sub} = 140 F t_w = 103.4°F R = 3950 ohm cc^{-1} pH = 7.60

Run No.	$q'' \times 10^{-6}$ B/hr ft^2	Indicated Temperature, t_{ind} Right MV	Center MV	Left MV	Mean MV	Mean °F	$t_{ind} - t_w$ F	h^* B/hr ft^2 F	h_{tc} B/hr ft^2 F	Temperature Correction 1/2 $\left(\frac{h^*}{h_{tc}}\right)$	$K_1(\sqrt{\beta}\, r_s)$	$K_o(\sqrt{\beta}\, r_s)$	t_s °F	$t_s - t_w$ F	$t_s - t_{sat}$ F
1	0.1742	2.190	2.142		2.156	127.9	24.5	7120	9208	0.880	1.563	0.887	136.4	33.0	
2	0.1975	2.275	2.250		2.263	132.7	29.3	6750		0.860	1.619	0.910	143.0	39.6	
3	0.3267	2.595	2.538		2.567	145.7	42.3	7720		0.917	1.485	0.855	160.0	56.6	
4	0.6538	3.500	3.462		3.481	185.5	82.1	7950		0.932	1.460	0.845	212.9	109.5	
5	0.7324	3.595	3.488		3.542	188.1	84.7	8700		0.974	1.377	0.810	215.6	112.2	
6	0.8168	3.811	3.760		3.786	198.5	95.1	8480		0.965	1.396	0.818	226.6	126.2	
7	0.9124	4.050	3.998		4.044	209.5	106.1	8600		0.970	1.383	0.812	234.0	140.6	0.6
8	1.0161	4.207	4.198		4.202	216.7	113.3	8920		0.990	1.348	0.797	2 2.5	149.1	5.7
9	1.1585	4.501	4.408		4.501	229.6	126.1	9180		1.000	1.327	0.788	2 ..	166.6	26.6
10	1.2983	4.835	4.795		4.815	243.3	139.9	9270		1.001	1.318	0.794	2 ..	184.6	44.6
11	1.4116	4.969	4.898		4.933	248.4	145.0	9670		1.025	1.280	0.767	284.0	190.6	50.6
12	1.5119	5.187	5.160		5.174	259.2	155.8	9730		1.030	1.268	0.762	306.2	204.8	64.8
13	1.6302	5.162	5.282		5.272	263.4	160.0	10200		1.052	1.232	0.746	312.6	209.2	69.2
14	1.6996	5.410	5.387		5.399	269.0	165.6	10260		1.050	1.211	0.736	320.4	217.0	77.0
15	1.8117	5.525	5.630		5.568	276.9	173.5	10600		1.072	1.195	0.729	330.8	227.4	87.4
16	1.9944	5.795	5.802		5.799	287.0	183.6	10860		1.085	1.179	0.722	342.0	239.4	99.4

NOTES: 1. h_{tc} was calculated from Equation (9) based on water temperature.

2. h^* was calculated based on indicated temperature.

TEST NO. 11

Results of Forced-Convection Surface-Boiling Heat Transfer

Date: 7-24-56 $p_{atr.}$ = 29.45 in. Hg t_{rm} = 92°F

V = 5 ft/sec p_{abs} = 53.81 in. Hg t_{sat} = 243°F Δt_{sub} = 80 F t_w = 163°F R = 4100 ohm cc^{-1} r = 0.25

Run	$q'' \times 10^{-6}$	Indicated Temperature, t_{ind}					$t_{ind} - t_w$	h^*	h_{tc}	Temperature Correction $\left(\frac{h^*}{h_{tc}}\right)^{1/2}$	$K_1(\sqrt{\beta}\, r_s)$	$K_o(\sqrt{\beta}\, r_s)$	t_s	$t_s - t_w$	$t_s - t_{sat}$
		Right	Center	Left	Mean										
No.	B/hr ft^2	MV	MV	MV	MV	°F	F	B/hr ft^2 F	B/hr ft^2 F				°F	F	F
1	0.1393	3.410	3.422		3.416	181.1	18.1	7606	11082	0.835	1.492	0.858	197.0	35.0	
2	0.1718	3.507	3.538		3.523	187.1	24.1	7130		0.804	1.563	0.881	196.2	33.2	
3	0.2723	3.842	3.853		3.846	194.5	31.5	8640		0.888	1.380	0.811	200.5	45.0	
4	0.4615	4.350	4.345		4.348	211.8	48.8	9000		0.835	1.492	0.858	234.0	72.0	
5	0.6560	4.695	4.700		4.700	238.0	75.0	8780		0.893	1.367	0.806	264.6	101.6	21.6
6	0.7402	4.784	4.806		4.795	242.2	79.0	9370		0.920	1.312	0.781	270.0	107.0	27.0
7	0.8096	4.932	4.953		4.943	248.7	85.8	9440		0.935	1.297	0.775	279.8	115.8	35.8
8	0.8642	5.140	5.140		5.150	257.0	95.0	9080		0.906	1.333	0.791	291.4	127.4	47.4
9	0.9201	5.255	5.261		5.259	263.0	100.0	9180		0.910	1.324	0.787	297.0	135.0	55.0
10	0.9859	5.387	5.391		5.389	268.3	105.3	9360		0.920	1.312	0.781	304.6	141.6	61.6
11	1.0507	5.500	5.510		5.505	273.7	110.7	9500		0.926	1.294	0.774	312.2	149.2	69.2
12	1.0982	5.625	5.610		5.617	278.8	115.8	9470		0.925	1.294	0.771	319.0	156.0	76.0
13	1.1612	5.680	5.720		5.700	282.5	119.6	9720		0.937	1.274	0.765	323.7	160.7	80.7
14	1.2147	5.740	5.780		5.760	285.0	122.0	10300		0.966	1.221	0.741	326.2	163.2	83.2
15	1.3365	5.790	5.828		5.809	287.5	124.5	10730		0.985	1.192	0.723	329.0	166.0	86.0

NOTES: 1. h_{tc} was calculated from Equation (9) based on water temperature.

2. h^* was calculated based on indicated temperature.

TEST NO. 12

Results of Forced-Convection Surface-Boiling Heat Transfer

Date: 7-7-56 p_{atm} = 29.44 in. Hg t_{rm} 90°F

V = 6.8 ft/sec p_{abs} = 61.80 in. Hg t_{sat} = 251.2°F Δt_{sub} = 140 F t_w = 111.2°F R = 3870 ohm cc^{-1} pH = 7.50

Run No.	$q'' \times 10^{-6}$ B/hr ft^2	Indicated Temperature, t_{ind} Right MV	Center MV	Left MV	Mean MV	Mean °F	$t_{ind} - t_w$ F	h^* B/hr ft^2 F	h_{tc} B/hr ft^2 F	Temperature Correction $\left(\frac{h^*}{h_{tc}}\right)^{1/2}$	$K_1(\sqrt{\beta}\, r_s)$	$K_o(\sqrt{\beta}\, r_s)$	t_s °F	$t_s - t_w$ F	$t_s - t_{sat}$ F
1	0.2114	2.415	2.419	2.319	2.351	136.5	25.3	8030	10920	0.860	1.450	0.841	145.7	34.5	
2	0.3284	2.730	2.677	2.796	2.734	153.2	42.0	7830		0.847	1.474	0.851	168.6	57.4	
3	0.6487	4.510	3.425		3.467	184.8	73.6	8830		0.900	1.361	0.803	210.8	99.6	
4	0.7328	3.702	3.652		3.677	192.8	81.6	8970		0.905	1.345	0.796	221.4	110.2	
5	0.7988	3.927	3.816		3.842	201.2	90.0	8870		0.903	1.354	0.800	232.8	121.6	
6	0.9244	4.150	3.861	Failure of Thermocouple	4.056	210.3	99.0	9320		0.925	1.312	0.781	241.6	133.4	
7	1.0181	4.280	4.118		4.199	216.5	105.3	9650		0.936	1.282	0.769	252.6	111.4	1.4
8	1.1594	4.508	4.467		4.488	238.9	127.7	9130		0.916	1.330	0.789	283.2	172.0	32.0
9	1.3060	4.820	4.715		4.768	240.9	129.7	10080		0.923	1.246	0.752	286.2	175.0	35.0
10	1.3985	5.012	4.955		4.984	250.7	139.5	10000		0.957	1.246	0.752	298.0	186.8	46.8
11	1.4952	5.288	5.176		5.228	261.4	150.2	9975		0.957	1.257	0.755	312.3	201.1	61.1
12	1.6253	5.377	5.385		5.331	266.0	154.8	10550		0.984	1.205	0.734	317.6	216.4	66.4
13	1.6901	5.542	5.477		5.509	274.0	162.8	10100		0.980	1.219	0.740	328.2	217.0	77.0
14	1.8340	5.678	5.630		5.624	279.2	168.0	10900		1.000	1.177	0.721	334.7	223.5	83.5
15	1.9903	5.924	5.885		5.904	291.8	180.6	11000		1.000	1.172	0.718	351.4	240.2	100.2
16	2.1772	6.108	5.986		6.047	297.9	186.7	11620	↓	1.032	1.125	0.696	358.1	246.9	106.9

NOTES: 1. h_{tc} was calculated from Equation (9) based on water temperature.

2. h^* was calculated based on indicated temperature.

TEST NO. 13

Results of Forced-Convection Surface-Boiling Heat Transfer

Date: 7-27-56 p_{atm} = 29.45 in. Hg t_{rm} = 92°F

V = 6.8 ft/sec p_{abs} = 61.71 in. Hg t_{sat} = 251.2°F Δt_{sub} = 80 F t_w = 171.2°F R = 4150 ohm cc^{-1} pH = 5.0

Run No.	$q'' \times 10^{-6}$ B/hr ft^2	Indicated Temperature, t_{ind} Right MV	Center MV	Left MV	Mean MV	Mean °F	$t_{ind} - t_w$ F	h^* B/hr ft^2 F	h_{tc} B/hr ft^2 F	$\left(\frac{h^*}{h_{tc}}\right)^{1/2}$	$K_1(\sqrt{\beta}\, r_s)$	$K_o(\sqrt{\beta}\, r_s)$	t_s °F	$t_s - t_{sat}$ F	$t_s - t_w$ F
1	0.1399	3.500	3.504	3.506	3.503	186.5	15.3	9130	13200	0.833	1.333	.791	192.3	21.1	
2	0.1621	3.542	3.586	3.578	3.569	189.3	18.1	8960		0.829	1.348	0.797	196.0	[illegible]	
3	0.2483		3.795	3.782	3.789	198.5	23.1	10730		0.826	1.192	0.729	206.[illegible]	[illegible]	
4	0.4196		4.240	4.364	4.302	220.8	49.6	8440		0.800	1.413	0.821	[illegible]	[illegible]	
5	0.6479		4.725	4.789	4.762	240.6	69.4	9340		0.840	1.303	0.778	247.2	[illegible]	[illegible]
6	0.7457	Failure of Thermocouple	4.827	4.839	4.833	244.1	72.9	10250		0.881	1.229	0.745	271.1	[illegible]	[illegible]
7	0.8180		5.002	4.844	4.923	248.1	76.9	10780		0.904	1.190	0.726	[illegible]	[illegible]	[illegible]
8	0.8673		5.086		5.086	255.2	84.0	10320		0.886	1.221	0.741	[illegible]	[illegible]	[illegible]
9	0.9271		5.238		5.238	261.9	90.7	10320		0.886	1.221	0.741	[illegible]	[illegible]	[illegible]
10	0.9922		5.390		5.390	268.5	97.3	10200		0.880	1.260	0.758	301.2	133.0	[illegible]
11	1.0335		5.478		5.478	271.5	100.3	10330		0.886	1.224	0.742	[illegible]	137.2	[illegible]
12	1.1018		5.547		5.547	275.5	104.3	10600		0.897	1.197	.730	313.6	142.4	[illegible]
13	1.1759		5.710		5.710	283.0	111.8	10550		0.896	1.198	0.731	324.0	152.[illegible]	[illegible]
14	1.2700		5.820		5.820	288.0	116.8	10900		0.910	1.177	0.721	330.3	159.1	[illegible]
15	1.3313		5.925		5.925	292.8	121.6	11000		0.910	1.172	0.718	336.8	165.6	[illegible]
16	1.4232		6.053		6.053	298.1	126.9	11220		0.912	1.152	0.708	341.0	172.9	[illegible]

NOTES: 1. h_{tc} was calculated from Equation (9) based on water temperature.

2. h^* was calculated based on indicated temperature.

TEST NO. 14

Forced-Convection Surface Boiling Heat Transfer from Single Wires at Burnout

Date	Run No.	E Volts	I Amps	$q''_{BO} \times 10^{-6}$ B/hr ft^2	V ft/sec	P_{abs} in. Hg	t_{sat} °F	t_w °F	Δt_{sub} F	ρ lb$_m$/ft^3	G x 10^{-6} lb$_m$/hr ft^2	$(\Delta t_{sub})^{0.8}$	$\left(\frac{G}{10^6}\right)^{0.2}$	$\left[\left(\frac{G}{10^6}\right)^{0.2} (\Delta t_{sub})^{0.8}\right]$	Location of Burnout from Center, inches Right	Left
3-13-56	1	23.25	651.2	1.9083	1	36.19	220.0	110.0	112.0	61.9	0.2229	43.4	0.740	32.1	1/4	-
3-14-56	2	24.20	668.8	2.0307	2	38.79	225.5	109	116.5	61.9	0.4459	44.8	0.851	38.1	2	-
3-14-56	3	24.50	663.2	2.0390	2	39.02	226.0	109.9	116.1	61.9	0.4459	44.8	0.851	38.1	-	2;4
3-14-56	4	24.60	691.2	2.1339	3	42.58	230.0	110.8	119.2	61.9	0.6685	45.5	0.923	42.0	4-1/4	-
3-18-56	5	25.20	699.2	2.2107	4	47.76	236.8	112.7	123.8	61.9	0.8914	47.0	0.477	45.8	-	1-1/4
3-18-56	6	27.40	756.8	2.6009	5	54.76	241.5	97.0	147.5	62.1	1.1178	54.0	1.023	55.2	0	0
4- 6-56	7	29.75	778.0	2.8071	6.8	60.78	250.0	127.9	122.1	61.6	1.5113	46.5	1.086	50.5	-	1-1/4
3-27-56	8	26.90	752.0	2.5382	1.1	36.15	222.0	61.1	160.9	62.4	0.2247	58.5	0.742	43.4	-	4-7/16
3-27-56	9	28.50	772.0	2.7577	2	38.40	225.0	57.0	168.0	62.5	0.4496	60.5	0.852	51.5	-	2-7/8
3-28-56	10	29.85	784.0	2.8386	3	42.2	229.7	56.5	173.2	62.5	0.6745	62.0	0.925	57.4	0	0
3-28-56	11	29.35	796.0	2.9320	4	47.74	236.3	64.1	172.2	62.4	0.8986	61.8	0.979	60.5	-	2-1/2
3-28-56	12	30.00	826.0	3.1161	5	53.75	243.0	69.3	173.7	62.4	1.1245	62.0	1.021	63.3	1-1/4	-
3-29-56	13	33.50	892.0	3.7502	6.8	61.10	251.0	52.1	198.9	62.4	1.5317	69.0	1.088	75.1	2	-
4- 7-56	14	20.10	564.0	1.4227	1	35.53	221.0	111.3	79.7	61.3	0.2207	33.2	0.740	24.6	1-7/	-
4- 5-56	15	21.40	594.0	1.5953	2	37.96	224.4	143.6	80.8	61.3	0.4414	33.8	0.849	28.7	1-3/8	-
4- 6-56	16	22.40	626.0	1.7429	3	41.42	228.7	140.2	88.5	61.3	0.6620	36.0	0.921	33.2	-	2-1/4
4- 6-56	17	23.70	658.0	1.9571	4	46.78	235.3	146.0	89.3	61.3	0.8820	36.2	0.975	35.3	2-3/4	-
4- 6-56	18	24.30	670.0	2.0433	5	53.47	242.7	147.0	94.7	61.2	1.1016	38.0	1.016	38.6	-	2-1/8
4- 7-56	19	25.60	700.0	2.2490	6.8	60.26	249.6	145.4	104.2	61.3	1.5028	41.0	1.085	44.5	2	-
4- 9-56	20	15.30	440.0	0.8146	1	36.03	221.5	174.5	47.5	60.9	0.2192	22.0	0.740	16.3	3	-
4-11-56	21	16.70	476.0	0.9976	2	37.88	224.5	179.2	45.3	60.6	0.4359	21.2	0.847	17.9	1/4	2-1/8
4-11-56	22	18.10	510.0	1.1585	3	41.25	232.7	173.5	55.2	60.7	0.6556	21.6	0.919	22.6	1	-
4-11-56	23	19.50	550.0	1.3460	4	46.65	235.2	175.5	59.7	60.7	0.8471	26.2	0.967	25.3	4-1/4	-
4-13-56	24	21.50	594.0	1.602*	5	52.70	242.2	173.1	64.1	60.6	1.0668	28.0	1.022	28.6	-	2-3/4
4-13-56	25	23.10	642.0	1.9812	6.8	60.27	249.7	173.0	76.7	60.7	1.4859	32.0	1.081	34.6	-	4-3/4
6-17-56	26*	23.20	638.0	1.8576	1	36.15	221.7	85	136.7	62.2	0.2239	51.0	0.7110	37.0	-	1-1/4
6-17-56	27*	28.40	770.0	2.7440	3	41.85	229.4	85	144.4	62.2	0.6718	52.0	0.9242	48.7	-1/4	-
6-18-56	28*	31.10	842.0	3.2864	5	54.44	243.8	85	158.8	62.2	1.1196	58.0	1.023	59.3	-3/4	-
6-19-56	29**	26.25	724.0	2.3851	2	38.32	224.8	85	139.8	62.2	0.4478	52.0	0.852	44.3	-	3
6-19-56	30**	29.70	784.0	2.9222	4	47.66	236.3	85	151.3	62.2	0.8957	55.5	0.978	54.3	-7 16	-
6-19-56	31**	32.50	868.0	3.5404	6.8	61.10	250.5	85	165.5	62.2	1.5227	59.8	1.088	65.1	-	4-1/8

NOTES: *These data were taken from simple matrices with Chromax as vertical elements.

**These data were taken from simple matrices with Teflon rod as vertical elements.

TEST NO. 15
Velocity Distribution Across Test Section
With 40-mesh Wire Screen Upstream

Date: 8-15-56 P_{atm} =29.33 in Hg t_{rm} =76 °F
SP. gr. of manometer fluid: 1.25

ΔP_o in RF	Mean Velocity ft/sec	ΔP in Green Fluid at Various Stations L5	L4	L3	L2	L1	0	R1	R2	R3	R4	R5
1.30	1	+0.2	+0.4	+0.4	+0.4	+0.4	+0.4	+0.4	+0.4	+0.4	+0.4	+0.2
		-0.2	-0.4	-0.4	-0.4	-0.4	-0.4	-0.4	-0.4	-0.4	-0.4	-0.2
		0.4	+0.8	+0.8	+0.8	+0.8	+0.8	+0.8	+0.8	+0.8	+0.8	0.4
	Local Velocity: ft/sec	0.73	1.04	1.04	1.04	1.04	1.04	1.04	1.04	1.04	1.04	0.73
4.64	2	1.2	+1.4	+1.5	+1.5	1.7	1.7	1.7	+1.4	1.4	1.4	1.2
		-1.2	-1.5	-1.7	-1.7	-1.8	-1.7	-1.7	-1.6	-1.6	-1.5	-1.2
		2.4	2.9	3.2	3.2	3.5	3.4	3.4	3.0	3.0	2.9	2.4
	Local Velocity: ft/sec	1.80	1.98	2.07	2.07	2.17	2.14	2.14	2.0	2.0	1.98	1.80
10.9	3	2.2	3.2	3.4	3.6	3.6	3.6	3.6	3.5	3.4	3.2	2.0
		-2.2	-3.3	-3.4	-3.7	-3.6	-3.6	-3.6	-3.6	-3.5	-3.2	-2.1
		4.4	6.5	6.8	7.3	7.2	7.2	7.2	7.1	6.9	6.4	4.1
	Local Velocity: ft/sec	2.43	2.95	3.02	3.14	3.11	3.11	3.11	3.09	3.04	2.94	2.35
19.6	4	4.0	5.5	5.9	6.2	6.2	6.1	6.1	6.1	5.8	5.5	4.0
		-4.0	-5.8	-5.9	-6.2	-6.2	-6.2	-6.2	-6.2	-5.9	-5.8	-4.0
		8.0	11.3	11.8	12.4	12.4	12.3	12.3	12.3	11.7	11.3	8.0
	Local Velocity: ft/sec	3.29	3.89	3.98	4.08	4.08	4.07	4.07	4.07	3.97	3.89	3.29
30.6	5	6.2	8.6	9.7	10.0	10.0	10.0	10.0	9.9	9.7	8.6	6.2
		-6.4	-8.7	-9.9	-10.1	-10.2	-10.2	-10.2	-10.1	-9.9	-8.6	-6.4
		12.6	17.3	19.6	20.1	20.2	20.2	20.2	20.0	19.8	17.2	12.6
	Local Velocity: ft/sec	4.12	4.81	5.14	5.20	5.20	5.20	5.20	5.18	5.16	4.80	4.12
43.8	6.8	12.4	15.8	17.0	17.6	17.7	17.7	17.7	17.8	16.7	15.8	12.4
		-12.6	-16.2	-17.0	-17.7	-17.8	-17.8	-17.8	-17.8	-16.9	-16.2	-12.6
		25.0	32.0	34.0	35.3	35.5	35.5	35.5	35.6	33.8	32.0	25.0
	Local Velocity: ft/sec	5.80	6.56	6.77	6.89	6.92	6.92	6.92	6.92	6.75	6.56	5.80

Computation: $V_{local} = \sqrt{2gR\ (1.25 - 1)}$
where R is in ft of manometer reading

TEST NO. 15 (cont'd.)
Velocity Distribution Across Test Section
Without Wire Screen Upstream

Date: 8-21-56 P_{atm} = 29.43 in Hg t_{rm} = 76 °F
SP. gr. of manometer fluid: 1.25

ΔP_o in "F	Mean Velocity ft/sec	ΔP in Green Fluid at Various Stations: L5	L4	L3	L2	L1	0	R1	R2	R3	R4	R5
43.8	6.8	+5.9	+10.0	14.7	+18.1	19.7	19.8	19.0	17.9	14.6	10.0	+5.9
		-6.2	-10.5	-15.2	-19.3	-20.5	-20.8	-20.0	-18.7	-15.2	-10.5	-6.2
		12.1	20.5	29.9	37.4	40.2	40.6	+39.0	36.6	29.8	20.5	12.1
	Local Velocity: ft/sec	4.02	5.25	6.34	7.00	7.36	7.39	7.24	7.02	6.34	5.25	4.02
30.6	5	+4.7	7.6	10.6	12.4	12.9	13.2	12.8	12.3	10.5	7.7	4.7
		-4.8	-7.9	-11.1	-13.0	-13.5	-13.7	-13.4	-12.9	-11.0	-8.0	-4.8
		9.5	15.5	21.7	25.4	26.4	26.9	26.2	25.2	21.5	15.7	9.5
	Local Velocity: ft/sec	3.57	4.56	5.39	5.84	5.96	6.01	5.92	5.80	5.38	4.59	3.57
19.6	4	3.0	4.8	6.5	7.9	8.2	8.3	8.2	7.7	6.6	5.2	3.0
		-3.1	-4.9	-6.7	-8.4	-8.6	-8.7	-8.6	-8.2	-6.8	-5.1	-3.1
		6.1	9.7	13.2	16.3	16.8	17.0	16.8	15.9	13.4	10.3	6.1
	Local Velocity: ft/sec	2.86	3.61	4.21	4.68	4.74	4.77	4.74	4.62	4.24	3.72	2.86
10.9	3	1.2	2.1	3.8	4.7	4.9	5.2	4.8	4.5	3.9	2.6	1.2
		-1.3	-2.2	-3.9	-4.9	-5.1	-5.3	-5.0	-4.7	-4.0	-1.8	-1.3
		2.5	4.3	7.7	9.6	10.0	10.5	9.8	9.2	7.9	4.4	2.5
	Local Velocity: ft/sec	1.83	2.40	3.21	3.58	3.67	3.76	3.63	4.51	3.26	2.42	1.83
4.64	2	+0.5	+1.0	1.6	2.0	2.3	2.3	2.3	2.0	1.6	1.0	0.5
		-0.6	-1.2	-1.8	-2.1	-2.4	-2.4	-2.4	-2.1	-1.8	1.1	-0.6
		1.1	2.2	3.4	4.1	4.7	4.7	4.7	4.1	3.4	2.1	1.1
	Local Velocity: ft/sec	1.21	1.71	2.14	2.55	2.51	2.51	2.51	2.55	2.14	1.67	1.21
1.3	1	0.1	0.2	0.3	0.5	0.6	0.6	0.55	0.5	0.3	0.2	0.1
		-0.1	-0.3	-0.3	-0.5	-0.6	-0.6	-0.55	-0.5	-0.4	-0.3	-0.1
		0.2	0.5	0.6	1.0	1.2	1.2	1.1	1.0	0.7	0.5	0.2
	Local Velocity: ft/sec	0.52	0.82	0.89	1.15	1.27	1.27	1.21	1.15	0.97	0.82	0.52

Computation: $V_{local} = \sqrt{2\,g\,R(1.25 - 1)}$
where R is in ft of manometer reading

TEST NO. 16

Forced-Convection Surface Boiling over a 1/8-in. Diameter Type 304 Stainless Steel Tube

Date: 7-2-56 p_{atm} = 29.48 in. Hg t_{rm} = 84°F Δt_{sub} = 144.3°F Electrical Conductivity: R = 3820 ohm cc^{-1}

V = 1 ft/sec p_{abs} = 37.88 in. Hg t_{sat} = 224.3°F Water Condition: pH = 7.50

Run	$q'' \times 10^{-6}$	Water Temp., t_w		Inner Tube Wall Temp.		R'_m	$\rho_m \times 10^8$	$I^2\rho_m^2 \times 10^8$	k_i	$\rho_i \times 10^8$	$k_i\rho_i \times 10^5$	$\frac{I^2\rho_m^2}{k_i - \rho_i}$	$t_i - t_s$	t_s	$t_s - t_w$
No.	B/hr ft^2	mv	°F	mv	°F	ohm/ft	ohm-ft	$(Am\text{-}ohm\text{-}ft)^2$	B/hr ft F	ohm-ft		x 10^3	F	°F	°F
1	0.0389	1.043	79.4	1.944	118.7	0.0559	256.3	4.3742	8.83	242.0	2.1369	2.0490	3.6	115.1	35.7
2	0.0458	1.042	79.4	2.125	126.7	0.0566	259.5	5.2118	8.86	243.5	2.1574	2.1271	4.2	122.5	43.1
3	0.0606	1.041	79.4	2.513	143.6	0.0562	257.7	7.7459	8.95	246.0	2.2017	3.5181	6.1	[illegible]	[illegible]
4	0.0806	1.040	79.4	2.900	160.3	0.0563	258.2	10.2507	9.02	248.0	2370	4.5823	8.0	152.3	72.9
5	0.1515	1.040	79.3	3.818	199.9	0.0566	259.5	17.5858	9.20	254.0	2.3368	7.5256	13.1	[illegible]	107.5
6	0.1633	1.044	79.4	3.879	202.5	0.0564	258.6	18.5167	9.22	254.0	2.3419	7.9067	13.7	[illegible]	[illegible]
7	0.1753	1.047	79.5	4.048	209.9	0.0567	260.0	19.9988	9.25	256.0	2.3680	8.4454	14.7	193.2	113.7
8	0.1996	1.055	79.8	4.287	220.3	0.0574	263.2	23. 475	9.28	257.0	2.3850	9.6635	16.8	203.5	123.7
9	0.2312	1.055	79.8	4.500	229.6	0.0571	261.8	26.5452	9.32	258.0	2.4046	11.0393	19.2	210.4	[illegible]
10	0.2654	1.055	79.8	4.663	236.6	0.0572	262.7	30.5498	9.37	259.0	2.4268	12.5985	21.9	214.7	134.7
11	0.3133	1.055	79.8	5.743	284.4	0.0576	264.1	36.2583	9.60	266.0	2.5536	14.1989	24.7	259.7	[illegible]
12	0.3707	1.055	79.8	6.057	298.4	0.0581	266.4	43.3677	9.65	268.0	2.5862	16.7689	29.2	269.2	[illegible]
13	0.4436	1.080	81.0	6.537	320.2	0.0587	269.2	52.3610	9.75	271.0	2.6423	19.8164	34.5	285.7	[illegible]
14	0.5595	1.083	81.1	7.094	343.3	0.0598	274.2	67.3073	9.86	274.0	2.7016	24.9139	43.4	299.9	219.9
15	0.6234	1.098	81.7	7.397	356.0	0.0603	276.5	75.5707	9.90	275.0	2.7225	27.7578	48.4	301.6	[illegible]
16	0.6772	1.110	81.8	7.632	369.6	0.0602	276.0	81.9532	9.98	278.0	2.7766	29.8381	52.0	317.6	[illegible]
17	0.7566	1.110	81.8	7.936	383.3	0.0605	277.4	92.3358	10.05	280.0	2.8140	32.8130	57.2	326.1	[illegible]
18	0.8346	1.110	81.8	8.180	394.0	0.0600	278.8	102.0850	10.10	281.0	2.8381	35.9695	62.7	331.3	[illegible]
19	0.9515	1.110	81.8	8.500	408.5	0.0602	276.1	115.2350	10.17	283.0	2.8781	40.0186	69.7	[illegible]	255.3
20	1.0564	1.110	81.8	8.802	434.6	0.0602	276.1	127.8940	10.30	287.0	2.9561	43.2644	75.4	359.2	[illegible]

TEST NO. 16 (Continued)

Forced-Convection Surface Boiling over a 1/8-in. Diameter Type 304 Stainless Steel Tube

Date: 7-2-56 p_{atm} = 29.48 in. Hg t_{rm} = 84°F Δt_{sub} = 82.6°F Electrical Conductivity: R = 4050 ohm cc^{-1}

V = 1 ft/sec p_{abs} = 36.68 in. Hg t_{sat} = 222.6°F Water Condition: pH = 7.93

Run	$q'' \times 10^{-6}$	Water Temp., t_w		Inner Tube Wall Temp.		R'_m	$\rho_m \times 10^8$	$I^2\rho_m^2 \times 10^8$	k_i	$\rho_i \times 10^6$	$k_i\rho_i \times 10^5$	$\frac{I^2\rho_m^2}{k_i - \rho_i}$	$t_i - t_s$	t_s	$t_s - t_w$
No.	B/hr ft^2	mv	°F	mv	°F	ohm/ft	ohm-ft	$(Am\text{-ohm-ft})^2$	B/hr ft F	ohm-ft		x 10^3	F	°F	°F
21	0.6049	2.465	140	3.716	196.8	0.0583	267.3	9.8814	9.18	253.0	2.3225	4.2545	7.4	189.4	49.4
21a	0.1237	2.465	140	4.325	221.5	0.0581	267.8	15.7089	9.30	256.4	2.3845	6.5879	11.5	210.0	70.0
22	0.2274	2.473	140.2	5.539	275.3	0.0594	272.4	27.3538	9.56	264.2	2.5257	10.8302	18.9	256.4	116.4
23	0.2782	"	"	5.861	290.3	0.0597	273.7	32.4121	9.60	266.5	2.5584	12.6689	22.1	268.2	128.2
24	0.2887	"	"	6.110	301.0	0.0601	275.6	37.2992	9.67	268.0	2.5916	14.3923	25.1	275.9	135.9
25	0.3121	"	"	6.330	311.0	0.0601	275.6	41.1619	9.72	269.5	2.6195	15.7146	27.4	283.6	143.6
26	0.3755	"	"	6.485	317.7	0.0602	276.5	44.3507	9.75	271.0	2.6423	16.7849	29.2	288.5	148.5
27	0.4632	"	"	6.682	326.6	0.0607	278.3	49.1815	9.78	272.0	2.6602	18.4890	32.2	294.4	154.4
28	0.5109	2.457	139.7	7.077	344.4	0.0610	279.7	66.3360	9.87	275.0	2.7143	24.4404	42.6	311.3	171.3
29	0.5782	"	"	7.239	352.0	0.0614	281.5	70.9382	9.90	276.0	2.7324	25.9619	45.2	306.8	166.8
30	0.6408	"	"	7.402	359.1	0.0615	282.0	74.2683	9.94	277.0	2.7534	26.9733	47.0	312.1	172.1
31	0.7114	"	"	7.562	366.6	0.0617	282.3	79.5782	9.97	278.0	2.7717	28.7110	50.0	316.6	176.6
32	0.6873	"	"	7.618	368.9	0.0620	281.3	81.9398	9.98	278.2	2.7764	29.5130	51.4	317.5	177.5
33	0.7357	"	"	7.759	375.3	0.0618	283.4	86.4072	10.03	279.4	2.7924	30.9437	53.9	321.4	181.4
34	0.7432	"	"	7.893	381.1	0.0621	284.8	92.8843	10.04	279.0	2.8012	33.1588	57.8	323.3	183.3
35	0.7373	"	"	8.081	389.5	0.0623	285.7	98.9499	10.07	281.0	2.8297	34.9684	60.9	328.6	188.6

*This is the mean temperature of two Alumel-Chromel thermocouple readings. Each of them was located 2-1/2-in. from the center.

TEST NO. 17

Temperature Indications of Soldered-on Thermocouples

Date: [illegible], p_{atm} = 29.18 in.Hg, t_{amb} = 86 °F,

(A) V=4 ft/sec, p_{abs} = 7.87 in.Hg; (B) V=5 ft/sec, p_{abs} = 54.07 in.Hg

t_w = 0.3 °F, Δt_{sub} = 140 F t_w = 20.7 °F, Δt_{sub} = 140 F

Run No.	q'' $\times 10^{-6}$ $\frac{B}{hr\ ft^2}$	t_{thrml} mv	F	Run No.	q'' $\times 10^{-6}$ $\frac{B}{hr\ ft^2}$	t_{thrml} mv	F
1	0.1455	2.062	124.0	1	[illegible]	[illegible]	133.2
2	0.1755	2.170	128.5	2	[illegible]	[illegible]	140.4
3	0.2181	[illegible]	134.3	3	[illegible]	[illegible]	147.7
4	0.3283	3.605	151.3	4	[illegible]	[illegible]	160.0
5	0.4512	3.620	191.5	5	[illegible]	[illegible]	178.0
6	0.7377	3.970	204.9	6	[illegible]	[illegible]	208.0
7	0.8119	4.106	212.3	7	[illegible]	[illegible]	221.0
8	0.9173	4.14	221.7	8	[illegible]	[illegible]	227.3
9	1.0198	4.496	229.2	9	[illegible]	[illegible]	[illegible]
10	1.1749	4.479	247.3	10	[illegible]	[illegible]	258.0
11	1.3289	5.078	42.0	11	[illegible]	[illegible]	[illegible]
12	1.4267	5.130	245.0	12	[illegible]	[illegible]	250.3
13	1.5295	[illegible]	264.0	13	[illegible]	[illegible]	[illegible]
				14	[illegible]	[illegible]	[illegible]

TEST NO. 18

Calibration of Power Factor of Power Transformer

Date: 9-2-46

Run No.	Voltage	Amperage			KVA	Watts			Power Factor KW/KVA
	Volts	Mtr Rdg	Transformer Ratio	Amps		Mtr. Rdg.	Transformer Ratio	KW	
1	3.45	1.25	80:1	100.0	0.345	3.75	80:1	0.300	0.870
2	4.75	1.49	"	119.2	0.566	5.75	"	0.460	0.813
3	4.[illegible]	1.78	"	[illegible]	0.[illegible]	8.50	"	0.680	0.[illegible]72
4	6.16	2.35	"	[illegible]	1.[illegible]	17.75	"	1.420	[illegible]92
5	8.26	3.13	"	251.0	2.[illegible]	5.75	"	2.[illegible]	0.[illegible]4
6	11.35	4.31	"	344.[illegible]	4.1[illegible]	51.25	"	4.100	0.[illegible]3
7	13.50	4.26	"	340.8	5.[illegible]4	65.75	"	5.260	0.[illegible]00
8	17.21	3.07	160:1	491.2	8.443	52.75	160:1	8.440	[illegible]000
9	22.[illegible]	3.04	"	638.4	14.[illegible]84	87.50	"	14.[illegible]	[illegible]000
10	[illegible].00	4.47	"	715.2	13.[illegible]	116.00	"	18.5[illegible]	0.[illegible]98
11	33.50	4.46	200:1	892.0	29.[illegible]2	146.38	200:1	29.[illegible]	1.[illegible]

TEST NO. 19

Calibration of Electrical Resistance
vs. Temperature for Chromax Wire

Date	Wire No.	Wire Condition	E_1 6" Wire mv	E_2 0.1 std D resistor mv	R' Ω/ft	ρ Ω / Cir Mil Ft	Temperature mv	Temperature °F
2-17-56	1	not annealed	32.360	81.95	0.0393	600.5	0.877	72*
"	"	"	32.185	81.44	0.0393	600.5	0.877	72*
"	"	"	32.155	81.44	0.0393	600.5	0.877	72*
2-17-56	"		33.910	83.44	0.0406	619.0	4.238	210.5*
"	"		33.750	83.10	0.0405	618.8	4.238	210.5*
"	"		33.740	82.95	0.0405	618.8	4.238	210.5*
2-18-56	2		17.200	81.150	0.0419	640.0	1.747	400
"	"		17.210	81.160	0.0419	640.0	1.747	400
"	"		17.200	81.155	0.0419	640.0	1.747	400
2-19-56	"		18.035	81.945	0.0441	673.0	2.812	668.5
"	"		18.085	82.020	0.0441	673.0	2.811	668.4
"	"		18.070	82.040	0.0440	672.5	2.810	668.3
6- 6-56	3	annealed	17.630	89.400	0.0395	603.6	0.220	100
"	"	"	17.625	89.400	0.0395	603.6	0.220	100
"	"	"	17.630	89.400	0.0395	603.6	0.220	100
6- 7-56	"		17.850	89.900	0.04015	613.4	0.501	176
"	"		17.855	88.900	0.04015	613.4	0.501	176
"	"		17.850	88.900	0.04015	613.4	0.501	176
6- 8-56	"		18.660	89.710	0.04160	635.6	1.273	357
"	"		18.660	89.710	0.04160	635.6	1.273	357
"	"		18.660	89.715	0.04160	635.6	1.273	357
6- 9-56	"		19.470	90.350	0.04310	658.6	2.206	550
"	"		19.465	90.352	0.04310	658.6	2.206	550
"	"		19.670	90.350	0.04310	658.6	2.206	550

Computation: $R' = 2(0.1)(E_1/E_2)$, Ω/ft

$\rho = R' A = (15230)R'$, Ω/ Cir Mil/ft

Note : 1. "*" Indicates temrerature was recorded with a copper-constantant thermocouple, others recorded with a platinum-platinum plus 100% rhodium thermocouple calibrated by the National Bureau of Standard.

2. Wire No.3 was annealed at 1800 °F for two hours and cooled inside inside the furnace.

BIBLIOGRAPHY

1. Jakob, M., and Fritz, W., "Versuche über den Verdampfungsvorgang", Forschung auf dem Gebiete des Ingenieurwesens, 2 (Dec., 1931) 435-447.

2. Jakob, M., and Linke, W., "Der Wäreübergang von einer Waagerechten Platte on seidendes Wasser", Forschung auf dem Gebeite des Ingenieurwesens, 4 (April, 1933), 75-81.

3. Jakob, M., and Linke, W., "Der Wäreübergang beim Verdampfen von Flüssigkeiten an sendrechten und waagerechten Flächen", Physik. Zeitschr. 36 (1935) 267-280.

4. Cryder, D. S., and Gilliland, E. R., "Heat Transfer from Metal Surfaces to Boiling Liquids", Refrig. Eng., 25 (Feb., 1933) 78-82.

5. Nukiyama, S., "The Maximum and Minimum Values of the Heat Q transmitted from Metal to Boiling Water under Atmospheric Pressure", Journal of Society of Mechanical Engineers, Japan, 37 (June, 1937) 367-374.

6. Drew, T. B., and Mueller, A. C., "Boiling", Trans. Amer. Inst. Chem. Engrs., 33 (1937) 447-473.

7. Cryder, D. S., and Finalborgo, A. C., "Heat Transmission from Metal Surfaces to Boiling Liquids: Effect of Temperature of the Liquid on the Liquid Film Coefficient", Trans. Amer. Inst. Chem. Engrs., 33 (1937) 346-362.

8. Akin, G. A., and McAdams, W. H., "Boiling: Heat Transfer in Natural Convection Evaporator", Trans. Amer. Inst. Chem. Engrs., 35 (April, 1939) 137-158.

9. Farber, E. A., and Scorah, R. L., "Heat Transfer to Water under Pressure", Trans. Amer. Soc. Mech. Engrs., 70 (May, 1948) 369-380.

10. Knowles, J. W., "Heat Transfer with Surface Boiling", Canadian Journal of Research, 26A (1948) 269-278.

11. McAdams, W. H., and Addoms, J. N., Rinaldo, P. M., and Day, R. S., "Heat Transfer from Single Horizontal Wires to Boiling Water", Chem. Eng. Prog., 44 (Aug., 1948) 639-646.

12. McAdams, W. H., Kennel, W. E., Minden, C. S., Carl, R., Picornell, P. M., and Dew, J. E., "Heat Transfer at High Rates to Water with Surface Boiling", Ind. and Eng. Chem., 41 (Sept., 1949) 1945-53.

13. Kreith, F., and Summerfield, M., "Heat Transfer to Water at High Flux Densities with and without Surface Boiling", Trans. Amer. Soc. Mech. Engrs., 71 (Oct., 1949) 805-814.

14. Dittus, F. W. and Boelter, L. M. K., Univer. of Calif. Pubs. Eng., 2 (1930) 443.

15. Gunther, F., "Photographic Study of Surface-Boiling Heat Transfer to Water with Forced Convection", Trans. Amer. Soc. Mech. Engrs., 73 (Feb., 1951) 115-123.

16A. Buchberg, H., Romie, F., Lipkis, R., and Greenfield, M., "Heat Transfer, Pressure Drop, and Burnout Studies with and without Surface Boiling for De-Aerated and Gassed Water at Elevated Pressures in a Forced Flow System", Heat Transfer and Fluid Mechanics Institute, (1951) 177-191.

16B. Buchberg, H., Romie, F., Lipkis, R., and Greenfield, M., "Studies in Boiling Heat Transfer", Final Report, Dept. of Engr., Univ. of Calif. at Los Angeles, AEC Research Contract No. AT-11-1-Gen-9 (March, 1951) III-A-7.

17. Colburn, A. P., "A Method of Correlating Forced Convection Heat Transfer Data and a Comparison with Fluid Friction", Trans. Amer. Inst. Chem. Engrs., 29 (1933) 174-210.

18. Rohsenow, W. M., and Clark, J. A., "Heat Transfer and Pressure Drop Data for High Heat Flux Densities to Water at High Sub-Critical Pressures", Heat Transfer and Fluid Mechanics Institute, (1951) 193-201.

19. Jens, W. H., and Lottes, P. A., "Analysis of Heat Transfer Burnout, Pressure Drop and Density Data for High Pressure Water", ANL-4627 (May 1951) 1-27.

20. Lowdermilk, W. H., and Weiland, W. F., "Some Measurements of Boiling Burnout", NACA RM E54K10 (Feb., 1955) 1-18.

21. Dingee, D. A., Epstein, H. M., Chastain, J. W., and Fawcett, S. L., "Burnout Heat Flux in a Rectangular Channel", Battelle Memorial Institute (Jan., 1956).

22. Davis, D. E., Nomography and Empirical Equations, Reinhold Publishing Co., New York (1955) 11-15.

23. McAdams, W. H., Heat Transmission, McGraw-Hill Co., New York, 3rd ed., (1955) 266-268.

24. ASME Research Committee, Flow Meters -- Their Theory and Applications, New York, 4th ed., (1937) 36-39.

25. Jakob, M., Heat Transfer, John Wiley & Sons, New York (1949), 185-189.

26. Boelter, L. M. K., Romie, F. E., Guibert, A. G., and Miller, M. A., "An Investigation of Aircraft Heaters XXVIII - Equations for Steady Temperature Distribution caused by Thermal Sources in Flat Plates applied to Calculation of Thermocouple Errors, Heater Corrections, and Heat Transfer by Pin-fin Plates", NACA TN 1452 (1948).

27. Boelter, L. M. K., and Lockhart, R. W., "An Investigation of Aircraft Heaters XXXV - Thermocouple Conduction Error observed in Measuring Surface Temperatures", NACA TN 2427 (July, 1951).

28. "Tables of the Bessel Functions $Y_o(x)$, $Y_1(x)$, $K_o(x)$, $K_1(x)$, 0 x 1", The National Bureau of Standards (1952).

29. "Allegheny Ludlum Blue Sheet — Allegheny Ludlum Stainless Steel, Chromium-Grades Type 302, 304, 304L and 305", Allegheny Ludlum Steel Corp., Pittsburgh, Penna.

30. "Nichrome and Other High Nickel Electrical Alloys", Driver-Harris Co., Harrison, New Jersey.

31. Janke, E., and Emde, F., "Table of Functions", Dover Publication (1945) 156-157.

32. Brown, A. I., and Marco, S. M., Introduction to Heat Transfer, McGraw-Hill, New York, 2nd ed., (1951).